DETERMINATION OF THERAPEUTIC POTENTIAL OF LUTEOLIN FOR ACUTE LYMPHOBLASTIC LEUKEMIA CELLS

A Thesis Submitted to
the Graduate School of Engineering and Sciences of
İzmir Institute of Technology
in Partial Fulfillment of the Requirements for the Degree of

MASTER OF SCIENCE

in Molecular Biology and Genetics
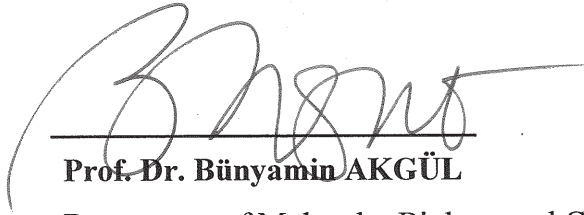
by
Sevim Beyza GÜRLER

November 2019
İZMİR

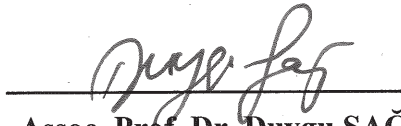We approve the thesis of **Sevim Beyza GÜRLER**

Examining Committee Members:

_____
Prof. Dr. Yusuf BARAN

Department of Molecular Biology and Genetics, İzmir Institute of Technology

_____
Prof. Dr. Bünyamin AKGÜL

Department of Molecular Biology and Genetics, İzmir Institute of Technology

_____
Assoc. Prof. Dr. Duygu SAĞ WINGENDER

İzmir International Biomedicine and Genome Institute, İzmir Dokuz Eylul University

18 November 2019

_____
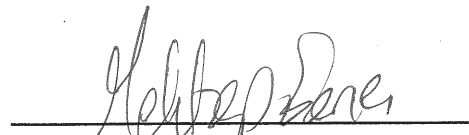**Prof. Dr. Yusuf BARAN**
Supervisor, Department of Molecular
Biology and Genetics,
İzmir Institute of Technology

_____
Prof. Dr. Bünyamin AKGÜL
Head of the Department of Molecular
Biology and Genetics

_____
Prof. Dr. Mehtap EANES
Dean of the Graduate School of
Engineering and Science

ACKNOWLEDGMENTS

ABSTRACT

DETERMINATION OF THERAPEUTIC POTENTIAL OF LUTEOLIN FOR ACUTE LYMPHOBLASTIC LEUKEMIA CELLS

Acute lymphoblastic leukemia (ALL) is a hematologic malignancy characterized by increased level of immature lymphoblasts in bone marrow and peripheral blood. The developments of lymphoblasts are genetically/epigenetically inhibited. One of the most common genetic abnormalities in ALL is BCR/ABL translocation which regulates the several pathways related to proliferation, anti-apoptotic and drug resistance through its aberrant tyrosine kinase activity. Although the current treatment strategies include targeting BCR/ABL via tyrosine kinase inhibitors; complete remission, overall survival and mortality of Ph+ ALL patients are still worse as compared to Ph- ALL patients. Therefore, new strategies combined with current treatments are needed for Ph+ ALL patients who are qualified as high risk group of ALL. Different studies showed thatluteolin has anti-cancer and anti-tumor effects on wide range cancer types including breast, colon, lung cancer except ALL in both *in vitro* and *in vivo.*

In this study, the dose and time dependent cytotoxic, apoptotic and cytostatic effects of luteolin on Philadelphia chromosome +ALL cells were determined for the first time. Besides, the effect of luteolin on cell growth and proliferation of two different healthy cell lines was shown. Moreover, the effect of luteolin on bioactive sphingolipids genes which regulate the several pathways including cell proliferation, apoptosis, drug resistance and senescence in cell was determined in Ph positive ALL cells for the first time. As a consequence, luteolin has cytotoxic, apoptotic and cytostatic effects on Ph positive ALL cells and bioactive sphingolipids genes are regulated in this therapeutic potential by luteolin.

ÖZET

AKUT LENFOBLASTİK LÖSEMİ (ALL) HÜCRELERİNDE LUTEOLİNİN TERAPÖTİK POTANSİYELİNİN BELİRLENMESİ

Akut lenfobalstik Lösemi (ALL) kemik iliğinde ve periferal kanda erken evredeki gelişimi genetik/epigenetik faktörlerle inhibe olmuş ve olgunlaşmamış lenfoblasthücrelerinin artışı ile karakterize malign bir hematolojik kanserdir. ALL'de karşımıza çıkan yaygın genetik anomalilerden biriPhiladelphia kromozomu olarak adlandırılan BCR/ABL translokasyonudur. BCR/ABL aşırı tirozinkinaz anlatımına sahip olup, kanserli hücrelerde hücre çoğalması, anti-apoptoz, metastaz ve ilaç dirençliliğiyleilişkili birçok yolağı aktive etmektedir. Günümüzde klasik kemoterapiye ek olarak BCR/ABL'i hedef alan, BCR/ABL'intirozinkinaz aktivitesini bastırmak veya inhibe etmek üzere tirozinkinaz inhibitörleri kullanılmaktadır. Yine de Ph kromozomu taşımayan ALL hastaları ile kıyaslandığında Ph kromozomu pozitif ALL hastalarında tam remisyon sağlanamamaktadır. Bu nedenle tedaviye yönelik yeni stratejilerin geliştirilmesi oldukça önem arz etmektedir. Yapılan birçok *in vitro* ve *in vivo*çalışmadabir flavonoid olan luteolinin meme, akciğer, kolon gibi birçok farklı kanser türlerinde anti- kanser ve anti-tümör etkiye sahip olduğu gösterilmiş olup ALL üzerindeki etkisi gösterilmemiştir.

Bu çalışmada, luteolininzamana ve doza bağımlı sitotoksik, apoptotik ve sitostatik etkileri Ph kromozomu pozitif ALL hücreleriiçinterapötikpotansiyeli ilk defa belirlenmiş olup, luteolinin hücre büyümesi ve çoğalması üzerine etkisi iki farklı sağlıklı hücre hatlarında da gösterilmiştir.Bunun yanı sıraluteolininhücre çoğalması, apoptoz, ilaç dirençliliği, yaşlanma gibi birçok metabolizmada rol alan biyoaktifsfingolipid genleri üzerine etkisi de Ph pozitif ALL hücrelerinde ilk defa çalışmamızla gösterilmiştir. Sonuç olarak, elde edilen bulgular luteolininPh pozitif ALL hücreleri üzerinde sitotoksik, apoptotik ve sitostatik etkileri olduğunu, bununla birlikte luteolinin bu terapötik potansiyeldebiyoaktifsphingolipid genlerini de regüle ettiğini gösterilmiştir.

To My LovelyGrandmother Sevim GÜRLER…

To My LovelyFamily…

ToLeukemiaPatients…

TABLE OF CONTENTS

LIST OF FIGURES

LIST OF TABLES

LIST OF ABBREVIATIONS

ABL1, Abelsontyrosinekinase 1

ALL, AcuteLymphoblasticLeukemia

Allo-HCT, Allogeneic hematopoietic cell transplantation

ATCC, American Type of Culture Collection

B-ALL, B cell lineage Acute Lymphobalstic Leukemia

BCR, Breakpoint cluster region

BSA, Bovine Serum Albumin

C1PP, Cer-1-Phosphate Phosphatase

CC, Coiled-Coil Domain

CDase, Ceramidase

CerCeramide (Cer),

CERS (LASS), Ceramide Synthase

CERT, Ceramide Transporter Protein

CK, Cer Kinase

CML, ChronicMyeloidLeukemia

CR, Complete Remission

DAG, Diacylglycerol

DES, DihydroceramideDesaturase

DMSO, Dimethylsulfoxide

DNMTs, DNA Methyltransferases

EFS, Event-free Survival

ERK, Extracellular Signal-regulated Kinases

FAB, French-American-British (FAB)

FDA, Food and Drug Administration

GCase, GlucosylCDase.

GCS, Glucosylceramidesynthase

GlcCer, Glycosylceramide (GlcCer)

GRB, Growth Factor Receptor-Bound Protein 2

HDACs, Histone Deacetylases

Hyper-CVAD, Hyper-fractionated cyclophosphamide, vincristine, doxorubicin, and dexamethasone (CVAD)

JAK, Janus Kinase (JAK)

KDS, 3-keto-dihydrosphingosine reductase

MRD, measurable residual disease

mTOR, Mammalian Target of Rapamycin

OS, Overall Survival

PAGE, Polyacrylamide Gel Electrophoresis

PC, Phosphatidylcholine

Ph, PhiladelphiaChromosome

Ph+ ALL, PhiladelphiaChromosomePositiveAcuteLymphoblasticLeukemia

PI, PropidiumIodide

PI3K, Phosphatidylinositol 3-Kinase

RFS, Relapse-free Survival

Rho/GEF, Ras Homolog Gene Family/Guanine Nucleotide Exchange Factors

S1P, Sphingosine-1-phosphate

SDS, Sodium DodesilSulphate

SH, Src Homology

SK, Sphingosine Kinase

SMase, Sphingomyelinase

SMS, SM Synthase

SPPase, Sphingosine Phosphate Phosphatase

SPT, Serine Palmitoyl Transferase

STAT, Signal Transducers and Activation of Transcription

TAE, Tris- Acetate- EDTA

TKI, Tyrosine Kinase Inhibitor

TMD, Transmembrane Domains

TRAIL, Tumor necrosis factor (TNF)-related apoptosis-inducing ligand-TNFSF10

VECs, Vascular Endothelial Cells

WHO, World Health Organization

CHAPTER 1

INTRODUCTION

Cancer is one of the most common diseases resulting in death in nowadays in all age, sexes and countries. In 2017, cancer has been reported as the second leading cause of death not only in the world but also in Turkey (Roser, 2019). Based on the data from World Health Organization (WHO), 18.078.957 new cases were estimated with 9.555.027 deaths caused by different cancer types in all around the world in 2018 while 210.537 new cases were estimated with 116.710 deaths in several cancer types for both sexes in Turkey in 2018 (Bray et al., 2018; Ferlay et al., 2018; Organization, 2019).

Besides, the incidence rate of cancer in males higher than females in the World and cancer mostly observed in Asia with high mortality rate. Likewise other cancer types, leukemia is mostly observed in Asia with high mortality and the incidence rate of leukemia in males is higher than in females (Bray et al., 2018; Ferlay et al., 2018; Organization, 2019).

According to American Cancer Society, 61.780 new leukemia cases with 22.840 deaths were estimated at the United States in 2019 (Siegel, Miller, & Jemal, 2019; Society, 2019). Moreover, 25.860 new leukemia cases with 9.690 deaths are expected in females while 35.920 new leukemia cases with 13,150 deaths in males were estimated (Siegel et al., 2019).

Based on the data from World Health Organization (WHO), the new cases rate of leukemia is 3.09% with 6.029 leukemia cases while the deaths rate of patients with leukemia is 4.31% with 4.681 deaths in Turkey in 2018. Leukemia is mostly observed in males with 8.5% as compared to females (Bray et al., 2018; Ferlay et al., 2018; Organization, 2019).

According to American Cancer Society, approximately 5.930 of new cases of Acute Lymphoblastic Leukemia (ALL) were estimated with approximately 1.500 deaths. Additionally, the numbers of new ALL cases are expected in females and males are 2.650 and 3.280, respectively, while the numbers of estimated deaths in females and males are 650 and 850, respectively, at the United States in 2019 (Siegel et al., 2019; Society, 2019).

1.1. Acute Lymphoblastic Leukemia (ALL)

Acute Lymphoblastic Leukemia (ALL) is a heterogeneous malign hematological cancer characterized by aberrant number of immature lymphoblast in bone marrow, peripheral blood and other organs (Malouf & Ottersbach, 2018; X. Thomas & Heiblig, 2016). The early development of lymphoblast precursor cells is blocked by genetic and/or epigenetic alterations such as chromosomal rearrangements, cooperative mutations, and aneuploidy during the hematopoiesis that is also result in the suppression of production of other normal blood cells and failure of normal immune response (Malouf & Ottersbach, 2018; Pui, Relling, & Downing, 2004; X. Thomas & Heiblig, 2016).

Amount of increased lymphoblast was determined as more than 30% in bone marrow or peripheral blood results in ALL according to French-American-British (FAB) Cooperative Group classification (Bennett et al., 1976, 1985; Lai, Hirsch-Ginsberg, & Bueso-Ramos, 2000). However, WHO Classification of Neoplastic Diseases of Hematopoietic and Lymphoid Tissues or Lymphomas proposed if number of lymphoblast is above 20%, it is sufficient for diagnosis (Harris et al., 1999; Lai et al., 2000). Moreover, 2008 WHO classification determines the current standards for ALL diagnosis combined with cell morphology, genetics/cytogenetics and immunophenotype studies (Vardiman et al., 2009).

According to WHO classification, ALL is grouped under different categories but mainly divided B- and T-lineage lymphoblastic leukemia based on the morphology, cytochemistry, immunophenotype, cytogenetic/genetic, genomics and chromosomal differences (Campo et al., 2011; Chiaretti, Zini, & Bassan, 2014; Lai et al., 2000) and B-lineage lymphoblastic leukemia is more seen type of ALL with 85% (Chiaretti et al., 2014).

Determination of genetic and/or epigenetic alterations in patients is a crucial step for treatment of B-ALL. The abnormalities affect the treatment progress, response of patients to treatment and efficiency of therapeutic drugs in both children and adults. For instance, trisomies (trisomy 4, 10 and 21), changes in chromosome numbers (hypodiploidy or hyperdiploidy), or chromosomal translocations such as t(4;11) MLLAF4, t(12;21) ETV6-RUNX1, t(1;19) E2A-PBX1 and t(9;22) BCR-ABL1 are genetic determinants of B-ALL (Malouf & Ottersbach, 2018). The case reports

indicated that the translocations t(4;11), t(1;19) and t(9;22) are related poor prognosis and leukemogenesis whereas patients who respond to treatment mostly have translocation t(12;21) (Rieder et al., 1996).

Besides, based on the translocation t(9;22) or transcriptional profile, there are three main types of B-cell ALL: Philadelphia chromosome positive B-lineage ALL (P. Nowell, 1960; P. C. Nowell, 2007), Philadelphia chromosome-like B-lineage ALL (Den Boer et al., 2009; Mullighan et al., 2009), Philadelphia chromosome negative B-lineage ALL. Ph-like ALL has similar transcriptional profile with Philadelphia chromosome positive ALL, although there is no (9;22) translocation occurs (Den Boer et al., 2009; Mullighan et al., 2009).

Whether presence of Philadelphia chromosome (Ph) or alterations in gene expressions related to Ph result in different outcome in the treatment strategies:

i. To treat the Philadelphia chromosome positive B-cell ALL, tyrosine kinase inhibitors such as imatinib, dasatinib, nilotinib and ponatinib are used (Malagola, Papayannidis, & Baccarani, 2016),

ii. To treat the Philadelphia chromosome-like B-cell ALL, a tyrosine kinase inhibitor dasatinib, JAK2 inhibitor ruxolitinib, blinatumomab and inotuzumab are used (Chiaretti, Messina, & Foa, 2019; Tasian, Loh, & Hunger, 2017),

iii. To treat the Philadelphia chromosome negative B-cell ALL in older adults, rituximab, ofatumumab, inotuzumab and blinatumumab are used (O'Dwyer & Liesveld, 2017),

in addition to classical chemotherapy or hematopoietic stem cell transplantation.

Several case reports have been showed that the importance of indication of genetic and/or epigenetic alterations in ALL patients due to that the mutations can change the treatment process. For instance, a recent study discovered a novel point mutation in BCR-ABL1 in a Ph+ ALL patient who had been treated with dasatinib 140 mg/day in addition to pediatric-inspired regimen.

Although the complete remission had achieved on day 29 of therapy, minimal residual disease or measurable residual disease (MRD) was detected in the patient. MRD which is a term of remained cancer cells in bone marrow that cause relapse after complete remission (Giebel et al., 2010) is used as a prognostic indicator in the treatment (Bassan et al., 2019).

Furthermore, they analyzed the bone marrow samples to find out mutations related to TKI resistance before allogeneic bone marrow transplantation. The novel

mutation was detected in *ABL1* domain of the fusion transcript. Then they changed the TKI regimen to bosutinib in post-induction therapy and *BCR-ABL1* levels decreased compared to dasatinib regimen. However, the patient died because of acute graft vs host disease complications at the end of the treatment (Vinhas et al., 2018).

1.1.1. Philadelphia Chromosome Positive ALL (Ph+ ALL)

One of the most frequent chromosomal abnormalities in ALL, the Philadelphia chromosome (Ph) was defined at the first time in 1960 in a chronic myeloid leukemia patient (P. Nowell, 1960; P. C. Nowell, 2007). A reciprocal translocation occurs between *BCR* gene located on chromosome 9 and *ABL1* gene located on chromosome 22 and chromosome 22 named as Philadelphia chromosome which contains BCR-ABL fusion gene (Bartram et al., 1983; Rowley, 1973). The transcript of BCR-ABL gene, BCR-ABL fusion protein has aberrant tyrosine kinase activity that changes signaling pathways related to cell proliferation, cell cycle and cell death of leukemic cells (Kurzrock, Gutterman, & Talpaz, 1988; S. Li, Ilaria, Million, Daley, & Van Etten, 1999) (Figure 1.1).

Although Philadelphia chromosome known as a hallmark of chronic myeloid leukemia due to that 95% of chronic myeloid leukemia patients have Ph (Z. J. Kang et al., 2016), ALL patients also experience a considerable amount of Ph. The incidence rate of Ph+ ALL in children is 2-5% while BCR-ABL presence in adolescents and adults with approximately 20% and 20-30%, respectively (Burmeister et al., 2008; Pullarkat, Slovak, Kopecky, Forman, & Appelbaum, 2008; Schultz et al., 2007). Besides, the incidence of presence of BCR-ABL is increasing with aging and the percentage of incidence rate of BCR-ABL is 50 in patients who 60 years old or more (Larson, 2006; D. A. Thomas, 2007).

De novo translocation of Ph chromosome observed dominantly while secondary Ph+ ALL after chemotherapy or radiation therapy have been experienced unfrequently in ALL patients (X. Thomas & Heiblig, 2016). Except a few observations in T-ALL, Ph chromosome is diagnosed widely in B-ALL patients (Mancini et al., 2005; Moorman et al., 2007; Stock, 2008).
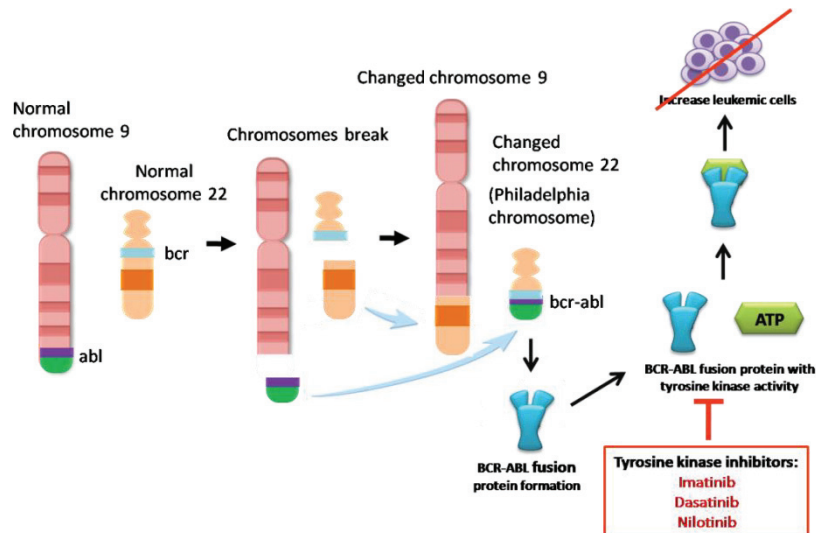
Figure 1.1. Philadelphia chromosome. This figure represents that reciprocal translocation occurs between BCR gene located on chromosome 22 and ABL gene located on chromosome 9. As a consequence of the translocation, BCR-ABL fusion protein which has aberrant tyrosine kinase activity is formed. Tyrosine kinase inhibitors generally use in addition to chemotherapy to prevent binding of ATP to BCR-ABL. Thus, cell proliferation of leukemic cells can be suppressed or inhibited.

.

1.1.2. Molecular Biology of BCR/ABL

Philadelphia chromosome is characterized by the reciprocal translocation between *Breakpoint cluster region* (*BCR*) gene located on long arm of chromosome 22 and proto-oncogene *Abelson tyrosine kinase 1* (*ABL1)* gene located on long arm of chromosome 9 that leads to *BCR-ABL1* fusion gene on chromosome 22 (Bartram et al., 1983; Rowley, 1973). As a consequence of head-to-tail fusion of the different breakpoints in 5′of the *BCR* gene with the sequences in upstream of the *ABL1* gene which encodes tyrosine kinase, three different transcripts of BCR-ABL occur: p190, p210 and p230 (Fainstein et al., 1987; Groffen et al., 1984; Saglio et al., 1990). Although the breakpoints locations of BCR and ABL gene are various (Score et al., 2010), the recombination generally occurs between intron 1, intron 13/14, or exon 19 of *BCR* and 140-kb region between exons 1b and 2 of *ABL1* (Figure 1.2a).

The fusion between exon13 of *BCR* and exon2 of *ABL* gene results in major 8.5-kilobase (kb) *BCR-ABL1* transcript (M-BCR, also known as b2a2 and b3a2) which

5

referred to as p210[BCR-ABL1] and these transcripts comprise a hybrid 210 kDa protein.7.5-kilobase (kb) transcript, p190[BCR-ABL1] (e1a2) known as the minor *BCR-ABL1* transcript (m-*BCR*) while p230[BCR-ABL1] (e19a2) named as macro *BCR-ABL1* transcript (μ-*BCR*) and the transcripts encode hybrid 190-kDa and 230-kDa proteins, respectively (S. Li et al., 1999). However, all fusion proteins consist the different portion of *BCR* sequence at the NH2 terminus, they contain same portion of *ABL* tyrosine kinase at the COOH terminus. These different types of BCR/ABL oncogene result in different lymphoid leukemogenic activity whereas similar CML-like syndrome was observed in mice (S. Li et al., 1999). Even if the transcripts produce distinct proteins, their common feature is their aberrant kinase activity comparing the wild-type ABL1 and they related to prognosis differently in both CML and ALL (Z. J. Kang et al., 2016).

p190[BCR-ABL] transcript mostly observed in childhood and adult Ph+ALL with approximately 85% and 50-70% rate, respectively (Gleissner et al., 2002; Pane et al., 2002; Rieder et al., 1996) and it increases the risk of relepse. Conversely, p210[BCR-ABL] transcript also observed in pediatric and adult Ph+ ALL patients with 15-20% and 30-50% rate, respectively while almost all CML patients have this transcript (Melo, 1996; Okamoto et al., 1997; Pane et al., 2002; Rieder et al., 1996; Westbrook et al., 1992). Besides, p230[BCR/ABL] transcript is mostly seen in neutrophilic leukemia patients (Chan et al., 1987). In addition, *BCR-ABL1* variant e3a2 (exon 3 of BCR and exon 2 of ABL) is similar to p190[BCR-ABL] transcript also seen in some cases (Soekarman et al., 1990).

As a consequence of BCR/ABL translocation, BCR/ABL protein comprises the distinct domains from both BCR and ABL. N-terminal coiled-coil domain (CC; aa 1-63), a Ser/Thr kinase domain (phosphorylated tyrosine 177, Y177) contain a region for binding of adaptor protein growth factor receptor-bound protein 2 (GRB2) and ras homolog gene family/Guanine nucleotide exchange factors (Rho/GEF) kinase domain (amino acids 298–413) in *BCR* (Fielding et al., 2009; He et al., 2002; Maru & Witte, 1991)get together thesrc homology (SH) domains (SH1/SH2), a proline-rich domain, and DNA- and actin-binding domains of *ABL* (Z. J. Kang et al., 2016) (Figure 1.2b).

The N-terminal coiled-coil domain (CC) and Ser/Thr kinase domain (Y177) of BCR have critical role in the activation of ABL1 kinase (Pendergast, Gishizky, Havlik, & Witte, 1993; Zhang, Subrahmanyam, Wong, Gross, & Ren, 2001). For this reason imatinib which is the first generation tyrosine kinase inhibitor (TKI) targets the CC domain to reduce the BCR/ABL kinase activity through disrupting its tetramerization (Beissert et al., 2008; Preyer, Vigneri, & Wang, 2011).
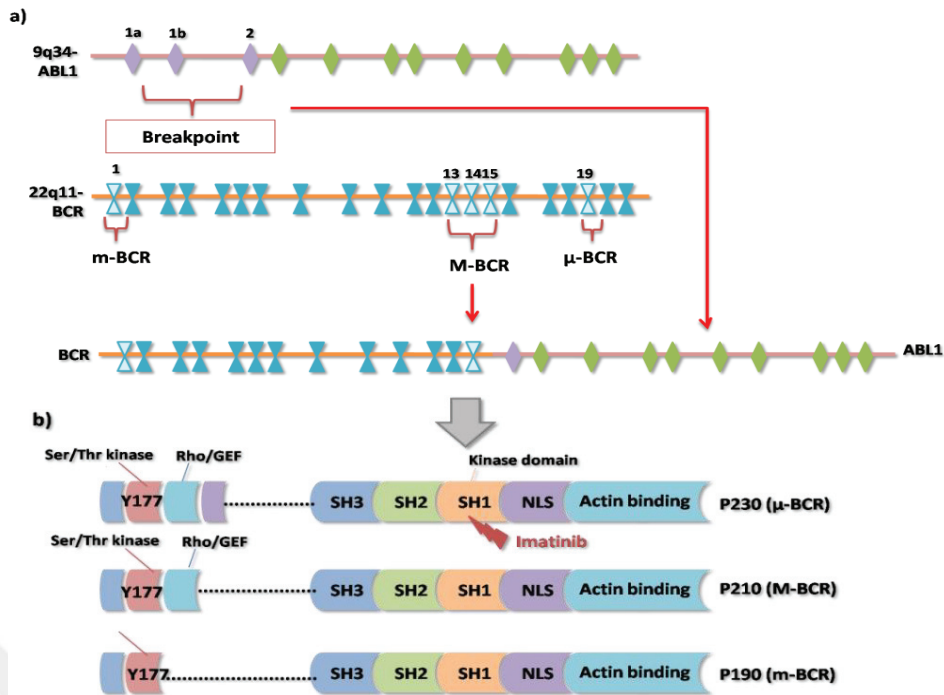
Figure 1.2. The translocation partners of Philadelphia chromosome: The breakpoint cluster region (*BCR*)-proto-oncogene tyrosine-protein kinase (*ABL1*) gene and protein. This figure was adapted from (Z. J. Kang et al., 2016).

On the other hand, Y177 is crucial for the leukemic cell proliferation, survival and progenitor expansion in CML. Mutation in GRB2-binding site of Y177 disallow the CML-like disease in $p210^{BCR-ABL1}$ as well as augments the imatinib sensitivity through inhibition of RAS and protein kinase B (PKB, also named AKT) activity (Chu, Li, Singh, & Bhatia, 2007). According to these results the prevention of tetramerization of BCR/ABL and targeting Y177 probably make a contribution to overcome imatinib resistance (Z. J. Kang et al., 2016).

Normally, ABL1 protein is found in low level during myeloid maturation in hematopoietic development whereas the autophosphorylation of activation loop through adenosine triphosphate (ATP) in SH1 domain acts as a switch between the inactive and active kinase structure (Dorey et al., 2001). When the SH2 domain blocks ABL1 activation the conformation named as "closed" while SH2 induces ABL1 activity through regulation of SH1 domain at C-terminus is "open" formation (W. Xu, Harrison, & Eck, 1997). Imatinib competitively bind the autophosphorylation site to prevent the binding of ATP and blocking the downstream BCR/ABL signaling pathways (Schindler et al., 2000).

1.1.3. Signaling Pathways in BCR/ABL Positive ALL

Aberrant tyrosine kinase activity of BCR/ABL fusion gene activates the signaling pathways that promote the cell proliferation, inhibits differentiation and cell death (Z. J. Kang et al., 2016; Sattler & Griffin, 2003) (Figure 1.3)

One of those pathways is JAK/STAT pathways. The activation of Janus kinase (JAK) 1-3 and also signal transducers and activation of transcription (STAT)1,3,5 and 6 are regulated by BCR/ABL in both CML and ALL (Frank & Varticovski, 1996; Ilaria & Van Etten, 1996). BCR/ABL1 kinase directly promotes the JAK2/STAT pathways which involve in cell growth and survival in CML while JAK1-3 activation requires an interaction between BCR/ABL and cytokine receptors (Tao, Lin, Sun, Samanta, & Arlinghaus, 2008; Warsch, Walz, & Sexl, 2013). JAK2 phosphorylates tyrosine 177 in Ser/Thr kinase domain of BCR/ABL and promotes the stability of BCR/ABL. On the other hand, inhibition of JAK2 does not affect on BCR/ABL although the phosphorylated Y177 is decreased (Samanta et al., 2011). Furthermore, JAK2 induces expression of oncogene c-Myc which has crucial role in BCR/ABL transformation (Sawyers, 1993; Xie, Lin, Sun, & Arlinghaus, 2002). The survivin which is a downstream gene of c-Mycalso is activated by JAK2/phosphatidylinositol 3-kinase (PI3K) signaling pathway (Fang et al., 2009). In addition, JAK2 induces the phosphorylation of STAT5 (p-STAT5) which is crucial for survival, growth and cell cycle process of both CML and lymphoid leukemic cells (Hoelbl et al., 2010).

Another important partner of STAT pathways, p-STAT3 was found as high level in imatinib resistant CML patients (Sayed, Badrawy, Gaber, & Khalaf, 2014)The STAT3 is regulated by BCR/ABL through phosphorylation of JAK1/2 and mitogen-activated protein kinase kinase (MEK) (Sayed et al., 2014). All together, JAK2 regulates the BCR/ABL stability as well as its oncogenic activity (Hoelbl et al., 2010).

Another signaling pathway regulated by BCR/ABL is the PI3K-AKT-mammalian target of rapamycin (mTOR) pathway and its downstream cascade in both Ph+ CML and ALL. The cells escape from cell cycle arrest through BCR/ABL independency of PI3K-AKT-mTOR pathway (Keeshan, Cotter, & McKenna, 2003). PI3K/mTOR contributes the BCR/ABL leukemogenesis and cell proliferation in mice with pre-B-ALL as well as PI3K and mTOR involves TKI resistance (Okabe et al., 2014). This studies performed by using dual inhibitor for both PI3K and mTOR, as a

consequence of the findings PI3K-AKT-mTOR pathway have a role in leukemogenesis by BCR-ABL1 and the PI3K inhibitors investigated for clinic(Barrett, Brown, Grupp, & Teachey, 2012). Unfortunately, clinical studies showed that the PI3K inhibitors are not useful for treatment strategies (Caino et al., 2015).
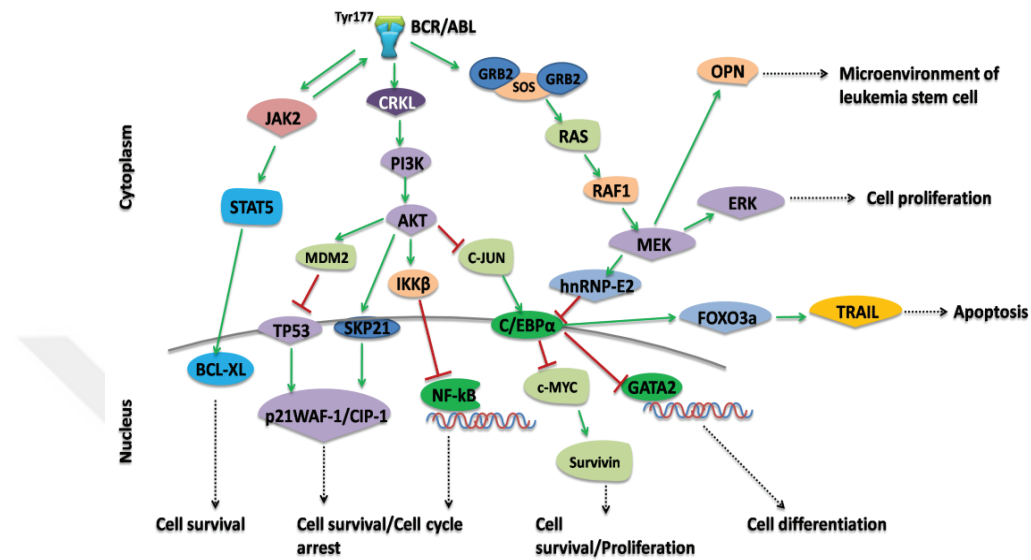
Figure 1.3. The pathways which are regulated by BCR/ABL are related to cell survival, cell proliferation, cell cycle, cell differentiation, and apoptosis. This figure was taken from (Z. J. Kang et al., 2016).

The activation of RAS/RAF/MEK/extracellular signal-regulated kinases (ERK) are regulated by BCR/ABL pathway cause uncontrolled proliferation Ph-positive CML and ALL (A. Jin et al., 2006; Mizuchi et al., 2005). The proliferative signals are promoted by RAS signaling which is activated by phosphorylation GRB2/GRB2-associated binding protein 2 (GAB2) at Y177 (Mandanas et al., 1993). Although the disruption of RAS signaling diminishes development of disease in CML, B-ALL development still become (Baum & Ren, 2008)This suggest that RAS signaling pathways can be target for CML pathogenesis in contrast to ALL.

BCR/ABL downregulates the Tumor necrosis factor (TNF)-related apoptosis-inducing ligand-TNFSF10 (TRAIL) which is a death receptor ligand in controlled cell death (Kuroda et al., 2013; Zhao et al., 1999). The imatinib treatment induces TRAIL-induced apoptosis suppress growth and inhibits cancer cell proliferation (Nimmanapalli et al., 2019; S. J. Park, Kim, Kim, Kang, & Kim, 2009; Raimondo et al., 2015).

1.1.4. Current Therapies in Ph + ALL Treatment

The treatment of Ph positive ALL patients contain combination of tyrosine kinase inhibitors and hyper-CVAD (hyper-fractionated cyclophosphamide, vincristine, doxorubicin, and dexamethasone [CVAD]) and stem cell transplantation to completely cure the patients (O. G. Ottmann & Pfeifer, 2009).

The wide range studies demonstrated that before the development of BCR-ABL tyrosine kinase inhibitors (pre-tyrosine kinase inhibitor era), the event-free survival (EFS) and 5- year overall survival (OS) rates of Ph+ ALL patients who treated with chemotherapy alone were significantly worse compared to Ph- patients even if Ph+ ALL patients ensured complete remission (CR) and Ph+ ALL are qualified as high risk group of ALL (Annino et al., 2002; Dombret et al., 2002; Gleissner et al., 2002; Moorman et al., 2007; Rieder et al., 1996; Rowe et al., 2005; Secker-Walker et al., 1997; X. Thomas et al., 1998; Westbrook et al., 1992). Moreover, the allogeneic hematopoietic cell transplantation (allo- HCT) was known as the best option for treatment of Ph+ ALL patients (Horowitz, Akasha, & Rowe, 2018). According to UKALLXII/ECOG 2993 study, patients who cured with allo-HCT showed considerately longer relapse-free survival (RFS) compared to patients treated with chemotherapy only(Fielding et al., 2009).Besides, the patients come up against some challenges such as age, lack of donor, other diseases.

Since developed tyrosine kinase inhibitors, the landscape of treatment changed. As a result of combination of the chemotherapy with the TKI, complete remission rate of newly diagnosed Ph positive ALL patients and their 3 years survival rate increased to 95% and 55% respectively (Yanada, Ohno, & Naoe, 2009).

1.1.4.1. Tyrosine Kinase Inhibitors

Tyrosine kinase inhibitors (TKI) have been developed to completely treat the Ph+ CML and ALL patients through targeting the BCR/ABL due to that the BCR/ABL is a main regulator molecule of disease prognosis.

Imatinib mesylate (Gleevec/Glivec; Novartis, Basel, Switzerland) is the first generation TKI is approved by Food and Drug Administration (FDA) in 2001 (Ribera, 2018). Constitutive activation of BCR/ABL protein forms when the adenosine triphosphate (ATP) binds to its binding domain. Imatinib competitively inhibits the activation of BCR/ABL protein by specifically binding of the ATP binding domain of BCR/ABL that is also result in inhibition of phosphorylation of BCR/ABL related pathways. In addition to inhibition of tyrosine kinase activity of BCR/ABL, imatinib also inhibits the c-kit and PDGFR tyrosine kinases (Druker et al., 2001).Although the combination of imatinib and classical chemotherapy show improve outcomes, patients can develop the resistance. The imatinib resistance may because of the mutations occur in ABL kinase domain including the gatekeeper mutations T3151 or F317L (Azam, Latek, & Daley, 2003), P-loop or activating loop mutations (N. P. Shah et al., 2002). After some of the patients who treated with imatinib did not response the treatment in first-lane therapy and developed the imatinib resistance, second and third generation TKIs was developed.

Dasatinib (Sprycel) which is a second generation TKI was approved by FDA in 2006 (Ribera, 2018). Dasatinib can bind both inactive and active form of BCR/ABL (Luo et al., 2006; O'Hare et al., 2005; Talpaz et al., 2006). It has been shown that dasatinib also inhibits other kinases such as SRC, c-KIT, ephrin A receptor kinases and PDGFRβ (O'Hare et al., 2005).

Another second generation TKI is nilotinib (Tasigna®; Novartis Pharmaceuticals, NJ, USA) which is an aminopyrimidine imatinib derivative was approved by FDA in 2007. Nilotinib also inhibits the c-KIT and PDGFR in addition to BCR/ABL inhibition (Saglio et al., 2010). Nilotinib competitively binds to inactive ABL kinase domain just as imatinib, but with high affinity (Bradeen et al., 2006).

Both dasatinib and nilotinib are more effective TKI than imatinib as 300 fold and 30-50 fold, respectively and they can overcome the nearly all mutations in BCR/ABL except the mutation threonine to isoleucine in codon 315 (T315I) (Bradeen et al., 2006; Daver et al., 2015; Luo et al., 2006; O'Hare et al., 2005; O. Ottmann et al., 2007; Saglio et al., 2010; Talpaz et al., 2006).

Ponatinib also known third generation tyrosine kinase inhibitor targets the T315I mutation was approved in 2016 (Ribera, 2018). Ponatinib is a pan-TKI just as dasatinib not only target BCR/ABL also inhibits the activity of other kinases including SRC, KIT (mast/stem-cell growth factor receptor), FLT3, RET (rearranged during transfection),

vascular endothelial growth factor receptor and as fibroblast growth factor receptor (Zhou et al., 2011).

Wide range studies demonstrated that the combination tyrosine kinase inhibitors and hyper-CVAD chemotherapy show good complete remission, overall survival and relapse free survival rates in newly diagnosed Ph+ ALL patients (Benjamini et al., 2014; Daver et al., 2015; Jabbour et al., 2015; Ravandi et al., 2010).

Although using TKIs in addition to classical chemotherapy is currently the most successful targeting treatment option for Ph chromosome positive leukemia, new strategies following genetic/epigenetic analysis are necessary for the patients who can develop resistance to TKIs or suffer from relapse.

1.1.4.2. Monoclonal Antibodies and Immunotherapy

Due to the fact that the chemotherapy regimens have some conflicts such as side effects, unsuccessful complete remissions, relapse or only cure some patient, new treatment strategies especially targeted therapies were needed. In addition to tyrosine kinase inhibitors which target BCR/ABL mutation, based on the surface markers of cancer cells antibody-based and cell-based strategies are developed and opened breakthrough new era for the treatment in recent years. For ALL treatment, antibody-based therapies involves the monoclonal antibodies such as rituximab, epratuzumab, alemtuzumab; the bi-specific T-cell engaging (BiTE[®]) antibody blinatumomab; and antibody-drug conjugate such as immunoconjugate inotuzumab ozogamicin antibodies while cell-based strategies include chimeric antigen receptor (CAR) T cells (Phelan & Advani, 2018; Portell & Advani, 2014).

The strategies based on the cell surface antigens of B-lymphoblast cells such as CD19, CD20, CD22 (Phelan & Advani, 2018; Wyatt & Bram, 2019).Antibody-based therapies target the tumor-specific antigens. Thus, the cancer cells and non-cancer cells are relatively separated (Wyatt & Bram, 2019). Monoclonal antibodies activates the antibody dependent cytotoxicity (ADCC), complement-dependent cytotoxicity or apoptosis directly following binding to their specific targets (Phelan & Advani, 2018).

CD20 which is expressed in malignant B lymphoblast cells as 30-50%related to poor prognosis and higher relapse rate (Hoelzer & Gokbuget, 2012; Phelan & Advani,

2018; Portell & Advani, 2014). CD20 involve in cell cycle progression, differentiation and apoptosis (Terwilliger & Abdul-Hay, 2017). Rituximab which is a first generated monoclonal humanized murine immunoglobulin G (IgG1) antibody targets the CD20+ cells (Portell & Advani, 2014; Terwilliger & Abdul-Hay, 2017). Phase studies showed that rituximab increased the overall survival and complete remission rate of patients when combined with hyper-CVAD chemotherapy regimen compared to patients treated with chemotherapy only (Hoelzer, Huettmann, & Kaul, 2010; Maury et al., 2016; Phelan & Advani, 2018; Portell & Advani, 2014; D. A. Thomas et al., 2010). Similar results were obtained from ofatumumab, obinutuzumaband REGN1979 which are another monoclonal antibodies effectively bind to different epitope of CD20 (Awasthi et al., 2015; Bazarbachi et al., 2018; Castillo, Milani, & Mendez-Allwood, 2009). The biallelic monoclonal antibody REGN1979 not only targets the CD20 also bind to CD3 which activates the T-cell immune response. These antibodies result in effective antibody-mediated cytotoxicity for the pre-B ALL, Ph- ALL or CLL (Terwilliger & Abdul-Hay, 2017). Obinutuzumab has been approved by FDA for the first-line CLL treatment, however for the pre-B ALL it should be studied (Phelan & Advani, 2018).

CD22 which is expressed as 90% in leukemic blasts of ALL patients is targeted by an unconjugated humanized monoclonal antibody, epratuzumab (N. N. Shah et al., 2015). Studies showed that epratuzumab enhance the chemotherapy and second remission in relapsed pediatric B-ALL patients compared to patients treated without epratuzumab (Raetz et al., 2015). Phase study of adult pre-B ALL patients with relapsed or refractory demonstrated that combination of clofarabine and cytarabine with epratuzumab enhance the therapy and complete remisson rate was significantly much more than therapy with clofarabine/cytarabine alone (Advani et al., 2014). Phase III studies of epratuzumab still ongoing (Phelan & Advani, 2018). Another CD22-targeted antibody is moxetumomab pasudodotox which is newly developed for treatment of both pediatric and adult ALL. Combotox which is a combination of anti-CD19 and anti-CD22 antibodies to treat the ALL patients with relapsed and refractory as well as epratuzumab (Terwilliger & Abdul-Hay, 2017). Moreover, the antibody – drug conjugate inotuzumab ozogamicin (InO) isa humanized monoclonal antibody targets CD22 antigens. InO attached to calicheamicin which is a cytotoxic agent through a nonimmunogenic linker. Calicheamicin induces dsDNA breaks and cell death(Hinman et al., 1993). Based on the phase studies showed that InO is a promising antibody and

enhance the overall survival rate of relapsed and refractory ALL patients, it has been approved by FDA in 2017 (Phelan & Advani, 2018).

CD19 is expressed in 90% of pre-B and mature ALL lymphoblasts and involved in activation of some signaling pathways such as the activation of c-myc, phosphorylation of src-family kinases and PI3K which are result in proliferation and differentiation (Chung et al., 2012; Fujimoto, Poe, Jansen, Sato, & Tedder, 1999; Otero, Omori, & Rickert, 2001). CD19 targeted by blinatumomab which is the first engineered antibody contains different regions of light and heavy chains of anti-CD19 and anti-CD3 which are connected through a non-immunogenic linker. Thus, this BİTEs not only bind to CD19-positive B cells also bind to CD3-positive cytotoxic T cells, thus the cytotoxic T cells are activated to inducing cell death (Phelan & Advani, 2018). According to studies, blinatumomab is seen as a promising strategy for Ph+ ALL patents with relapse or refractory combined with second generation tyrosine kinase inhibitors (Martinelli et al., 2017).Another CD19-targeted antibodies; coltuximab ravtansine (SAR3419), denintuzumab mafodotin (SGN-CD19A) and ADCT-402 conjugated-monoclonal antibodies have been used in phase studies to determine the therapeutic potential of these monoclonal antibodies for Ph-, Ph+ ALL patients with relapsed/refractory (Terwilliger & Abdul-Hay, 2017).

Moreover, CD52 targeted monoclonal antibody alemtuzumab has been investigated for the treatment of both T- and B- ALL and AML patients (Tibes et al., 2006). Besides, CD52 has found highly expressed in Ph positive ALL patients. Therefore, alemtuzumab can be attractive treatment option for Ph positive ALL patients however, development of alemtuzumab is slow (Portell & Advani, 2014).

Due to the fact that antibodies specifically bind to their antigens, monoclonal antibodies has been seen the best option in targeted treatment instead of classical strategies. According to several trials, ALL patients with relapsed/refractory treated more efficiently than only chemotherapy. Ongoing studies focused on the Ph+ ALL patients treated with current TKIs to eliminate the poor progression of patients through using monoclonal antibodies.

Another targeted strategy is chimeric antigen receptor (CAR) T cells which are genetically engineered T cells. T lymphocyte cells are obtained from patients' peripheral blood and genetically stimulate to transcribe receptors which target the antigen on the malignant cells, for instance CD19 on B-ALL, attached with other co-

stimulatory membrane proteins which attached the CD3 to activate the T cell (Portell & Advani, 2014; Rafei, Kantarjian, & Jabbour, 2019).

1.2. Sphingolipid Metabolism

Sphingolipids are one of the major lipid classes of eukaryotic cell membrane and were firstly identified by J. L. W. Thudichum in 1876 (Bartke & Hannun, 2009). Sphingolipids involve the cell membrane structure and modulate the fluidity and functions of membrane (Futerman & Hannun, 2004; Goni & Alonso, 2006). In addition to structural roles of sphingolipids in membrane, sphingolipids also contribute to several signaling pathways related to cell growth, cell proliferation, differentiation, survival, cell cycle, apoptosis and inflammation (Y. A. Hannun & Obeid, 2008; Simons & Ikonen, 1997; van Meer, Voelker, & Feigenson, 2008). Moreover, sphingolipids regulate the activities of transmembrane and peripheral membrane proteins (Lingwood & Simons, 2010).

Sphingolipids are *de novo* arises from serine and palmitoyl-CoA which are firstly convert to3-keto-dihydrosphingosinethrough serine palmitoyl transferase (SPT)in endoplasmic reticulum and then undergoes the dihydroceramide, ceramide, ceramide-1-phophate, sphingosine, sphingosine-1-phosphate, sphingomyelin and glucosylceramide by different enzymes that glycosylated, phosphorylated or add head group to ceramide (Figure 1.4) (Y. A. Hannun & Obeid, 2008).

Sphingolipids are defined by their characteristic long-chain sphingoid bases (18 carbon amino-alcohol backbone) in which the most common types are sphingosine, dihydrosphingosine (sphinganine) and phytosphingosine. This sphingoid base serve as a backbone which comprises the sphingolipids together with a fatty acid or head group attached the sphingoid backbone. Additions of either multifarious head group, distinct fatty acid based on the different chain lengths, introduction of a double bond(s), degree of saturation or hydroxylation of fatty acyl chain define the biological properties of sphingolipids (Gault, Obeid, & Hannun, 2010; Y. A. Hannun & Obeid, 2008; Lahiri & Futerman, 2007; Menaldino et al., 2003; Patwardhan, Beverly, & Siskind, 2016). The biological features of sphingolipids depend on their subcellular location, amount and the cell types (Patwardhan et al., 2016).
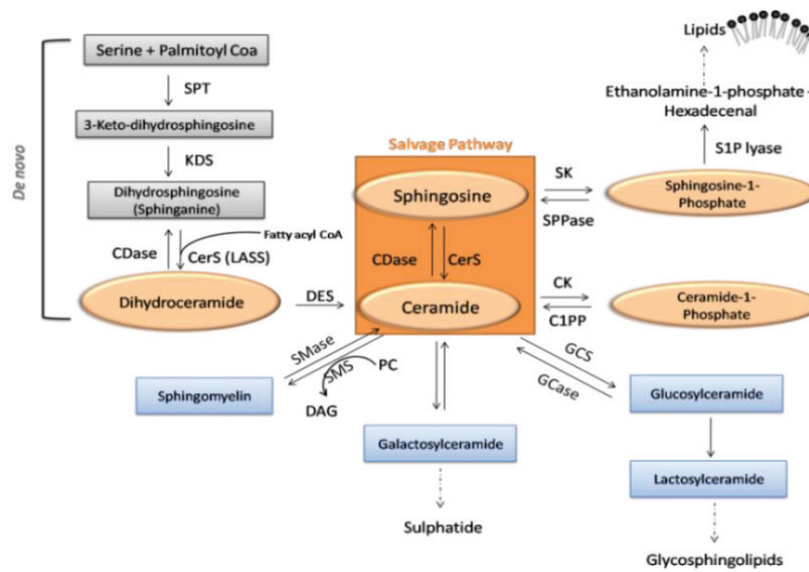
Figure 1.4. Sphingolipid metabolism. SPT, serine palmitoyl transferase; KDS, 3-keto-dihydrosphingosine reductase; CDase, ceramidase; CERS (LASS), ceramide synthase; SK, Sphingosine kinase; SPPase, Sphingosine phosphate phosphatase; DES, dihydroceramide desaturase; CK, Cer kinase; C1PP, Cer-1-phosphate phosphatase; SMase, sphingomyelinase; SMS, SM synthase; PC, phosphatidylcholine; DAG, diacylglycerol; GCS, glucosylceramidesynthase; GCase, glucosyl CDase. Orange partners of figure indicate the bioactive sphingolipids. This figure adapted from (Bartke & Hannun, 2009).
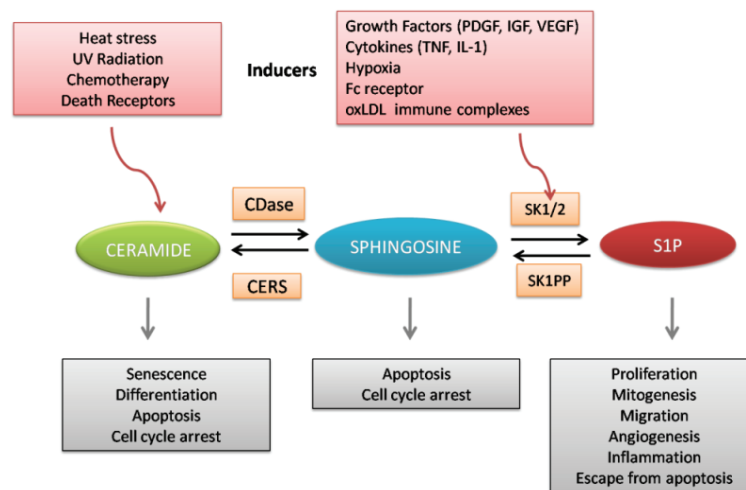
Figure 1.5. Sphingolipid rheostat. The biological processes in cells are regulated by ceramide, sphingosine and sphingosine-1-phospate in a harmony. CDase, ceramidase; CerS, ceramide synthase; SK1 /2, sphingosine kinase 1/2; S1P, sphingosine-1-phosphate. This figure is adapted from (Y. A. Hannun & Obeid, 2008).

Sphingolipid metabolism is a highly complex network whose partners interconnect and interconvert each other and each process might be in different subcellular localization (Yusuf A. Hannun & Obeid, 2017). The partners of sphingolipids are in harmony in cells, the balance between apoptotic and anti-apoptotic metabolits called as "Sphingolipid Rheostat" (Figure 1.5).When the harmony is broken through imbalances in sphingolipids level cause aberrant cellular mechanism that end up various disease including COPD, Alzheimer's disease, autoimmune diseases, asthma, diabetes, inflammatory bowel disease, chronic heart failure, sepsis, and cancer (Baranowski & Gorski, 2011; Kolter, 2011; Russo, Ross, & Cowart, 2013; van Echten-Deckert & Walter, 2012; Yang & Uhlig, 2011).

1.2.1. Bioactive Sphingolipids

Sphingolipid metabolism in which each pathway is a universe have been studied and reported in a wide range. One of the sphingolipids universes is bioactive sphingolipids. Bioactive sphingolipids such as ceramide (Cer), sphingosine, sphingosine-1-phosphate (S1P) and glycosylceramide (GlcCer) known as bioeffector molecules due to that they have a role as signaling molecules or second messengers in cells.

Bioactive sphingolipids play important roles in cell proliferation, apoptosis, cell migration, angiogenesis, senescence and drug resistance in cancer cells(Dressler, Mathias, & Kolesnick, 1992; Y. Hannun & Bell, 1987; Ogretmen & Hannun, 2004). Bioactive sphingolipids influence the particular proteins such as kinases, phosphatases, membrane receptors and other enzymes(Yusuf A. Hannun & Obeid, 2017). Therefore, sphingolipids-based cancer therapies are topical issue in current landscape (Shaw et al., 2018).

Ceramide is the central molecule of bioactive sphingolipids as both product and precursor of distinct bioactive sphingolipids (Bartke & Hannun, 2009). Ceramide comprise from sphingosine which is a fatty acyl chain with amide-linkage found in different length from C14 to C26 (Y. A. Hannun & Obeid, 2011; Ponnusamy et al., 2010; Saddoughi, Song, & Ogretmen, 2008). Ceramide is synthesized from at least two distinct pathways: one of those is de novo synthesis of ceramide either from sphingosine

through ceramide synthase (CerS) named as salvage pathway (Kitatani, Idkowiak-Baldys, & Hannun, 2008; Pewzner-Jung, Ben-Dor, & Futerman, 2006) or from sphinganine through LASS genes/CerS genes(Y. A. Hannun & Obeid, 2002; Linn et al., 2001). Another pathway is catabolism of complex lipids especially sphingomyelin to ceramide (Bartke & Hannun, 2009; Ogretmen & Hannun, 2004).

Ceramides contribute and regulate the programmed cell death chemotherapeutic drug and radiation sensitivity, cellular stress, cell cycle arrest, autophagy and drug resistance related signaling pathways (Cruickshanks et al., 2015; Nganga, Oleinik, & Ogretmen, 2018; Obeid, Linardic, Karolak, & Hannun, 1993; Patwardhan et al., 2016). Accordingly, ceramides known as tumor suppressor lipids and can be potential biomarkers or targets for treatment of diseases especially cancer (S. Brachtendorf, El-Hindi, & Grosch, 2019; Kurz, Parnham, Geisslinger, & Schiffmann, 2019; J. W. Park, Park, & Futerman, 2014; Saddoughi & Ogretmen, 2013). These physiological and pathophysiological specific roles of ceramides are determined by their acyl chain lengths in cell (Grosch, Schiffmann, & Geisslinger, 2012; Saddoughi & Ogretmen, 2013). Ceramide turns into sphingosine which is then converted to sphingosine-1-phosphate by phosphorylation through sphingosine kinase-1 and -2 enzymes (Saddoughi & Ogretmen, 2013) in Golgi apparatus. Hereby ceramide is transported from ER to Golgi by ceramide transporter protein, CERT (Hanada, Kumagai, Tomishige, & Yamaji, 2009). In contrast to ceramide, sphingosine-1-phosphate promotes cell survival, proliferation, invasion, migration and drug resistance (Ogretmen & Hannun, 2004) (Figure 1.5).

1.2.2. Ceramide Synthases

Six mammalian genes named longevity-assurance homolog (LASS1-6)/ Cer synthase (CerS1-6) encode for ceramide synthase proteins(Bartke & Hannun, 2009). Several studies showed that the substrate specificities of sphingosine N-acyl transferase known as ceramide synthases by using normal-phase thin-layer chromatography approach: CerS1 generates C18 ceramide (Venkataraman et al., 2002), CerS2 generates C22–C26 cermide (Laviad et al., 2008), CerS3 generates C18–C20 ceramide (Mizutani, Kihara, & Igarashi, 2006), CerS4 generates C18–C20 ceramide (Riebeling, Allegood,

Wang, Merrill, & Futerman, 2003), CerS5 generates C16 ceramide (Riebeling et al., 2003) and CerS6 generates C14–C16 ceramide (Luttgeharm, Cahoon, & Markham, 2015; Mizutani, Kihara, & Igarashi, 2005).

These acyl chain specificity of ceramide synthases are determined by eleven residues in between the last two putative transmembrane domains (TMDs) of the CerS (Tidhar et al., 2018). The mammalian CerS expression changes depend on cell types and development. The tissue distribution and properties of mammalian ceramide synthaseswere shown in Figure 1.6 (Levy & Futerman, 2010; Mullen, Hannun, & Obeid, 2012).

CerS gene	Location on Chromosome	Gene Size	Protein Size (Da)	Acyl Chain Length Specificity
CerS1	19p12	25,837	39,536	C18
CerS2	1q21.2	9,792	44,876	C20-C26
CerS3	15q26.3	144,326	46,217	C22-C36
CerS4	19p13.2	53,046	46,399	C18-C20
CerS5	12q13.3	37,565	45,752	C16
CerS6	2q24.3	318,394	44,890	C14 and C16
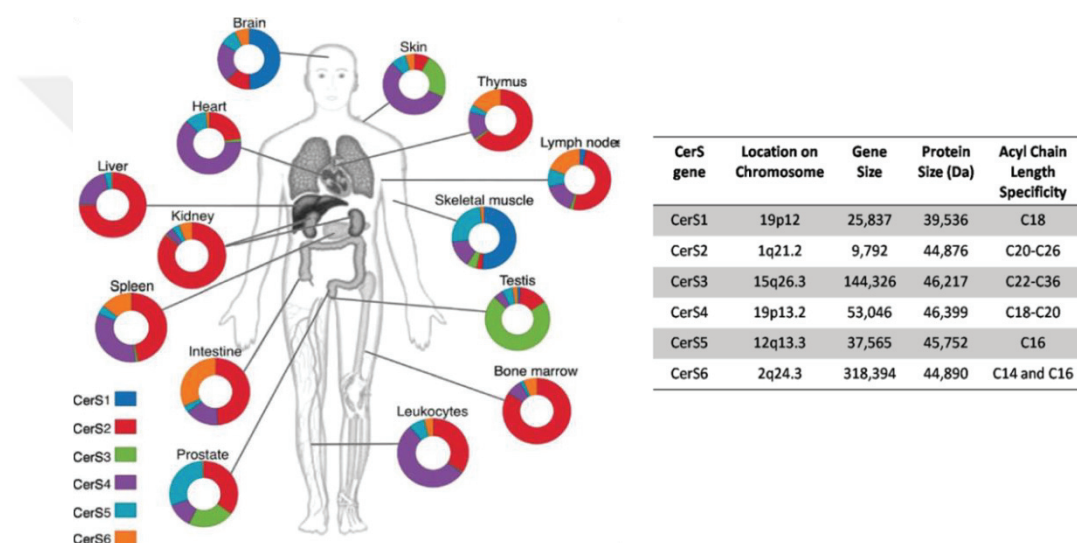
Figure 1.6. The tissue distribution and properties of ceramide synthase genes. This figure is adapted from (Levy & Futerman, 2010).

Our previous studies showed that dasatinib and imatinib treatment increase the CERS genes mRNA level and leads to apoptosis in K562 cells whereas S1P generation enhanced in imatinib-resistance K562 cells (Baran et al., 2007; Gencer Akcok, Ural, Avcu, & Baran, 2011) as well as docetaxel induces the LASS genes expression in prostate cancer (Bassoy & Baran, 2012). Moreover, the increment in LASS genes expression in resveratrol-induced apoptosis of HL60 cells also shown previously by our group (Cakir, Saydam, Sahin, & Baran, 2011).

CERS1 (also known as *LASS1*) mainly expressed in human skin, brain and skeletal muscle and generates the C18-ceramide. Studies demonstrated that *CERS1* overexpression elevates C18-ceramide that result in cell death in head and neck cancer cells (HNCC). Normally, *CERS1* and C18-ceramide highly expressed in healthy tissues

comparing with cancer cells (Koybasi et al., 2004; Senkal et al., 2007). Besides, the overexpression of CERS1 increases the C18-ceraide leads to autophagy in glioma cells (Z. Wang et al., 2017) as well as the relation between overexpression level of *CERS1* and its product C18-ceramide and lethal mitophagy, which is an autophagy subtype characterized with damaged mitochondria, has been shown in several studies. According to these studies elevated CERS1/C18-ceramide level leads to mitophagy in AML (Dany et al., 2016) and HNSCC (Sentelle et al., 2012) following treatment.

CERS2 (also known as *LASS2*) is mostly expressed in kidney, liver, lung, brain, breast, heart, adipose tissues and peripheral blood leukocytes and generates the long chain ceramides from C20 to C26. Low level of CERS2 related to tumor progression and poor prognosis in hepatocellular carcinoma patients (Ruan et al., 2016). According a study, CERS2 overexpression related to less metastasis ability in breast cancer patients and it proved that *CERS2* mRNA and protein level was found in MCF-7 cells more than MDA-MB-231 which has more invasion and migration ability than MCF-7. Besides, the expression of CERS2 regulates the invasion and metastasis ability of breast cancer cells through regulating V-ATPase activity and MMP-2 and -9 (Fan et al., 2015). On the other hand, CERS2 downregulation increased C16 ceramide level and enhance the apoptosis in HeLa cells following cisplatin/UV radiation application (Sassa, Suto, Okayasu, & Kihara, 2012). Besides a study showed that CERS2 downregulation decreased the migration ability of bladder cancer cells (Aldoghachi et al., 2019) and controversial result obtained from another study, migration ability of bladder cancer cells enhanced when CERS2 expression downregulated (H. Wang et al., 2017).

CERS3 (also known as *LASS3*) mostly expressed in testis tissues and skin however, its expression is limited in other tissues and generates different ceramides from C18- to C26- ceramide (S. Brachtendorf et al., 2019). However, the knowledge about the role of CERS3 is limited; there is no significant relation between CERS3 and cancer in the literature.

CERS4 (also known as *LASS4*) mostly expressed in almost all human tissues with low level however, CERS4 highly expressed in testis tissues and generates the C18 and C20 ceramide(S. Brachtendorf et al., 2019). CERS4 highly expressed in cancerous cells such as liver cancer (J. Chen et al., 2017) and ER positive breast cancer (Schiffmann et al., 2009). On the other hand high expression level of CERS4 decreased the proliferation and induced apoptosis in colon cancer and breast cancer tissues (Hartmann et al., 2012). Moreover decreasing CERS4 expression in HNSCC and renal

cell carcinoma patients enhance migration ability of liver cancer cells in vitro and metastasis ability of mammary cancer cells to liver *in vivo* (Gencer et al., 2017).

CERS5 (also known as *LASS5*) is mostly expressed in human brain and generates mainly C14- and C16 ceramides. According to studies CERS5 was found highly expressed in breast cancer tissues (Wegner et al., 2014) and colorectal cancer patients (Fitzgerald et al., 2014), CERS5 enhanced the cell proliferation and decreased the overall survival of patients. On the other hand after drug and ionizing radiation CERS5 expression increased and triggered C16-ceramide that result in apoptosis in breast cancer (J. Jin et al., 2009) and cervix cancer cells (Mesicek et al., 2010), respectively. Besides irradiation increased the expression of CERS5 in leukemia cells that result in p53 activation (Panjarian et al., 2008). Likewise, another study showed that p53 controls the response of CERS5 to chemotherapy in colon cancer cells (Sebastian Brachtendorf et al., 2018).

CERS6 (also known as *LASS6*) is expressed almost in all tissues and generates the C14- and C16-ceramides. CERS6 known as oncoprotein due to the fact that CERS6 expression highly elevated in cancer cells especially, invasive and metastatic cancer cells including breast cancer (Edmond et al., 2015; Erez-Roman, Pienik, & Futerman, 2010; Schiffmann et al., 2009). CERS6 overexpression significantly related to carcinogenesis, poor prognosis and survival in gastric cancer in both in vitro and in vivo. Moreover, suppressing of CERS6 suppressed the cell proliferation and enhanced the cell cycle arrest. Depletion of CERS6 repressed cell cycle regulators cyclins A, B, CDK1, and the JAK2/STAT3 signaling pathway as well as silencing CERS6 decreased the migration and invasion of gastric cancer cells whereas accelerated CER6 expression promoted the invasion and migration (Uen et al., 2018).Moreover, downregulation of CERS6 sensitizes the ALL cells to ABT-737 drug through regulation of CD95/Fas-associated protein with death domain (FADD) whereas overexpression of CERS6 prevented the drug-related apoptosis in ALL cells (Verlekar, Wei, Cho, Yang, & Kang, 2018). Conversely, CERS6 positively regulates the drug resistance in cancer cells. For instance, CERS6 expression level was found fewer in cisplatin-resistant oral squamous cell carcinoma (OSCC) and activates the autophagy whereas CERS6 expression related to apoptosis in cisplatin-sensitive OSCC cells. After transfection of cisplatin-resistant OSCC cells with lentivirus of CERS6 gene, these cells sensitized to cisplatin and apoptosis was enhanced. These results were also confirmed in xenograft mice model (S. Li, Wu, Ding, Yu, & Ai, 2018).

1.2.3. Sphingosine Kinase -1 and -2

Sphingosine Kinase -1 and -2 (SK-1 and -2) are enzymes which are responsible for the conversion of ceramide to S1P by phosphorylation of sphingosine (Saddoughi & Ogretmen, 2013). The studies demonstrated that increased levels of SK1 and SK2 related to poor prognosis and accelerated proliferation of cancer cells.

A microarray study that performed in tissue samples of different types of breast cancer patients demonstrated that *Sphingosine kinase-1* is highly expressed in ER-negative tissues whereas the dihydroceramidsynthases (*LASS4, LASS6*) and glucosylceramidsynthase (*GCS*) were higher in ER-positive tissues. Moreover, high expression level of SK-1 was related to poor outcome of patients (Ruckhaberle et al., 2008). Another study showed that high expression level of SK-1 related to gemcitabine-resistance in pancreatic cancer cells and up-regulating ceramide level or down-regulating SK-1 level sensitizes the pancreatic cancer cells to gemcitabine-induced cell death. The *SK-1* expression level also found as highly expressed in pancreatic adenocarcinoma tissues (Guillermet-Guibert et al., 2009). Another study showed that mRNA and protein level of *SK-1* were highly expressed in gastric cancer cells and tissues that related to poor prognosis and survival of gastric cancer patients (W. Li et al., 2009). Another recent study indicated that the expedited replicative cellular senescence was related to decreased transcription of SK-1 (Kim et al., 2019).

A study showed that the inhibition of SK-2 reduces cell viability and proliferation, promotes caspase-dependent apoptosis through inhibition of Myc expression in ALL cells. Moreover, the contribution of SK-2 to ALL development was shown in immunodeficient mice (Wallington-Beddoe et al., 2014)

1.2.4. Glycosylceramide Synthase

Our group previously showed that nilotinib induces apoptosis through increasing expression level of LASS genes while decreasing SK-1 and GCS expression that result in *de novo* ceramide generation and accumulation in chronic myeloid leukemia cells. Besides, ceramide generation related to sensitivity of CML cells to nilotinib as well

(Camgoz, Gencer, Ural, Avcu, & Baran, 2011). Another study demonstrated that rising level of ceramide by ceramide analogs and decreasing level of UDPglucose ceramide glucosyltransferase (UGCG) by siRNA sensitizes breast cancer cells to chemotherapy (Che, Huang, Xu, & Zhang, 2017). Another study showed that the inhibition of GCS sensitizes the P53-mutant-ovarian cancer cells to doxorubicin and reactivates the P53-mediated apoptosis in these cells (Y. Y. Liu et al., 2011).

The studies implicated the crucial role of bioactive sphingolipids in tumorigenesis, cancer progression and drug-resistance as well as cellular processes like proliferation, differentiation, apoptosis and senescence; development of novel therapeutics to target bioactive sphingolipids became important for current treatment strategies. Therefore, inhibitors of GCS, SK , AC, S1PR, CK were developed with purpose to downregulates the proliferation whereas the aim of development of synthetic ceramide analogs upregulates the apoptosis in cancer (Adan-Gokbulut, Kartal-Yandim, Iskender, & Baran, 2013).

In addition to bioactive sphingolipids inhibitors, the effects of natural compounds on bioactive sphingolipids metabolism have been studied. For instance, a study showed that combination of radiation and resveratrol induces cell death through increasing ceramide level in prostate cancer (Scarlatti et al., 2007). Our previous study showed that resveratrol induces apoptosis and regulates the bioactive sphingolipids genes in HL-60 AML in a dose dependent manner (Cakir et al., 2011) and a supportive study showed that resveratrol induces apoptosis through regulation of SK-1 pathway in K562 CML cells (Tian & Yu, 2015). Another flavonoid genistein also inhibits the growth and induces apoptosis in melanoma cells (Ji et al., 2012).

1.3. Flavonoids

When the fruits, vegetables and traditional plants have been discovered to contain certain compounds which can be used for treatment of distinct diseases including cancer, the studies in that area have been accelerated to understand the properties of them in twenty century. Several *in vitro* and *in vivo* studies showed that the compounds which are known as "phytochemicals" in nowadays, have the anti-oxidation, anti-inflammation and anti-carcinogenic features. Flavonoids, one of the

phytochemicals, are polyphenol secondary metabolites of plants and have an important position in human diet. Up to now, approximately 10000 flavonoids are described as the anti-oxidant, prooxidant, anti-inflammatory, anti-viral/bacterial, anti-diabetic, cardio protective, anti-cancer, anti-aging (Prochazkova, Bousova, & Wilhelmova, 2011).

1.3.1. Luteolin
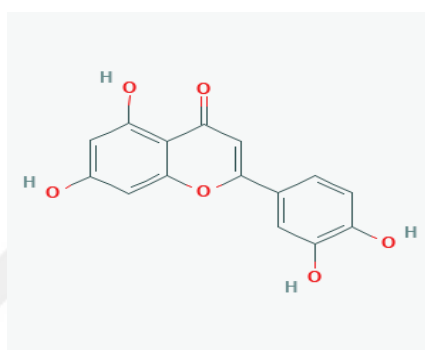
Figure 1.7. Chemical structure of luteolin. This figure was taken from PubChem, NCBI (PubChem).

Luteolin also known as 3',4',5,7-tetrahydroxyflavone is mostly studied type of flavones and has antioxidant activity (K. A. Kang et al., 2017). Likewise, other flavonoids, luteolin play role in pathogenesis of several diseases including cancer through regulating the signaling pathways. The chemical structure of luteolin was shown in Figure 1.7.

1.3.2. Luteolin and Cancer

Anti-cancer effects of luteolin on cell lines, tumor tissues or mouse models of different cancer types have been investigated in a wide range. In this part, the recent studies about anti-cancer effects of luteolin on various cancer types including leukemia were reviewed.

Several studies have been demonstrated that luteolin inhibits cell proliferation and growth in various cancer types such as breast cancer (Cook, Liang, Besch-Williford, & Hyder, 2017), prostate cancer(Han et al., 2016), pancreatic cancer(Z. Li, Zhang, Chen, & Li, 2018), non-small cell lung cancer cells, (Yu et al., 2019), esophageal carcinoma (P. Chen et al., 2017), and hepatocellular carcinoma (Im, Yeo, & Lee, 2018; Lee & Kwon, 2019), human placental choriocarcinoma cells (Lim, Yang, Bazer, & Song, 2016) and melanoma (C. Li, Wang, Shen, Wei, & Li, 2019) with dose and time dependently.

Luteolin induces apoptosis through intrinsic and/or extrinsic apoptotic pathways in several cancer types including hepatocellular carcinoma (Im et al., 2018; Lee & Kwon, 2019), colon cancer (K. A. Kang et al., 2017), esophageal carcinoma (P. Chen et al., 2017), gliomablastoma (Q. Wang, Wang, Jia, Pan, & Ding, 2017), cholangiocarcinoma cells (Kittiratphatthana, Kukongviriyapan, Prawan, & Senggunprai, 2016) and human placental choriocarcinoma cells (Lim et al., 2016). Luteolin down regulated the mitochondrial membrane potential that leads to apoptosis in esophageal carcinoma (P. Chen et al., 2017) and gliomablastoma (Q. Wang, H. Wang, Y. Jia, H. Pan, et al., 2017) in both *in vitro* and *in vivo*. Although luteolin promoted caspase-dependent apoptosis through preventing AKT/osteopontin pathway in human hepatocellular carcinoma cells, luteolin has low toxic effect on mouse normal hepatocyte cells (Im et al., 2018). Studies showed the low toxic effect of luteolin on normal mouse vascular endothelial cells (VECs) (Q. Wang, H. Wang, Y. Jia, H. Pan, et al., 2017) and normal human colon FHC cells (K. A. Kang et al., 2017) as well. A recent study demonstrated that luteolin inhibited cell proliferation and induced both apoptosis and autophagy through endoplasmic reticulum stress in P53-null Hep3B hepatocellular carcinoma cells (Lee & Kwon, 2019). Hadi et al. 2015, demonstrated that luteolin induces apoptosis through increasing endogeneous ceramide level in colon cancer cells Caco-2. Moreover, luteolin inhibits the both expression and activity of SK-1 and -2 that leads to sphingosine-1-phosphate reduction (Abdel Hadi et al., 2015).

In addition to anti-proliferative and apoptotic effects of luteolin, anti-migration, anti-invasion and anti-metastatic effects of luteolin in various cancer types was also shown in both *in vitro* and *in vivo*. For instance, luteolin prevents migration and lung metastasis ability of triple-negative breast cancer cells(Cook et al., 2017) while luteolin inhibits the migration and invasion through upregulating miR‑384/pleiotrophin axis in colorectal cancer cells (Y. Yao, Rao, Zheng, & Wang, 2019). Luteolin inhibits the

invasion and metastasis through down regulation of matrix metalloproteases (MMPs) in glioblastoma cells (Q. Wang, H. Wang, Y. Jia, H. Ding, et al., 2017), melanoma cells (X. Yao, Jiang, Yu, & Yan, 2019), pancreatic cancer cells (X. Huang et al., 2015). Various studies showed that luteolin downregulates or inhibits epithelial-mesenchymal transition (EMT) in colorectal cancer (Y. Liu et al., 2017), triple-negative breast cancer (Lin et al., 2017), pancreatic cancer (X. Huang et al., 2015), glioblastoma cells (Q. Wang, H. Wang, Y. Jia, H. Ding, et al., 2017), gastric cancer (Zang et al., 2017) and melanoma (C. Li et al., 2019).

Luteolin regulates signaling pathways not only genetically but also epigenetically regulates in cells. For instance, luteolin extinguished cell proliferation and cellular transformation colorectal cancer cells through decreasing methylation of Nuclear factor erythroid 2- related factor 2 (Nrf2) promoter in a dose-dependent manner as well. Moreover, protein level and enzymatic activity of DNA methyltransferases (DNMTs) and histone deacetylases (HDACs) was decreased by luteolin in a dose-dependent manner as well (Zuo et al., 2018).This study recently supported that luteolin increased Nrf2 expression through repression DNA methyltransferases expression and augmentation ten-eleven translocation (TET) DNA demethylases activation in colon cancer. Moreover, the interaction between Nrf2 and P53 that involved in the apoptotic effect of luteolin on colon cancer was shown (K. A. Kang et al., 2019). Besides, various concentration exposure of luteolin leads to Fas/FasL-mediated apoptosis via increasing acetylation of histone H3 and increasing level of nuclear accumulation of c-Jun in human HL-60 leukemia cells (S. W. Wang et al., 2018).

In classical chemotherapy, patients can develop resistance to chemotherapeutic drugs. In that point, opening a new window to overcome the drug resistance is important phenomenon in cancer therapy. It has been documented; luteolin does not only reverse drug resistance but also enhance the therapeutic effects of chemotherapeutic drugs on cancer cells. For instance, a recent study indicated that luteolin sensitizes the drug-resistant cells against chemotherapeutic drugs in ovarian cancer (H. Wang, Luo, Qiao, Wu, & Huang, 2018). Luteolin enhanced anti-proliferative and apoptotic effect of cisplatin onto cisplatin-resistance ovarian cancer cells as well as inhibiting the migration and invasion ability of ovarian cancer cells. Besides, luteolin enhanced the anti-tumor effect of cisplatin in xenograft in vivo model (H. Wang et al., 2018). Another study demonstrated that luteolin leads to apoptosis in colorectal carcinoma cells which were arrested at G0/G1 by chemotherapeutic drug oxaliplatin

(Jang, Moon, Oh, & Kim, 2019). Furthermore, cell viability and EMT was downregulated by luteolin in paclitaxel-resistant ovarian cancer cells (Dia & Pangloli, 2017). Another study showed that luteolin synergistically enhance the anti-cancer effect of 5-fluorouracil (5-FU) on human hepatocellular carcinoma cells (H. Xu et al., 2016).

1.4. Aim of Project

Although the current treatment strategies for Ph positive ALL include the targeting BCR/ABL; complete remission, overall survival and mortality of Ph+ ALL patients are still worse compared to Ph- ALL patients. Therefore, new strategies combined with current treatments are needed for Ph+ ALL patients who are qualified as high risk group of ALL.

Due to that the bioactive sphingolipids regulates the several biological processes in cells, they considered as therapeutic target. Besides, some studies showed that flavonoids contribute the bioactive sphingolipids-based cell death or suppression/inhibition of cell proliferation in cancer cells. Only one study showed that luteolin induces apoptosis through increasing endogeneous ceramide level in colon cancer cells. Moreover, luteolin inhibits the both expression and activity of SK-1 and -2 and thereby resulting in the reduction of S1P (Abdel Hadi et al., 2015).

According to this background information, we hypothesized that luteolin might have cytotoxic, apoptotic and cytostatic effects on Philadelphia chromosome positive acute lymphoblastic leukemia cells. Besides, luteolin might regulate the bioactive sphingolipids genes in possible therapeutic potential of luteolin.

In this study, the cytotoxic, apoptotic and cytostatic effects of luteolin on Philadelphia chromosome positive acute lymphoblastic leukemia cells were determined for the first time. Moreover, the roles of bioactive sphingolipids genes in therapeutic potential of luteolin on Ph positive ALL cells was investigated for the first time as well.

CHAPTER 2

MATERIALS AND METHODS

2.1. Materials

2.1.1. Cell Lines

SD-1 cells, Philadelphia chromosome + ALL (Ph+ ALL) cells were obtained from German Collection of Microorganisms and Cell Cultures, Germany.

10 μM imatinib resistance SD-1 cells referred as SD-1R were generated by Dr. Yağmur KİRAZ in our laboratory.

Normal lymphoblast HCC1937 BL cell line was provided from Lisa Wiesmuller, Department of Obstetrics and Gynecology, University of Ulm, Germany.

Normal epithelial lung BEAS-2B cell line was used from stocks in our laboratory. BEAS-2B cell line was obtained from American Type of Culture Collection, USA.

2.1.2. Luteolin

Luteolin was obtained from Santa Cruz Biotechnology, USA. The stock solution of Luteolin was prepared as 10 mM with sterile DMSO under dark and stored at – 20ºC.

2.1.3. Chemicals

RPMI Media 1640, heat inactivated fetal bovine serum (FBS), Dulbecco's phosphate buffer saline (PBS) 10X, RNase/Dnase free water were obtained from Gibco,

Thermo Fischer Scientific, USA. PBS 10X was diluted with distilled water and used as PBS 1X and stored at both room temperature and +4 ºC. FBS was aliquated as 15 mL and stored at -20 ºC.

Penicillin/Streptomycin, L-glutamine, Trypsin-EDTA and Prestained Standard protein marker were obtained from EuroClone, Germany. Both Penicillin/Streptomycin and L-glutamine were aliquated as 10 ml and stored at -20 ºC as well as Prestained Standard protein marker.

*Dimethyl sulfoxide (*DMSO), Tween-20, Ethidium bromide, 3-(4, 5-Dimethylthiazol-2-yl)-2-5-diphenyltetrazolium bromide (MTT) powder and Trypan blue powder were obtained from Sigma Aldrich, USA. DMSO was stored at room temperature. MTT stock solution was prepared as 5 mg/ml in 1X PBS and stored at -20 ºC. Trypan blue was prepared as 0,4% in PBS 1X and stored at room temperature.

Annexin V-FITC, Annexin V binding solution and Propidium Iodide (PI) were obtained from BioLegend, USA. Dyes and solution were stored at +4 ºC.

JC-1 mitochondrial membrane potential kit was obtained from Cayman Chemical, USA. Kit was stored at -20 ºC.

NucleoSpin RNA isolation kit was obtained from Macherey-Nagel, Germany. Kit was stored at +4 ºC.

RevertAid first strand cDNA synthesis kit, Taq DNA polymerase kit, DyNAmo HS SYBR Green qPCR kit, 6X loading dye, 50 kb Gene Ruler, Pierce™ BCA Protein Assay Kit were obtained from Thermo Ficher Scientific, USA. Except Pierce™ BCA Protein Assay Kitall kits were stored at -20 ºC.

Tris- Acetate- EDTA (TAE) 10 X was obtained from Vivantis Technologies, Malaysia. Chemical was stored at room temperature.

BSA powder was obtained from Santa Cruz Biotechnology, USA and was stored at +4 ºC.

Sodium Chloride (NaCl), Tris-hydrochlorid, NP-40, Triton X-100 were obtained from AppliChem GmbH, Germany. Chemicals were stored at room temperature.

Blotting-grade blocker (Non-fat dry milk), Ammonium Persulfate, Laemmli 4X buffer, β-mercaptoethanol, TEMED, 10X TGS buffer for SDS-PAGE, Mini-PROTEAN TGX Stain-Free Gels, 10% TGX Stain-Free FastCast Acrylamide Kit, Trans-Blot Turbo 5X Transfer Buffer, Trans-Blot Turbo Mini-Size PDVF Membrane, Trans-Blot Turbo Mini-Size Transfer Stacks, 10X TBS (Tris-Buffered Saline), Clarity™ Western ECL Substrate were obtained from Bio-Rad, USA.

2.1.4. Primers

Ceramide synthase (CERS)-1, -2, -4, -5, -6; Sphingosine kinase (SK-1, and -2) and β-actin primers were obtained from Sentebiolab Biotech, TURKEY. Sequences of primers were designed by using NCBI Primer Blast Tool. Primers used in this study showed in Table 2.1.

Table 2.1. Sequences forward and reverse primers used in this study.

Primers	Sequence
CERS 1 Forward	5'- ACGCTACGCTATACATGGACAC -3'
CERS 1 Reverse	5'- AGGAGGAGACGATGAGGATGAG -3'
CERS 2 Forward	5'- AGTAGAGCTTTTGTCCCGGC -3'
CERS 2 Reverse	5'- GCTGGCTTCTCGGAACTTCT -3'
CERS 4 Forward	5'- CTTCGTGGCGGTCATCCTG -3'
CERS 4 Reverse	5'- TGTAACAGCAGCACCAGAGAG -3'
CERS 5 Forward	5'- TCAGGGGAAAGGTATCGAAGG -3'
CERS 5 Reverse	5'- CTGCCTCCCATGTGACCATT -3'
CERS 6 Forward	5'- GGGATCTTAGCCTGGTTCTGG -3'
CERS 6 Reverse	5'- GCCTCCTCCGTGTTCTTCAG -3'

2.1.5. Antibodies

The antibodies used in this study and their brands, dilutions and secondary antibodies are showed in Table 2.2.

Table 2.2. Dilutions and brands of primary antibodies and their secondary antibodies used in this study.

First Antibody	Dilution	Brand	Secondary antibody	Dilution
SK-1	**1:1000**, in 5% non fat dry milk in TBST-20	Abcam	Anti-rabbit, Biorad	**1:2000**, in 5% non fat dry milk in TBST-20
SK-2	**2 μg/ml,** in 5% non fat dry milk in TBST-20	Sigma Aldrich	Anti-mouse, Biorad	**1:2000**, in 5% non fat dry milk in TBST-20
GCS	**2 μg/ml,** in5% non fat dry milk in TBST-20	Sigma Aldrich	Anti-mouse, Biorad	**1:2000**, in 5% non fat dry milk in TBST-20
ABL	**1:1000**, in 5% non fat dry milk in TBST-20	Santa Cruz	Anti-mouse, Biorad	**1:2000,** in 5% non fat dry milk in TBST-20
GAPDH	**1:15000**, in 5% non fat dry milk in TBST-20	Proteintech	Anti-mouse, Biorad	**1:3000**, in 5% non fat dry milk in TBST-20

2.2. Methods

2.2.1. Cell Culture Conditions

SD-1, SD-1R and HCC1937 BL cells were maintained as $0,3-0,5 \times 10^6$ cells/ml in RPMI medium that contains 15% heat-inactivated fetal bovine serum (HI-FBS), 1% L-glutamine and 1% Penicillin-Streptomycin in 75 cm^2 tissue culture flasks. For SD-1R cells, 10 μM imatinib was added to flask to maintain the resistance. When the cell number reached to $1-1,5 \times 10^6$ cells/ml, cells were cultured.

BEAS-2B cells were maintained in DMEM high glucose medium which contains 10% fetal bovine serum (FBS), 1% L-glutamine and 1% Penicillin-Streptomycin in 75 cm^2 tissue culture flasks. Cells were cultured when their confluence reached to 90%.

The cells were incubated at 37 °C in 5% CO_2 incubator (Thermo Scientific, USA).

2.2.2. Thawing Frozen Cells

SD-1, SD-1R, HCC1937 BL or BEAS-2B cells were frozen and stored at -80 C° for further studies when they may be needed. In case, cells were quickly thawed to obtain the highest percentage of viable cells. When the ice crystals melted, the cells were taken into a sterile falcon tube that contains 4 ml fresh complete media. Then, the falcon tube was centrifuged at 800 rpm for 5 min to remove DMSO from content. After centrifugation, supernatant was removed, cells were resuspended in fresh complete media and cultured in 25 cm^2 tissue culture flask. The cells were incubated at 5% CO_2, 37 °C in CO_2 incubator (Thermo Scientific, USA).

2.2.3. Freezing Cells

SD-1, SD-1R, HCC1937 BL or BEAS-2B cells were frozen in cryogenic vials at -80 °C to use in further studies when needed. Each cryogenic vial contained 2×10^6 cells in 1 mL as 500 µL Freezing Mix 1 + 500 µL Freezing Mix 2 (Table 2.3).

Table 2.3. Preparation of freezing mixtures.

	Contents of freezing mix	
Freezing Mix 1	6 mL culture media (not complete)	4 mL FBS
Freezing Mix 2	8 mL culture media (not complete)	2 mL DMSO

The cells cultured were harvested and the content was centrifuged at 800 rpm for 5 minutes. After centrifuge, supernatant was removed carefully and the pellet was resuspended with Freezing Mix 1. The amount of Freezing Mix 1 calculated as each cryogenic vial contains 500 µL. The content was transferred into the cryogenic vials.

Then, 500 µL Freezing Mix 2 was put into each cryogenic vial immediately. The cryogenic vials were incubated in -20 °C fridge overnight. Finally, the cells were stored at -80 ° C freezer.

2.2.4. Maintenance of Cells

2.2.4.1. Maintenance of SD-1, SD-1R Cells and HCC1937 BL Cells

SD-1, SD-1R and HCC1937 BL cells were cultured when the cell number reached to 1-1,5x10^6 cells/ml. SD-1, SD-1R or HCC1937 BL cells were collected from 75 cm^2 tissue culture flask into a sterile falcon tube. The falcon tube was centrifuged at 600 rpm for 5 minutes. Next, supernatant was removed and the pellet was resuspended in 10 mL fresh complete RPMI 1640 medium. 30 µL content was taken and mixed with 30 µL trypan blue dyes. 10 µL of mixture was put into clean Neubauer hemacytometer (MARIEN SUPERIOR, GERMANY) to count the cell number. The cells were counted under Carl-Zeiss 12V DC 30W light microscopy at 10X magnification.
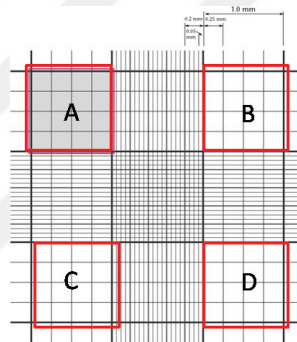
Figure 2.1. The view of hemacytometer squares under the light microscope.

Each square of the hemacytometer (Figure 2.1) (with cover slip in place) represents a total volume of 10^{-4} cm^3. Since 1 cm^3 is equivalent to 1 mL, the subsequent cell concentration per mL and the total number of cells was determined using the following equations:

$$Cells\ per\ mL = \frac{A+B+C+D}{4} \times the\ dilution\ factor \times 10^4 \qquad (2.1)$$

$$Total\ cell\ number = Cells\ per\ mL \times the\ total\ volume\ of\ resuspended\ cells\ in\ falcon$$
$$(2.2)$$

After cell counting, SD-1, SD-1R or HCC1937 BL cells were seeded into 75 cm^2 tissue culture flask as 0,3x10^6 – 0,5x10^6 cells/mL in complete RPMI 1640 media.

2.2.4.1. Maintenance of BEAS-2B Cells

BEAS-2B cells were cultured when their confluence reached to 90%. The medium of BEAS-2B cells in 75 cm^2 tissue culture flask was removed and cells were washed with 1X PBS. The PBS was discarded and 1 mL Trypsin-EDTA solution was put into flask. The cells were incubated at 5% CO_2, 37 °C in CO_2 incubator (Thermo Scientific, USA) for 1-5 minutes until all cells are suspend. The suspend cells were collected with 4 mL complete culture medium and centrifuged at 1000 rpm for 5 minutes. After centrifugation, supernatant was removed and the pellet was resuspended in 10 mL fresh complete DMEM high glucose medium. 30 μL of content was taken and mixed with 30 μL trypan blue dyes. 10 μL mixture was put into clean Neubauer hemacytometer MARIEN SUPERIOR, GERMANY to count the cells number. The cells were counted under Carl-Zeiss 12V DC 30W light microscopy at 10X magnification. The subsequent cell concentration per mL and the total number of cells was determined using the equations 2.1 and 2.2.

After cell counting, BEAS-2B cells were seeded into 75 cm^2 tissue culture flask as 1×10^6 cells in complete DMEM high glucose media.

2.2.5. Drug Preparation and Stock Solutions

Luteolin (Synonym: 3′,4′,5,7-Tetrahydroxyflavone) and imatinib (Synonym: 3′,4′,5,7-Tetrahydroxyflavone) powder were obtained from Santa Cruz Chemicals and Sigma, USA, respectively. Luteolin and imatinib were dissolved in DMSO and water using below calculation (2.3 and 2.4), respectively. 10 mM stock solution was prepared from this content using below equation (2.5). The drugs were stored at -20 ^{0}C and dark.

$$Mole(n) = \frac{Weight(m)}{Molecular\ weight(MA)} \qquad (2.3)$$

$$Molarity(M) = \frac{Mole(n)}{Volume(V)} \qquad (2.4)$$

$$M1 \times V1 = M2 \times V2 \tag{2.5}$$

2.2.6. Measurement of Cell Proliferation by MTT

The cytotoxic effect of Luteolin on SD-1, SD-1R, HCC1937 BL cells and BEAS-2B were determined by using MTT assay. Moreover, the cytotoxic effect of imatinib on SD-1 cells is also determined by using this method.

10.000 cells/100 µL of SD-1, SD-1R or HCC1937 BL cells and 5.000 cells/100 µL BEAS-2B cells were seeded into each well of 96-well plates. BEAS-2B cells were incubated overnight at 5% CO_2, 37 °C in CO_2 incubator before application of drugs.

Luteolin were prepared as 0-5-10-20-30-40-50-100 µM doses while imatinib was prepared as 0-1-5-10-20-50 µM doses. 100 µL drug doses were applied onto dedicated wells and the final concentration of DMSO in each well was under the 0,1%. 96-well-plates were incubated at 5% CO_2, 37 °C in CO_2 incubator (Thermo Scientific, USA) for 24 and/or 48 hours. When incubation time was completed, 20 µL of MTT stock solutions (5 mg/mL) was added into each well and 96-well-plates were incubated at 5% CO_2, 37 °C in CO_2 incubator for 4 hours. After incubation time was completed, plates were centrifuged at 1400 rpm, 4 °C for 10 minutes to precipitate formazan crystals. Then, supernatant was removed carefully and 100 µL of DMSO was added to each well to dissolve the formazan crystals. Plates were incubated at room temperature in rotator shaker for 10-15 minutes, then they were read in a microplate reader (Multiskan Go, Thermo Scientific, USA) at 570 nm.

2.2.7. Trypan Blue Dye Exclusion Method to Measure Cell Viability

The effect of Luteolin on viability of SD-1, SD-1R, HCC1937 BL and BEAS-2B cells were determined by trypan blue dye exclusion assay. Moreover, the cytotoxic effects of imatinib on SD-1 cells were also determined by using this method.

0,3x10^6 SD-1, SD-1R, and HCC1937 BL cells and 25.000 BEAS-2B cells were seeded in 1 mL complete culture media into 6-well plate. BEAS-2B cells were incubated overnight at 5% CO_2, 37 °C in CO_2 incubator before application of drugs. 0-5-10-20-30-40-50-100 µM of Luteolin was applied while0-1-5-10-20--50 µM of imatinib was applied with three replicates. 6-well-plates were incubated at 5% CO_2, 37 °C in CO_2 incubator (Thermo Scientific, USA) for 48 hours.

When incubation time completed, cells were pipetted gently, 30 µL cells were taken and mixed with 30 µL trypan blue dye. 10 µL was taken from mixture and put to clean Neubauer hemacytometer (with cover slip in place) to count the cell number. The cells were counted under Zeiss light microscopy at 10X magnification. Each square of the hemacytometer (with cover slip in place) represents a total volume of 10^{-4} cm^3. Since 1 cm^3 is equivalent to 1 mL, the subsequent cell concentration per mL and the total number of cells was determined using the following equations:

$$\text{Cells per mL} = (A+B+C+D)/4 \times \text{the dilution factor} \times 10^4$$

Thus, cell number of control and luteolin treated SD-1, SD-1R, HCC1937 BL and BEAS-2B cells were determined.

2.2.8. Measurement of Apoptosis Rate by Annexin-V/PI Double Staining by Flow Cytometry

Apoptotic effects of luteolin on SD-1 cells were determined by using Annexin-V/PI Double Staining by flow cytometry. SD-1 cells were seeded as 0,6x10^6 cells in 2 mL complete RPMI 1640 media at 6-well plates. Luteolin was applied as 0-10-20-40 µM to desired wells and 6-well-plates were incubated at 5% CO_2, 37 °C in CO_2 incubator (Thermo Scientific, USA) for 48 hours.

When incubation time completed, cells were collected in different falcons and centrifuged at 1000 rpm for 10 minutes (0 µM Luteolin- exposed cells -1 and -2 were divided into two 15 mL falcon to stained as below for introducing cells to flow cytometry). After centrifugation, supernatant was removed and cells were dissolved in 1 mL cold PBS 1X. Then, falcons were centrifuged again at 1000 rpm for 10 minutes and

supernatant was removed after centrifugation. The pellets were dissolved in 200 µL Annexin binding buffer and 2 µL Annexin and PI dyes were added as defined below (Figure 2.2).

Untreated control cells (0 µM Luteolin) and experiment cells (exposed to 10-, 20-, and 40 µM of luteolin) were stained with both 2 µL Annexin and 2 µL PI. Cells were incubated at room temperature for 15 minutes before analysis at flow cytometry.
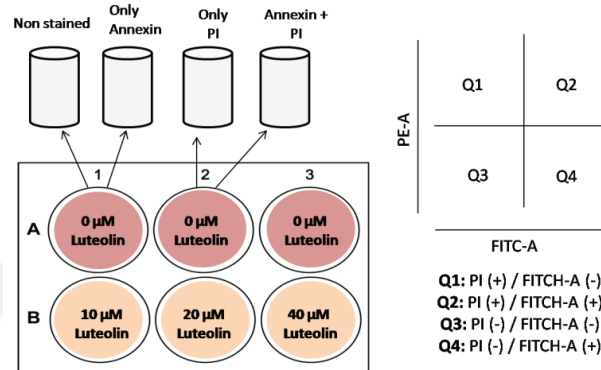
Figure 2.2. AnnexinV-PI double staining.

As a consequence of whether AnnexinV dye (FITC-A) binds to phosphatidylserine in outer membrane of cells and PI dye binds to DNA fragments in nucleus, cells divided to 4 quadrant in flow cytometry, (BD FACS Canto, USA) in two channel. Normally phosphatidylserine found in inner membrane of cells while it moves to outer membrane by flip-flop in apoptosis. AnnexinV-FITC dye binds to phosphatidylserine found in outer membrane of death cells. Besides, DNA fragments of cells which goes to cell death can be visualized through PI dye. PI dye can bind to DNA fragments in the nucleus of death cells. Thus, death cells can be visualized by double staining of AnnexinV-PI.

2.2.9. Detection of Loss of Mitochondrial Membrane Potential

The effect of Luteolin on loss of mitochondrial membrane potential of SD-1 cells was determined by using JC-1 Mitochondrial Membrane Potential Kit by flow cytometry. SD-1 cells were seeded as $0,6 \times 10^6$ cells in 2 mL complete RPMI-1640

media at 6-well plates. Luteolin was applied as 0-10-20-40 µM and 6-well-plates were incubated at 5% CO_2, 37 °C in CO_2 incubator (Thermo Scientific, USA)for 48 hours.

When 48 hours incubation time completed, 100 µL of JC-1 staining solution was prepared and applied to each well, was mixed gently. The plates were incubated at 5% CO_2, 37 °C in CO_2 incubator (Thermo Scientific, USA) for 20 minutes.

After incubation, cells were collected in different falcons and centrifuged at 1000 rpm for 5 minutes. After centrifugation, supernatant was removed and cells were dissolved in 1 mL of JC-1 assay buffer.

Then, falcons were centrifuged again at 1000 rpm for 5 minutes and supernatant was removed after centrifugation. The pellets were dissolved in 500 µL JC-1 assay buffer and the mitochondrial membrane potential was detected by flow cytometry (BD FACS Canto, USA),immediately.

- Preparation of JC-1 staining solution: 100 µL JC-1 dye + 900 µL complete RPMI medium 1640
- Preparation of JC-1 assay buffer: 1 Cell based assay buffer tablet + 100 mL distilled water

2.2.10. Analysis of Cell Cycle Profiles

The possible cytostatic effects of Luteolin on SD-1 cells was determined by using Flow Cytometry. $0,6X10^6$ cells in 2 mL SD-1 cells were seeded in RPMI-1640 media in 6-well plates. Luteolin was applied as 0-10-20-40 µM and 6-well-plates were incubated at 5% CO_2, 37 °C in CO_2 incubator (Thermo Scientific, USA) for 48 hours.

2.2.10.1. Fixation

When 48 hour incubation time was completed, cells were collected in different falcons and centrifuged at 1000 rpm for 5 minutes. After centrifugation, supernatants were discarded and the pellets were dissolved in 1 mL cold PBS. Falcons were

incubated on ice for 15 minutes and then 4 mL -20 °C absolute ethanol was added into each falcon. Falcons were incubated at -20 °C at least 24 hours.

2.2.10.2. Staining

After incubation time was completed, falcons were centrifuged at 1000 rpm for 10 minutes. Supernatants were discarded and the pellets were dissolved in 5 mL cold PBS. Falcons were centrifuged at 1000 rpm for 10 minutes again and then supernatants were discarded and the pellets were dissolved in 250 µL 0,1% TritonX100 in 1X PBS. Then, 25 µL RNase A was added into each falcons and falcons were incubated at 5% CO_2, 37 °C in CO_2 incubator (Thermo Scientific, USA) for 30 minutes. After incubation time completed, 25 µL PI dye was added into each falcon and falcons were incubated at room temperature for 10 minutes. Then, cell cycle profiles of cells were examined by BD FACS Canto, USA flow cytometry.

2.2.11. Quantification of Expression Levels of Sphingolipid Genes

The effects of Luteolin on expression levels of sphingolipid genes in SD-1 cells were determined by qRT-PCR. Sequences of primers were described above in Table 2.1. Before performing qRT-PCR, total RNAs were isolated from luteolin applied SD-1 cells after different concentration of luteolin application for 48 hours.

SD-1 cells were seeded in 8 mL complete RPMI-1640 medium as $0{,}3\mathrm{x}10^6$ cells/mL in 100 mm petri dishes. Luteolin was applied the petri dishes as 0-10-20-40 µM and petri dishes were incubated at 5% CO_2, 37 °C in CO_2 incubator (Thermo Scientific, USA) for 48 hours.

When 48 hour incubation was completed, cells were collected in different 15 mL falcons and centrifuged at 1000 rpm for 10 minutes. After centrifugation, supernatants were discarded, the pellets were dissolved in 1 mL 1X PBS and contents carried to 1,5

mL eppendorf to centrifuge at 1000 rpm for 10 minutes. After centrifugation, supernatants were discarded and pellets were used for total RNA isolation.

2.2.11.1. Total RNA Isolation from Cells and Quantification of RNA

Macherey-Nagel NucleoSpin®RNA isolation kit was used for the total RNA isolation from SD-1 cells. According to manifacturer's protocol, isolation was performed and all steps were performed at room temperature.

After collecting cells, the pellets were well dissolved in 350 µL of lysis buffer of Macherey-Nagel NucleoSpin®RNA isolation kit that contain 3,5 µL β-mercaptoethanol. Contents were applied to Macherey-Nagel NucleoSpin®RNA fitler in collection tube and were centrifuged at 11,000 g for 1 minutes. The lysate was passed at least 5 times through a 0.9 mm diameter needle (20-gauge) fitted to a syringe.

The flow-through were discarded, 350 µL 70% ethanol was added into each tube and the lysates were homogenized by pipetting. The samples were applied to new Macherey-Nagel NucleoSpin®RNA filter (spin column) in new collection tube and centrifuged at 11,000 g for 30 seconds. The spin columns were put into new collection tube and 350 µL Membrane Desalting Buffer (MDB) was applied to spin columns. The columns were centrifuged again at 11,000 g for 1 minute. DNase reaction mixture was prepared by 10 µL reconstituted rDNase was mixed with 90 µL Reaction Buffer for rDNase. Then, 95 µL DNase reaction mixtures were added directly to center of silica membrane of the spin columns. The columns were incubated at room temperature for 15 minutes. After incubation time completed, 200 µL Buffer RAW2 was added to columns and columns were centrifuged at 11,000 g for 30 seconds. Thus, Buffer RAW2 inactivated the rDNase. Columns were put into new collection tube and 600 µL Buffer RA3 was added into each column. Columns were centrifuged at 11,000 g for 30 seconds. After centrifuge, 250 µL Buffer RA3 was added to columns and columns were centrifuged again at 11,000 g for 2 minutes.

Columns were put into nuclease-free tubes for elution. 50 µL RNase-free water was applied to each column and columns were incubated at room temperature for 5 minutes and then, columns were centrifuged at 11,000 g for 1 minute. Thus, Total RNAs were eluted.

After RNA isolation, RNAs were quantified by NanoDrop ND1000 Spectrometer, Thermo Fischer, USA. The ratio between the absorbance values at 260 nm and 280 nm (A_{260}/A_{280}) determines the nucleic acid purity. Generally, pure RNA have a ratio of ~2.0.

If RNAs do not use in PCR directly, RNAs can be stored at -80^{0}C.

2.2.11.2. Conversion of Total RNA to cDNA by Reverse Transcriptase Reaction

Total RNAs from luteolin treatedSD-1 cells were converted to cDNA through Thermo Scientific RevertAid Reverse Transcriptase Kit, USA. Based on the manufacturer's manual, reaction was performed in two steps.

Step 1: Template RNA and primers were added into nuclease-free tube on ice as indicated order in Table 2.4. Tubes were centrifuged briefly and incubated at 65 °C for 5 min in Applied Biosystem PCR machine, USA.

Table 2.4. Components of first step of cDNA conversion reaction.

Components	Final Concentration	Volume
Template RNA (Total RNA)	1 µg	It was calculated based on the RNA ratio in per µL
Primer (Random hexamer)	0,2 µg (100 pmol)	1 µL
DEPC- treated water		to 12,5 µL
Total Volume:		**12,5 µL**

Step 2: After incubation, 7,5 µL of master mix (Table 2.5) was added into each tube on ice and mixed gently, centrifuged briefly. Based on the manifacturer's manual, tubes were incubated at 25 °C for 5 minutes followed by incubation at 42 °C for 60 minutes. The termination reaction was performed at 70 °C for 10 min.

If cDNAs do not use in qRT-PCR directly, cDNAs should be stored at -20 °C.

Table 2.5. Master Mix of step 2 of cDNA conversion reaction.

Components	Final Concentration	Volume
5X Reaction Buffer	1 X	4 µL
Thermo Scientific™ RiboLock RNase Inhibitor	20 U	0,5 µL
dNTP Mix (10 mM each)	1 mM each	2 µL
RevertAid Reverse Transcriptase	200 U	1 µL
Total Volume:		**20 µL**

2.2.11.3. Detection of Expression Levels of Bioactive Sphingolipid Genes by Quantitative Real-Time PCR (qRT-PCR)

Before Quantitative Reverse Transcriptase Reaction (qRT-PCR) was performed, gradient PCR and agarose gel electrophoresis had performed to understand annealing temperature of each primer. After determination of annealing temperature of each primer, qRT-PCR was performed to determine the effects of luteolin on expression levels of CERS 1, CERS 2, CERS 4, CERS 5, CERS6, SK-1, and SK-2 genes through Thermo Scientific DyNAmo HS SYBR Green qPCR Kits, USA. Beta actin was used as positive internal control. Based on the manufacturer's manual, 18 µL of master mix (Table 2.6) was prepared and added into 96-well-plate qRT-PCR plate on ice as indicated. 2µL of cDNA was put into 96-well plate directly. Then, based on the PCR conditions of each primer, qRT-PCR was performed for each gene (Table 2.6-2.10).

Table 2.6. Components of master mix for qRT-PCR.

Components	Final Concentration	Volume
2X Master mix	1X	10 µL
Forward Primer	0.3 µM	0,6 µL
Reverse Primer	0.3 µM	0,6 µL
Template DNA	<10 ng/µL	2 µL directly put into 96-well plate.
Nuclease free water	Up to 20 µL	6,8 µL
Total Volume:		**20 µL**

Table 2.7. qRT-PCR Conditions of CERS 1, CERS5, and GCS.

	Temperature	Time	Cycle
Initial Denaturation	95 ^{0}C	15 minutes	1 cycle
Denaturation	94 ^{0}C	10 seconds	40 cycles
Annealing	50 ^{0}C	20 seconds	
Extension	72 ^{0}C	30 seconds	
Melting Curve	95 ^{0}C	1 minutes	1 cycle
	55 ^{0}C	2 minutes	
	95 ^{0}C	Continuous	
Cooling	40 ^{0}C	10 minutes	1 cycle

Table 2.8. qRT-PCR Conditions of CERS 2, CERS 4 and Beta actin.

	Temperature	Time	Cycle
Initial Denaturation	95 ^{0}C	15 minutes	1 cycle
Denaturation	94 ^{0}C	10 seconds	40 cycles
Annealing	52 ^{0}C	20 seconds	
Extension	72 ^{0}C	30 seconds	
Melting Curve	95 ^{0}C	1 minutes	1 cycle
	57 ^{0}C	2 minutes	
	95 ^{0}C	Continuous	
Cooling	40 ^{0}C	10 minutes	1 cycle

Table 2.9. qRT-PCR Conditions of CERS 3 and CERS 6.

	Temperature	Time	Cycle
Initial Denaturation	95 ^{0}C	15 minutes	1 cycle
Denaturation	94 ^{0}C	10 seconds	40 cycles
Annealing	60 ^{0}C	20 seconds	
Extension	72 ^{0}C	30 seconds	
Melting Curve	95 ^{0}C	1 minutes	1 cycle
	65 ^{0}C	2 minutes	
	95 ^{0}C	Continuous	
Cooling	40 ^{0}C	10 minutes	1 cycle

Table 2.10. qRT-PCR Conditions of SK-1 and SK-2.

	Temperature	Time	Cycle
Initial Denaturation	95 ^{0}C	15 minutes	1 cycle
Denaturation	94 ^{0}C	10 seconds	
Annealing	58 ^{0}C	20 seconds	40 cycles
Extension	72 ^{0}C	30 seconds	
Melting Curve	95 ^{0}C	1 minutes	
	63 ^{0}C	2 minutes	1 cycle
	95 ^{0}C	Continuous	
Cooling	40 ^{0}C	10 minutes	1 cycle

During the experiment Roche LightCycler480, Switzerland qRT-PCR machine was used.

2.2.12. Western Blotting Analyses

Western blotting was performed to determine the effects of luteolin on SK-1, SK-2, and GCS protein levels in SD-1 cells. GAPDH was used as protein loading control.

2.2.12.1. Total Protein Isolation

Total proteins were isolated from luteolin exposed SD-1 cells. Firstly, SD-1 cells were seeded into 100 mm petri dishes as $0,3X10^6$ cells/mL. Petri dishes were exposed 0-,10-,20-, and 40 μM of luteolin and incubated at 5% CO_2, 37 °C in CO_2 incubator (Thermo Scientific, USA) for 48 hours.

After incubation, cells were collected from each petri to desired falcons and centrifuged at 1000 rpm for 10 minutes. After centrifugation, supernatants were discarded and pellets were dissolved in 1X PBS. Contents were carried into 1,5 mL

eppendorf and centrifuged again at 1000 rpm for 10 minutes. After centrifugation, supernatant was discarded and cell pellet was dissolved in lysis buffer (10 mM Tris-HCl + 1 mM EDTA + 0,1% TritonX).

If content use in western blotting directly, content was centrifuged at 14000 rpm for 20 minutes at 4°C, supernatant carry to new eppendorf carefully and use in BCA assay. If content does not use western blotting directly, it can be stored at -80 °C until using in western blotting.

2.2.12.2. Determination of Protein Concentration by Bicinchoninic Acid (BCA) Assay

Total protein concentration was determined by using Pierce BCA Protein Assay Kit, Thermo Scientific, USA. According to manufacturer's protocol, each sample from cell lysate preparation were diluted as 1:10 ratio by using 2,5 µL samples + 22,5 µL sterile dH$_2$O. 10 µL was taken from diluted content and was put into 96-well plate with two replicates. At the same time, Bovine Serum Albumin (BSA) standards were prepared from BSA 2 mg/mL main stock (shown in Table 2.11) and 10 µL of each one was put into 96-well plate as well.

Table 2.11. Preparation of BSA standards.

Bovine Serum Albumin Standards (BSA)	Volume of BSA main stock (2 mg/mL) (µL)	Volume of dH$_2$O (µL)
2 mg/mL	25	0
1,5 mg/mL	18,75	6,25
1 mg/mL	12,5	12,5
0,75 mg/mL	9,38	15,62
0,5 mg/mL	6,25	18,75
0,25 mg/mL	3,13	21,87
0 mg/mL	0	25

The BCA working reagent was prepared as 1:50 dilution using Copper (II) Sulfate and Bicinchoninic Acid Reagent, respectively. 200 μL BCA mixture was put into each samples in 96-well plate. All process was performed at room temperature. The 96-well plate was incubated at 5% CO_2, 37 °C in CO_2 incubator (Thermo Scientific, USA) for 30 minutes. After incubation completed, the well plate was read in microplate reader (Multiskan Go, Thermo Scientific, USA) at 595 nm. According to absorbance value of BSA standards, a graph was drawn to calculate the total protein concentration as μg/μL.

2.2.12.3. SDS Polyacrylamide Gel Electrophoresis (SDS-PAGE)

According to standard curve of BCA assay, 40 μg total protein was taken from each 0-, 10-, 20-, and 40 μM luteolin treated SD-1 cells and was diluted in lysis buffer up to 15 μL. Then, 5 μL of 4X Laemmli Buffer containing β-mercaptoethanol as 1:10 dilution ratio was added into protein-lysis buffer mixture. As a consequence of dilution, total protein amount of all samples ready for loading is 40 μg in 20 μL. Before loading the protein samples SDS-PAGE cassette, samples were denatured at 95 ºC for 10 minutes in Dry Block Heating temperature. After denaturation completed, samples were spin-down shortly before using in SDS-PAGE.

In order to separate the proteins, Bio-Rad 10% TGX Stain Free FastCast Acrylamide Kit was used. According to manifacturer's gel preparing manual, resolver (separating) gel and stacker (collecting) gels of SDS-PAGE were prepared.

3 ml of Resolver A solution and 3 ml of Resolver B solution were mixed in 15 mL falcon tube and 500 μL was taken from mixture to 1.5 ml Eppendorf tube for sealing gel preparation. 10 μL of 10% APS and 1 μL of TEMED were added into eppendorf tube, respectively. As a consequence of that TEMED increases the polymerization of gel, sealing gel pour immediately within two glasses of WB System, which is already assembled. 30 μL of 10% APS and 3 μL of TEMED was added into the remaining resolver A and B mixture. Then, 5 mL mixture was poured immediately to WB system. For preparing of stacker gel, 1 mL of Stacker A solution and 1 mL of Stacker B solution into 15 ml of falcon tube. 10 μL of 10% APS and 2 μL of TEMED

were added to the mixture. WB system was filled immediately with this mixture and 10 wells comb (1 mm comb; Well width: 5.08 mm) were inserted. SDS-PAGE gel was allowed polymerization for 30 minutes.

After polymerization, the gel was placed into the Mini Tank of WB which was fulfilled with 1X Bio-Rad (Tris/Glycine/SDS) running buffer until the company recommended line. After 10 wells comb was removed carefully, 5 µL of the Euro-Clone Prestained Standard protein marker and 20 µL of the protein samples were loaded into the desired wells. Finally, the gel was run at 100 V for 90 minutes to separate the proteins.

2.2.12.4. Transfer of Proteins from Polyacrylamide Gel to PVDF Membrane

Following protein separation through SDS-PAGE, proteins were transferred from gel to Bio-Rad PVDF membrane by using Bio-Rad Trans-Blot Turbo Transfer System. Firstly, the PVDF membrane was incubated in absolute methanol to activate those for 5 minutes and two transfer stacks were washed with 1X Transfer Buffer at the same time. The first transfer stack was put into the cassette of blotting device and the active PVDF membrane was placed on the transfer stack. Then, SDS-PAGE gel was taken from glasses of WB system carefully and placed onto the PVDF membrane. Lastly, the second transfer stack was put onto the gel carefully. All steps were performed in wet condition by 1X Transfer Buffer and both the stacks and gel became smooth by a cylindrical tube to remove bubbles in each step. The cassette was locked with its cover and placed to Bio-Rad's Trans-Blotting device. The blotting was started to transfer whole proteins from gel to PVDF membrane under conditions which are constant 1.3 miliampher (mA), 25 voltage (V) for 15-20 minutes at room temperature.

After blotting of whole proteins, the membrane was blocked in either 5%non-fat dry milk or BSA in 0.1% 1X TBS-Tween20 at room temperature for 60 minutes under shaking conditions. The membrane was washed with 0.1% 1X TBS-Tween20 for 10 minutes at room temperature under shaking conditions. Then, the membrane was incubated with primary antibodies of interested proteins at 4ºC for overnight under shaking conditions. The properties of each antibody were shown in Table 2.2 in detail.

2.2.12.5. Detection of Desired Proteins by Specific Antibodies

After overnight incubation of membrane with primary antibody, the membrane was washed in 0.1% 1X TBS-Tween20 for 10 minutes at room temperature under shaking conditions for three times. Then, the membrane was incubated with secondary antibody of primary antibody at room temperature for 2 hours under shaking conditions. The properties of each secondary antibody for interested proteins were shown in Table 2.2. Following the incubation of membrane with secondary antibody, the membrane was washed with0.1% 1X TBS-Tween20 for 10 minutes at room temperature under shaking conditions three times.

The protein of interest was visualized by using Clarity^{TM} Western ECL Substrate. 100 μL of ECL Solution A and 100 μL of ECL Solution B was mixed in an Eppendorf tube. At the same time, the tray of the fusion machine was prepared to take the proper view of the membrane. Then, the membrane was placed into this tray and the air bubbles were removed with the help of a tip. The prepared visualizing solution was poured onto the protein of interest based on the molecular weights which were determined by the marker protein weight as kD. After that, the tray was placed into the Fusion machine immediately and the view of the marker was snapped. Following the chemoillumisence light application to the membrane for a time period, the view of antibody-bound desired proteins was taken.

After detection of proteins of interest, the membranes were washed with 0.1% 1X TBS-Tween20 for 10 minutes at room temperature under shaking conditions and then incubated with GAPDH antibody as an internal control at 4ºC for overnight under shaking conditions. The steps mentioned above were repeated for GAPDH antibody visualization.

2.2.13. Statistical Analysis

The GraphPad Prism 7.0 was used for both statistical analysis and drawing graphs. Statistical analysis was done using paired t-test to compare the control and experiments while one-way Anova was used for comparison of all set, $p < 0.05$: *,

p<0.01: **, p<0.001: *** were accepted significant. The error bars represent the standard deviations. The error bars are not seen when they are smaller than the thickness of the lines on the graphs. Experiments were performed as three different experiments (n=3).

CHAPTER 3

RESULTS AND DISCUSSION

3.1. Dose and Time Dependent Cytotoxic Effects of Luteolin on SD-1, HCC1937 BL and BEAS-2B Cell Lines

The cytotoxic effect of increasing concentration of luteolin (0-, 5-, 10-, 20-, 30-, 40-, 50-, and 100 μM) on SD-1, HCC1937 BL and BEAS-2B cell lines were determined by using MTT assay. Normal lymphoblast HCC1937 BL cell line and normal epithelial lung BEAS-2B cell line were used to determine the cytotoxic effect of luteolin on healthy cells and compared to Ph positive ALL cells. Based on the graphs, the IC values were determined.

MTT results showed that luteolin has cytotoxic effects on SD-1 cells both for 24- and 48 hours (Figure 3.1.A) in a dose dependent manner. IC50 value of luteolin on SD-1 cells was determined as 17.67 μM.

On the other hand, luteolin also has dose dependent cytotoxic effect on HCC1937 BL cell line. However, there was a significant difference between 24- and 48 hours trails (Figure 3.1.B). In 24 hour trail, HCC1937 BL cells are more proliferative than 48 hour trail. Luteolin has more cytotoxic effects of on SD-1 cells as compared to HCC1937 BL cell lines. IC50 value of Luteolin for HCC1937 BL cells was determined as 27.20 μM.

In addition, the cytotoxic effect of luteolin on BEAS-2B cell line for 48 hours was determined. As shown in Figure 3.1.C, increased luteolin concentration decreases the proliferation of BEAS-2B cells but not as much as SD-1 and HCC1937 BL cell lines (Figure 3.1.C). There was no significant decrease in proliferation of BEAS-2B cells even in the highest concentration of luteolin (100 μM) as compared to both SD-1 and HCC1937 BL cells (Figure 3.1.C). IC50 value of BEAS-2B could not be determined due to that the viability of BEAS-2B cells was more than 50% even during 100 μM luteolin application.

Figure 3.1. The dose and time dependent anti-proliferative effects of luteolin on
A. SD-1, B. HCC1937 BL, and C.BEAS-2B cell lines. Experiments were performed as three different experiments (n=3). Statistical analysis was done using paired t-test, $p<0.05$:*, $p<0.01$: ** were accepted significant. The error bars represent the standard deviations. The error bars are not seen when they are smaller than the thickness of the lines on the graphs.

Figure 3.1 indicated that increasing concentration of luteolin has cytotoxic effect on SD-1 cells and HCC1937 BL cells in a time and dose dependent manner while the luteolin was more effective on proliferation of SD-1 cells than HCC1937 BL cells. In contrast, there was no significant change determined for BEAS-2B cell proliferation. These data was in agreement with the literature since several studies also showed cytotoxic effects of luteolin on several cancer types including leukemia.

For instance, Lim *et al*, showed that luteolin inhibits the proliferation of JAR and JEG-3 human placental choriocarcinoma cells. They applied the luteolin as 0-, 5-, 10-, 20-, 50-, and 100 μM and almost all doses of luteolin significantly decreased the viability of both cell lines (Lim *et al*., 2016). Another study showed that application of luteolin as 0-, 20-, 40-, 60-, 80-, and 100 μM, cell proliferation and growth significantly decreased in esophageal carcinoma cells (P. Chen *et al*., 2017). Recently, it was shown that the proliferation of non-small cell lung cancer cells was suppressed by different concentrations of luteolin (Yu et al., 2019).

Taken together all these studies performed in different cancer types support the cytotoxic effect of luteolin on SD-1 cell lines.

3.2. The Effect of Luteolin on Viability of SD-1, HCC1937 BL and BEAS-2B Cell Lines

Following the determination of the cytotoxic effect of luteolin on SD-1, HCC1937 BL and BEAS-2B cells, dose dependent effect of luteolin on cell viability of SD-1, HCC1937 BL and BEAS-2B cells was determined by trypan-blue dye exclusion method.

Following application of increasing concentrations of luteolin (0 to 100 μM) for 48 hours onto cells, cell numbers of each cell types were determined.

Normal lymphoblast HCC1937 BL cell line and normal epithelial lung BEAS-2B cell line were used to determine the effect of luteolin on viability of healthy cells and compared to Ph positive ALL, SD-1 cells.

Figure 3.2.A shows increasing luteolin doses gradually decreases the cell viability of SD-1 cells (Figure 3.2.A) and similar results were observed for HCC1937 BL cells (Figure 3.2.B).
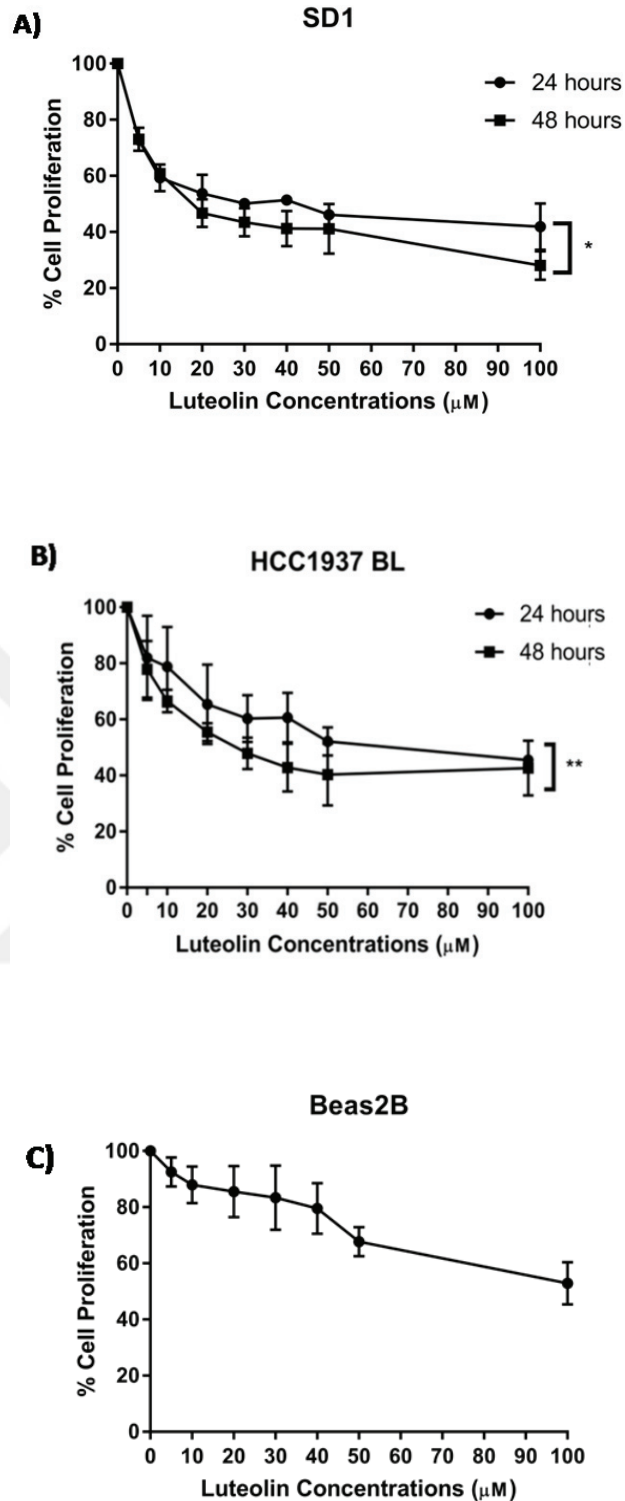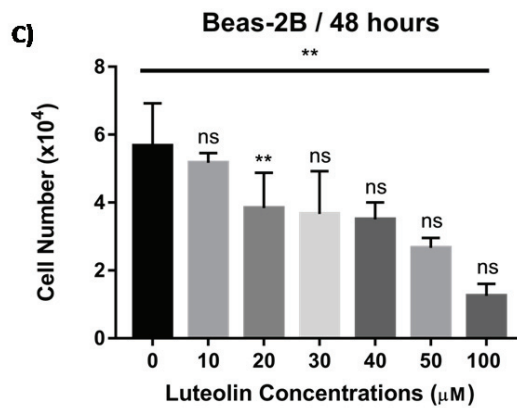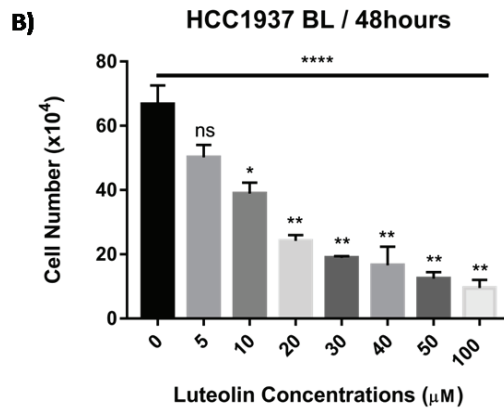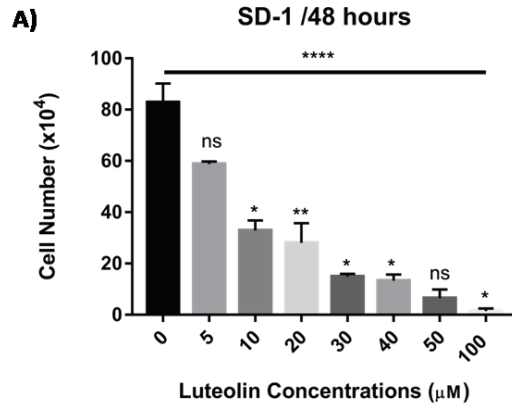
Figure 3.2. The dose and time dependent effect of luteolin on cell viability of A. SD-1, B. HCC1937 BL, and C. BEAS-2Bcell lines. Experiments were performed as three different experiments (n=3). Statistical analysis was done using paired t-test to compare the control and experiments while one-way Anova was used for comparison of all, $p < 0.05$: *, $p < 0.01$: **, $p < 0.001$: *** were accepted significant. The error bars represent the standard deviations.

However, the viability of SD-1 cells is minute amount at 100 μM luteolin exposure (Figure 3.2.A) while HCC1937 BL cells were still alive (Figure 3.2.B). On the other hand, the viability of BEAS-2Bcells were slightly decreased, however these decreases are not significant as compared to control cells (Figure 3.2.C). When the cell viability of SD-1 cells comparing to BEAS-2B cells viability, a remarkable difference between the viability of cells can be observed.

Taken together all these data revealed that luteolin has significant cytotoxic effects on both cell proliferation and viability of SD-1 cells as compared to normal BEAS-2B epithelial lung cells. Although, the MTT and trypan blue results of HCC1937 BL were similar to results of SD-1 cells, even a little difference was observed between them. SD-1 cells are affected from luteolin as compared to both healthy cell lines, HCC1937 BL and BEAS-2B. Decreasing cell viability after luteolin treatment on SD-1 cell line, it was revealed that luteolin has cytotoxic effect on several cancer types including leukemia.

A study showed that application of luteolin as 0-100 μM, cell proliferation and growth significantly decreased in esophageal carcinoma cells (P. Chen *et al*., 2017). Lim *et al*, showed that luteolin inhibits the cell proliferation in human placental choriocarcinoma cells. They applied the luteolin as 0-100 μM and almost all doses (except control) of luteolin significantly decrased the viability of both cell lines (Lim et al., 2016). A study showed that luteolin has little cytotoxic effect on healthy cell lines as compared to human hepatocellular carcinoma cells in dose dependent manner (Im et al., 2018).Taken together all these studies performed in different cancer types support not only anti-proliferative and cytotoxic effect of luteolin on SD-1 cell linesbut also low cytotoxicity of luteolin on healthy HCC1937 BL and BEAS-2B cells.

3.3. Apoptotic Effect of Luteolin on SD-1 Cell Line

Furthermore, the apoptotic effect of different concentration of luteolin (0-, 10-, 20-, and 40 μM) on SD-1 cells for 48 hours was determined by AnnexinV-PI double staining by flow cytometry. In this experiment, X axis represents Annexin-FITC channel while Y axis represents PI channel. The quadrants show alive or dead cells as a consequence of binding of dyes as their properties.

The Q3 quadrant shows the percentage of viability of cells, 89,2%, 76,2%, 64,7% and 38,0% was found for control, 10-, 20-, and 40 μM luteolin exposed SD-1 cells, respectively. The increasing concentration of luteolin enhances the apoptosis which is represented by Q2 and Q4 (Figure 3.3).
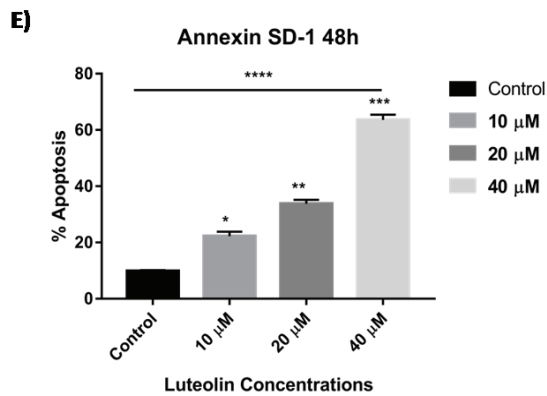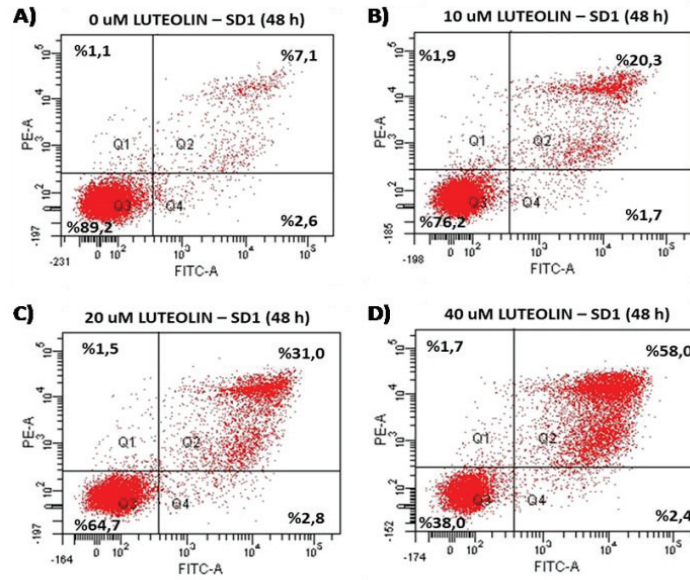
Figure 3.3. Apoptotic effect of luteolin on SD-1 cells in different concentration for 48 hours was determined by Annexin-PI double staining by flow cytometry. Experiments were performed as three different experiments (n=3). Statistical analysis was done using paired t-test to compare the control and experiments while one-way Anova was used for comparison of all, p<0.05: *, p<0.01: **, p<0.001: *** were accepted significant. The error bars represent the standard deviations.

As compared to untreated control cells (Figure 3.3.A), 10 μM luteolin application increased the percentage of apoptosis as 12.3% (Figure 3.3.B). Besides, percentage of apoptosis was increased from 9.7% to 32% when the 20 μM luteolin was applied (Figure 3.3.C). Moreover, the apoptosis rate was significantly increased from 9.7% to 60.4% in 40 μM luteolin-treated SD-1 cells (Figure 3.3.D).

In Figure 3.3.E, statistical analysis of three independent experiments was shown. The increased apoptosis rate by step-wise increasing concentration of luteolin is statistically significant. As a result, the graph demonstrated that percentage of apoptosis of SD-1 cells exposed to different concentration of luteolin based on the statistical analysis of three independent experiments. Luteolin significantly enhances apoptosis in SD-1 cell line in different concentrations (Figure 3.3.E).

The result of apoptotic effect of luteolin on SD-1 Ph positive ALL cells was expected due to that several studies indicated that luteolin has cytotoxic effect on several cancer types including leukemia. For instance, Lim *et al* showed that luteolin induces apoptosis in JAR and JEG-3 human placental choriocarcinoma cells in a dose dependent manner. According to their AnnexinV-PI staining 10-, and 20 μM luteolin significantly increased the apoptosis in these cell lines (Lim *et al*., 2016).

Another study showed that following application of luteolin, apoptosis is enhanced through activating caspase-3 in esophageal carcinoma cells EC1 and KYSE450 in a dose dependent manner (P. Chen *et al*., 2017). Previous studies showed that luteolin also has apoptotic effect on leukemias. For instance, according to Cheng AC *et al*., luteolin increases the caspase-dependent apoptosis in HL-60 acute premyeloblastic leukemia cells in a dose dependent manner (Cheng, Huang, Lai, & Pan, 2005). Taken together all these studies performed in different cancer types support the apoptotic effect of luteolin on SD-1 cell lines.

3.4. The Effect of Luteolin on Mitochondrial Membrane Potential of SD-1 cells

Loss of mitochondrial membrane potential (MMP) of SD-1 cells in response to step-wise increasing luteolin concentrations (0-, 10-, 20-, and 40 μM) for 48 hours was determined by JC-1 mitochondrial membrane potential assay by flow cytometry.

According to results increased concentration of luteolin changes the mitochondrial membrane potential which is marker of mitochondrial cell death.
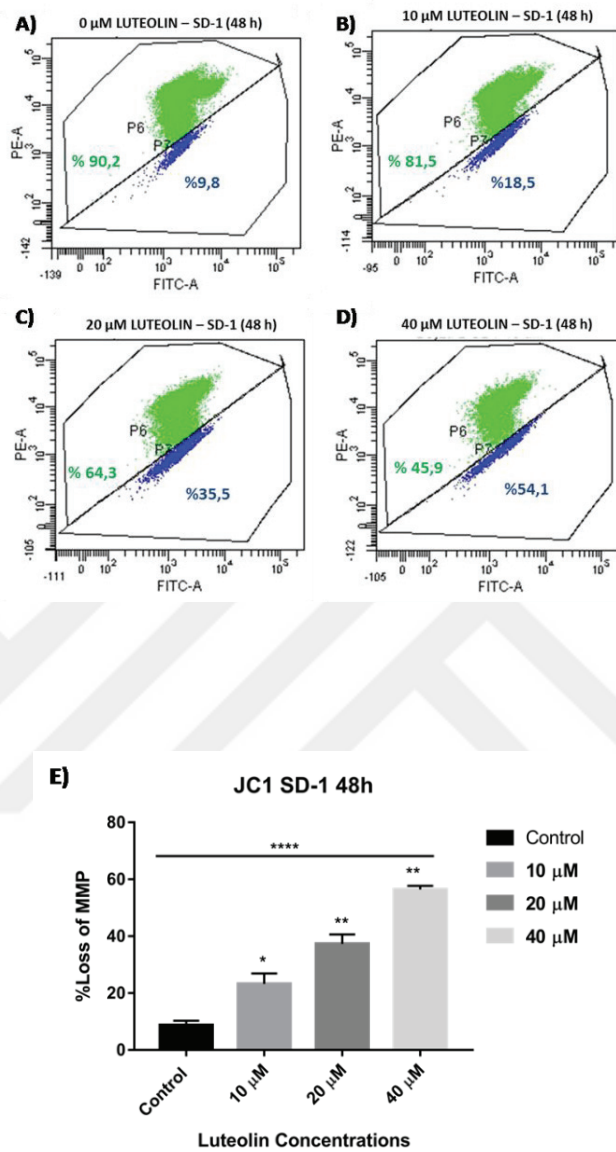
Figure 3.4. Loss of mitochondrial membrane potential of SD-1 cells after applying different concentration of luteolin for 48 hours. Experiments were performed as three different experiments (n=3). Statistical analysis was done using paired t-test to compare the control and experiments while one-way Anova was used for comparison of all, $p<0.05$: *, $p<0.01$: **, $p<0.001$: *** were accepted significant. The error bars represent the standard deviations. The error bars are not seen when they are smaller than the thickness of the lines on the graphs.

Compared to control cells (Figure 3.4.A) which are not exposed to luteolin, 10 μM luteolin applications double the percentage of loss of mitochondrial membrane

potential (Figure 3.4.B) while the cell viability of control cells and 10 μM luteolin exposed cells are 90.2% and 81,5%, respectively. Next, loss of mitochondrial membrane potential of SD-1 cells is increased from 9,8% to 35.5% when 20 μM luteolin was applied (Figure 3.4.C). Furthermore, the cell viability of SD-1 cells were 45,9% at 40 μM dose while the dead cells found as 54.1% (Figure 3.4.D).

Consequently, the loss of mitochondrial membrane potential of SD-1 cells gradually increased when the luteolin applied as step-wise increasing concentrations. The graph shows the percentage of loss of mitochondrial membrane potential of SD-1 cells according to the statistical analysis of three independent experiments (Figure 3.4.E).

Loss of mitochondrial membrane potential significantly increased in SD-1 cells when luteolin was exposed. This data supports the AnnexinV-PI double staining results of SD-1 cells. The results in Ph positive ALL cells, SD-1 cell line, was expected due to that several studies indicated that luteolin has apoptotic effect on several cancer types including leukemia. For instance, Lim et al, showed that luteolin induces the apoptosis in JAR and JEG-3 human placental choriocarcinoma cells in dose dependent manner. According to their JC-1 mitochondrial membrane potential assay 10 and 20 μM luteolin significantly increased the loss of MMP in the JEG-3 cell lines while 5, 10 and 20 μM luteolin significantly increased the loss of MMP in JAR cells (Lim et al., 2016). Another study showed that application of luteolin significantly decreased mitochondrial membrane potential of esophageal carcinoma cells in dose dependent manner (P. Chen et al., 2017). Previous study showed that luteolin decreases the mitochondrial membrane potential in acute premyeloblastic leukemia HL-60 cells after 1,5 hours (Cheng et al., 2005).

3.5. The Cytostatic Effects of Luteolin on SD-1 Cells

Furthermore, the effect of luteolin on cell cycle event of SD-1 cells after applying step-wise increasing luteolin concentrations (0-, 10-, 20-, and 40 μM) for 48 hours was determined by PI staining by flow cytometry. According to results increased concentration of luteolin promotes the cell cycle arrest.

56.18%, 7.63% and 36.19% of control cells were in G1 phase, G2 phase and S phase (Figure 3.5.A)while 10 μM luteolin applications enhances the cell cycle arrest at G1 stage with 62.75% and at G2 phase with 10.88% (Figure 3.5.B).

Next, the cell cycle of 20 μM luteolin exposed SD-1 cells is arrested at G2 phase with 16.75% while the cells at G1 and S phase with 61.92% and 21.32%, respectively (Figure 3.5.C).
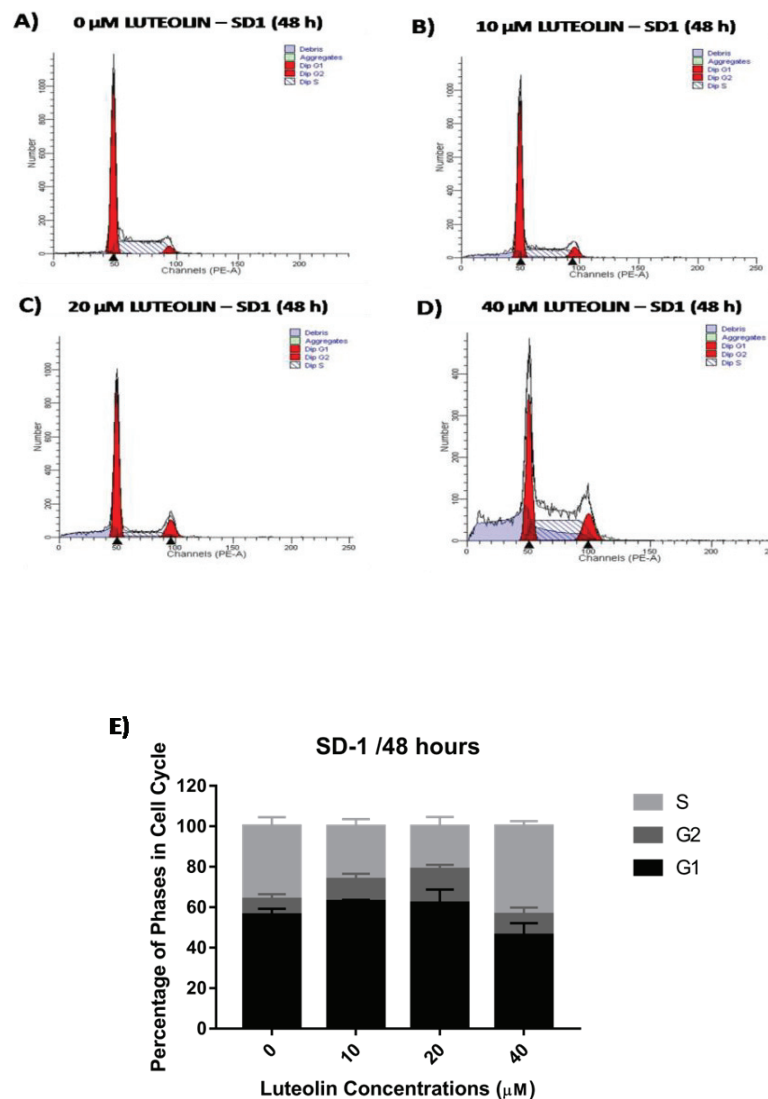
Figure 3.5. Cytostatic effect of luteolin on SD-1 cells for 48 hours was determined by cell cycle arrest assay (PI staining) by flow cytometry. Experiments were performed as three different experiments (n=3). The error bars represent the standard deviations. The error bars are not seen when they are smaller than the thickness of the lines on the graphs.

Furthermore, SD-1 cells were arrested at S phase of cell cycle with 43.62%, at G1 and G2 phase with 46.09% and 10.29% (Figure 3.5.D) after 20 μM luteolin application for 48 hours. As a consequence of three independent experiments, luteolin enhances the cell cycle arrest in SD-1 cells in a dose dependent manner. The graph demonstrates the percentage of phases in cell cycle (Figure 3.5.E).

The cell cycle arrest because of the luteolin application in SD-1 Ph positive ALL cells, it was expected due to the fact that several studies indicated that luteolin has cytostatic effect on several cancer types including leukemia. A study showed that luteolin induced the cell cycle arrest in esophageal carcinoma cells EC1 and KYSE450 in dose dependent manner. The cell population of EC1 and KYSE450 arrested at G2/M phase while decreased at S phase. (P. Chen et al., 2017).

Recently it was shown that when the luteolin applied as 20-, 40-, and 80 μM, luteolin induces cell cycle arrest at G2/M phase in non-small cell lung cancer (Yu et al., 2019). Another study demonstrated that 10-, and 30 μM luteolin application blocks the cell cycle progression in MDA-MB-231 breast cancer cell lines (L. Huang, Jin, & Lan, 2019). Taken together all these studies performed in different cancer types support the cytostatic effect of luteolin on SD-1 cell lines.

3.6. The Expression Levels of *CERS1* Gene in SD-1 Cells in Response to Different Concentrations of Luteolin

Following determination of cytotoxic, apoptotic and cytostatic effects of luteolin on SD-1 cells, the role of bioactive sphingolipids genes in therapeutic potential of luteolin on SD-1 cells was determined by using qRT-PCR. Experiments were performed as two different experiments (n=2). *Beta actin* gene was used as internal control to normalize the expression level of *CERS 1-6, SK-1 and SK-2* genes The error bars represent the standard deviations. The error bars are not seen when they are smaller than the thickness of the lines on the graphs.

Figure 3.6 showed that, 10-, and 20 μM luteolin application on SD-1 cells for 48 hours gradually increased the expression level of *CERS1* gene as compared to SD-1 control cells (Figure 3.6).

Figure 3.6. The expression level of *CERS1* gene. Experiments were performed as two different experiments (n=2). *Beta actin* gene was used as internal control. The error bars represent the standard deviations. The error bars are not seen when they are smaller than the thickness of the lines on the graphs.

Although there is no study showed the effect of luteolin on CERS genes expression, it has been known that increased *CERS1* expression and its product C18-ceramide related to apoptosis in different cancer types (Baran et al., 2007; Camgoz et al., 2011; Koybasi et al., 2004; Ponnusamy et al., 2010; Senkal et al., 2007). This result was expected as a consequence of our previous study showed that LASS1 gene expression increased in resveratrol induced-apoptosis in HL60 cells (Cakir et al., 2011).

3.7. The Expression Levels of *CERS2* Gene in SD-1 Cells in Response to Different Concentrations of Luteolin

Figure 3.7 shows that the expression level of *CERS2* gene is increased as approximately 50% in 10 µM luteolin exposed cells while *CERS2* expression is slightly decreased by increasing of luteolin to 20 µM, however, both 10 µM and 20 µM luteolin application enhanced the *CERS2* gene expression in SD-1 cells compared to control cells.

Although there is no study showed the effect of luteolin on *CERS* genes expression, this result was expected as a consequence of our previous study that showed *LASS2* gene expression increased in resveratrol induced-apoptosis in HL60 cells (Cakir et al., 2011). Each ceramide chain are produced by different *CERS* genes and they play

61

role in different signaling pathway in different types of cells, this increment in *CERS2* expression in luteolin exposed cells can be obtained or following the increased luteolin application the signaling pathways related to *CERS2* gene might be activated.

Figure 3.7. The expression level of *CerS2* gene. Experiments were performed as two different experiments (n=2). *Beta actin* gene was used as internal control. The error bars represent the standard deviations. The error bars are not seen when they are smaller than the thickness of the lines on the graphs.

3.8. The Expression Levels of *CERS4* Gene in SD-1 Cells in Response to Different Concentrations of Luteolin

The Figure 3.8 indicated that expression level of *CERS4* is gradually increased in different concentration of luteolin exposed cells. In the 20 µM luteolin exposed SD-1 cells, the expression level of *CERS4* was increased 1.5 times higher than expression levels in control cells, however, the increment in *CERS4* expression level in 10µM luteolin exposed SD-1 cells was approximately 50% compared to control cells.

Although there is no study showed the effect of luteolin on CERS genes expression, it has been known that ceramide synthase 4 was highly expressed and promoted the cell proliferation in liver cancer cells and tissues. Moreover, suppression of *CERS4* gene expression result in cell cycle arrest at G0/G1 phase and suppression of development of liver tumor through regulating NF-kB (J. Chen et al., 2017).

This result was expected as a consequence of our previous study showed that *LASS4* gene expression increased in resveratrol which is a flavonoid induced-apoptosis

in HL60 cells (Cakir et al., 2011). This increment in *CERS4* expression in luteolin exposed SD-1 cells after 48 hours application might be obtained by the signaling pathways related to *CERS4* gene might be activated or downregulated following the increased luteolin application.
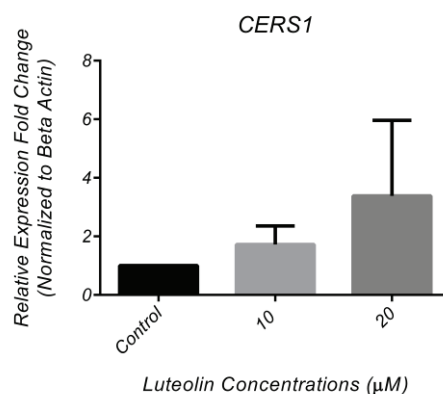

Figure 3.8. The expression level of *CerS4* gene. Experiments were performed as two different experiments (n=2). *Beta actin* gene was used as internal control. The error bars represent the standard deviations. The error bars are not seen when they are smaller than the thickness of the lines on the graphs.

3.9. The Expression Levels of *CERS5* Gene in SD-1 Cells in Response to Different Concentrations of Luteolin

.

Figure 3.9. The expression level of *CERS5* gene. Experiments were performed as two different experiments (n=2). *Beta actin* gene was used as internal control. The error bars represent the standard deviations. The error bars are not seen when they are smaller than the thickness of the lines on the graphs.

The Figure 3.9 shows that the expression level of *CERS5* gene significantly increased in both 10 μM and 20 μM luteolin exposed SD-1 cells (Figure 3.9).In the 20 μM luteolin exposed SD-1 cells, the expression level of *CERS5*was increased approximately10-fold higher than expression levels in control cells, however, the increment in *CERS5* expression level in 10 μM luteolin exposed SD-1 cells was approximately 5-fold higher compared to control cells.

Although there is no study showed the effect of luteolin on CERS genes expression, this result was expected as a consequence of our previous study showed that *LASS5* gene expression increased in resveratrol which is a flavonoid induced-apoptosis in HL60 cells (Cakir et al., 2011)

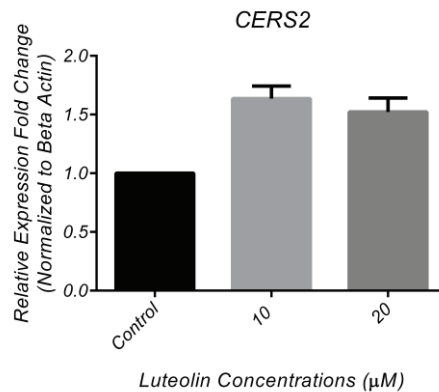## 3.10. The Expression Levels of *CERS6* Gene in SD-1 Cells in Response to Different Concentrations of Luteolin

Figure 3.10. The expression level of *CERS6* gene. Experiments were performed as two different experiments (n=2). *Beta actin* gene was used as internal control. The error bars represent the standard deviations. The error bars are not seen when they are smaller than the thickness of the lines on the graphs.

The Figure 3.10 shows that after 48 hours luteolin application the expression level of *CERS6* gene did not significantly changed in 10 μM luteolin exposed cells however, 20 μM luteolin application slightly decreased the expression level of *CERS6* gene compared to control cells (Figure 3.10).

According to recent studies, *CERS6* is highly expressed and related to poor prognosis and drug resistance in different cancer cells (S. Li et al., 2018; Uen et al., 2018; Verlekar et al., 2018) and considered as a target for treatment (Fekry, Esmaeilniakooshkghazi, Krupenko, & Krupenko, 2016).

3.11. The Expression Levels of *SK-1* Gene in SD-1 Cells in Response to Different Concentrations of Luteolin

Figure 3.11 demonstrated that following 48 hours of luteolin application, the expression level of *SK-1* gene was not changed in 10-, and 20 µM luteolin treated cells. *SK-1* can be considered as a target for treatment of different types of cancer since increased levels of *SK-1* and *SK-2* were shown to be related with cell proliferation, survival, growth and drug resistance (Lu et al., 2017; Pchejetski et al., 2005; Sobue et al., 2008; Zheng et al., 2019).
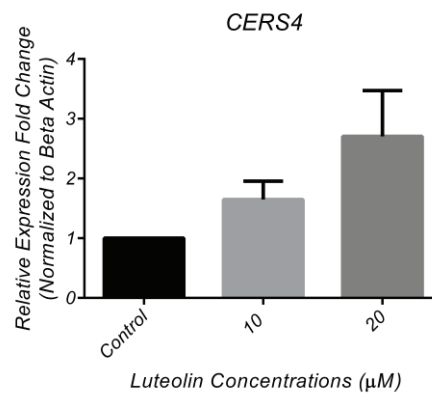

Figure 3.11. The expression level of *SK-1* gene. Experiments were performed as two different experiments (n=2). *Beta actin* gene was used as internal control. The error bars represent the standard deviations. The error bars are not seen when they are smaller than the thickness of the lines on the graphs.

Although there is no study showing the effect of luteolin on *SK-1* gene expression, this result was expected as a consequence of our previous study showing that *SK-1* gene expression decreased in resveratrol induced-apoptosis in HL60 cells

(Cakir et al., 2011). On the other hand, Abdel Hadi et al., showed that luteolin application decreased SK-1 activity in colon cancer cells (Abdel Hadi et al., 2015).

3.12. The Expression Levels of *SK-2* Gene in SD-1 Cells in Response to Different Concentrations of Luteolin

Figure 3.12 demonstrated that the expression level of *SK-2* gene was fluctuated depending on the concentrations. Therefore, the increment in expression level of *SK-2* gene in 10-, and 20 μM luteolin treated SD-1 cells probably due to that the activation of different pathways which affect to *SK-2* activity during the cell death of SD-1 cells.
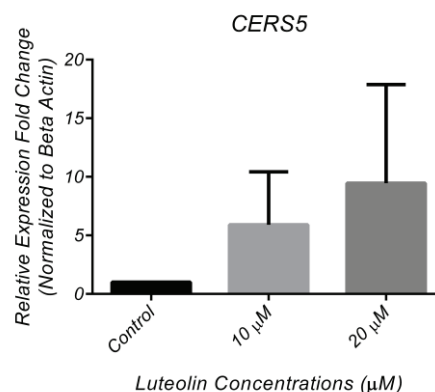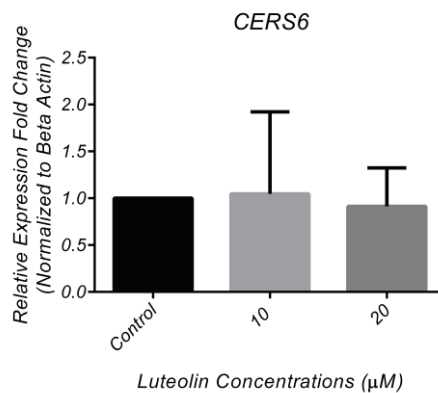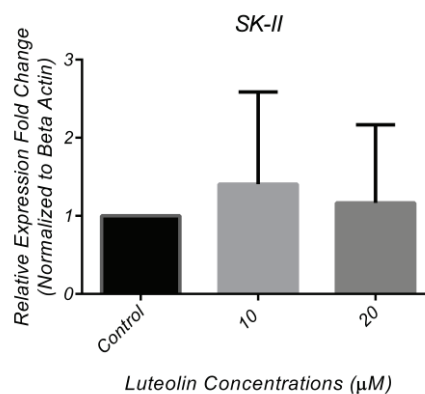

Figure 3.12. The expression level of *SK-2* gene. Experiments were performed as two different experiments (n=2). *Beta actin* gene was used as internal control. The error bars represent the standard deviations. The error bars are not seen when they are smaller than the thickness of the lines on the graphs.

SK-2 can be considered as a target for treatment of different types of cancer since increased levels of *SK-1* and *SK-2* were shown to be related with cell proliferation, survival, growth and drug resistance (Lu et al., 2017; Pchejetski et al., 2005; Sobue et al., 2008; Zheng et al., 2019). Therefore, fluctuation in *SK-2* gene expression was expected after luteolin application for 48 hours. *SK-1* and *SK-2* genes activate the related-signaling pathways.

3.13. The Protein Levels of *SK-1* in SD-1 Cells in Response to Different Concentrations of Luteolin

Figure 3.13 demonstrated that the protein levels of *SK-1* significantly decreased in 10 µM luteolin treated cells after 48 hours. Although the protein level of *SK-1* was also decreased after 20 µM luteolin application for 48 hours, the change was not statistically significant. There is no study showing the effect of luteolin on protein level of *SK-1* in leukemias. *SK-1* gene expression was decreased in resveratrol induced-apoptosis in HL60 cells (Cakir et al., 2011) as well as Abdel Hadi et al, showed that after luteolin application SK-1 activity decreased in colon cancer cells (Abdel Hadi et al., 2015).
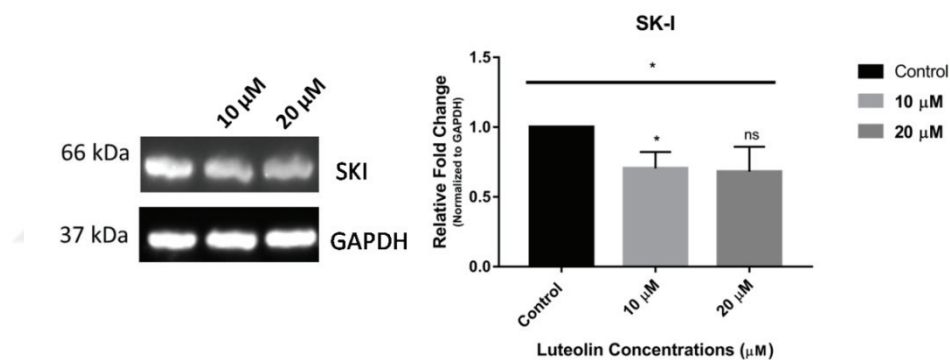
Figure 3.13. The protein level of *SK-1* gene. Experiments were performed as three different experiments (n=3). *GAPDH* was used as internal control. Statistical analysis was done using paired t-test to compare the control and experiments while one-way Anova was used for comparison of all, $p<0.05$: *, $p<0.01$: **, $p<0.001$: *** were accepted significant. The error bars represent the standard deviations.

3.14. The Protein Levels of *SK-2* in SD-1 Cells in Response to Different Concentrations of Luteolin

As shown in Figure 3.14 the changes in protein level of *SK-2* in both 10 µM and 20 µM luteolin treated SD-1 cells was not statistically significant. However the protein

level of *SK-2* decreased slightly after 10 µM luteolin application while increased slightly after 20 µM luteolin application.
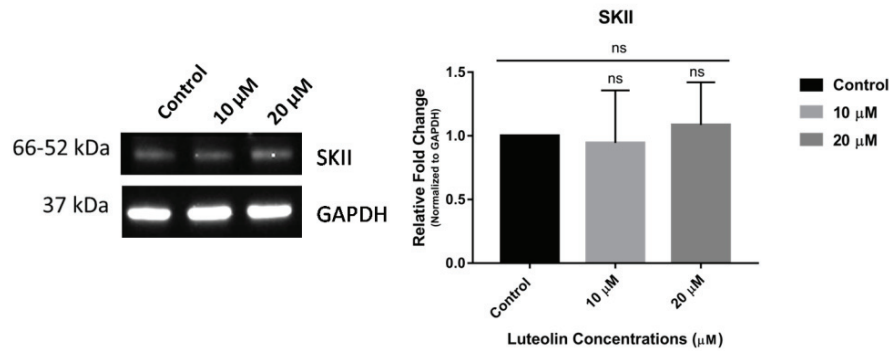
Figure 3.14. The protein level of *SK-II* gene. Experiments were performed as three different experiments (n=3). *GAPDH* was used as internal control. Statistical analysis was done using paired t-test to compare the control and experiments while one-way Anova was used for comparison of all, $p < 0.05$: *, $p < 0.01$: **, $p < 0.001$: *** were accepted significant. The error bars represent the standard deviations.

3.15. The Protein Levels of *GCS* in SD-1 Cells in Response to Different Concentrations of Luteolin
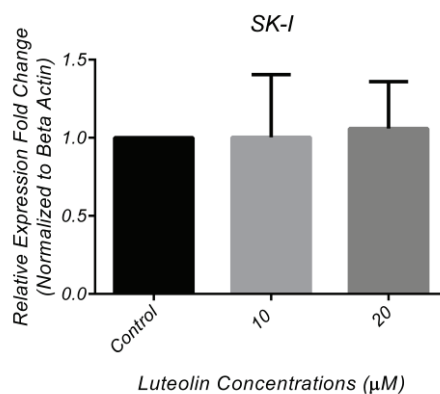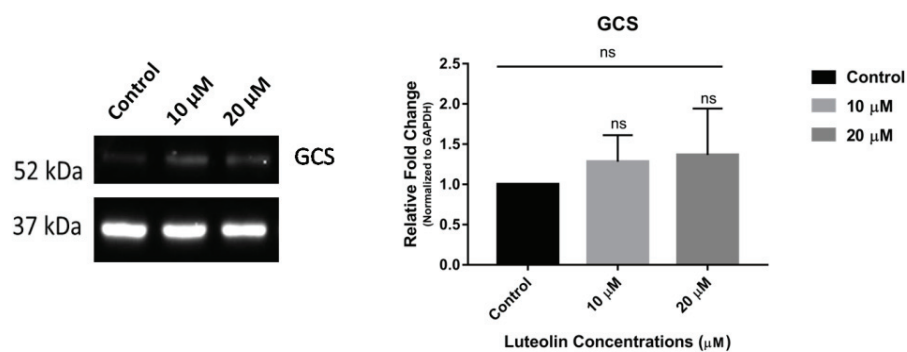

Figure 3.15. The expression level of *GCS* gene. Experiments were performed as three different experiments (n=3). *GAPDH* was used as internal control. The error bars represent the standard deviations. Statistical analysis was done using paired t-test to compare the control and experiments while one-way Anova was used for comparison of all, $p < 0.05$: *, $p < 0.01$: **, $p < 0.001$: *** were accepted significant. The error bars represent the standard deviations.

As shown in Figure 3.15 the changes in protein level of *GCS* in both 10 μM and 20 μM luteolin exposed SD-1 cell was not statistically significant. However the protein level of *GCS* increased slightly after 10 μM and 20 μM luteolin application. There is no study showing the effect of luteolin on protein level of *GCS*. It was shown before that *GCS* gene expression was decreased in resveratrol treated HL60 cells (Cakir et al., 2011).

3.16. Cytotoxic Effects of Luteolin on Imatinib Resistant SD-1 Cells

The cytotoxic effect of increasing concentration of luteolin (0-, 5-, 10-, 20-, 30-, 40-, 50-, and 100 μM) on SD-1 imatinib resistant cell lines were determined by using MTT assay. As a consequence of the MTT results, luteolin has a dose dependent cytotoxic effects on SD-1 imatinib resistant cells (Figure 3.12). IC50 value of luteolin on SD-1 cells was determined as 50 μM.

.
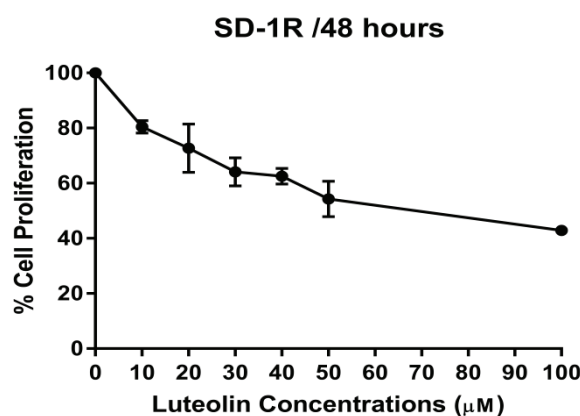
Figure 3.16. The dose dependent anti-proliferative effect of luteolin on SD-1 imatinib resistant SD-1R cells. Experiments were performed as two different experiments (n=2). The error bars represent the standard deviations. The error bars are not seen when they are smaller than the thickness of the lines on the graphs.

It has been documented; luteolin does not only reverse drug resistance but also enhance the therapeutic effects of chemotherapeutic drugs on several cancer cells including ovarian cancer (H. Wang et al., 2018) (Dia & Pangloli, 2017), colorectal

carcinoma (Jang et al., 2019) and human hepatocellular carcinoma cells (H. Xu et al., 2016). Therefore, the result of cytotoxic effect of luteolin on imatinib-resistant SD-1R cells was expected

3.17. The Effect of Luteolin on Imatinib Resistant SD-1 Cell Viability

The effect of increasing concentration of luteolin on viability of SD-1 imatinib resistant cell lines was determined by using trypan-blue dye exclusion method. Following 48 hours application of increasing concentrations of imatinib (0-, 5-, 10-, 20-, 30-, 40-, 50-, and 100 μM) to cells, cell numbers of each cell types were determined.

Following step-wise application of luteolin concentrations, the cell viability of SD-1 cells resistant to 10 μM imatinib was significantly decreased (Figure 3.17). This result supports the cytotoxic effect of increasing concentration of luteolin on SD-1 imatinib resistant cell lines (Figure 3.16).
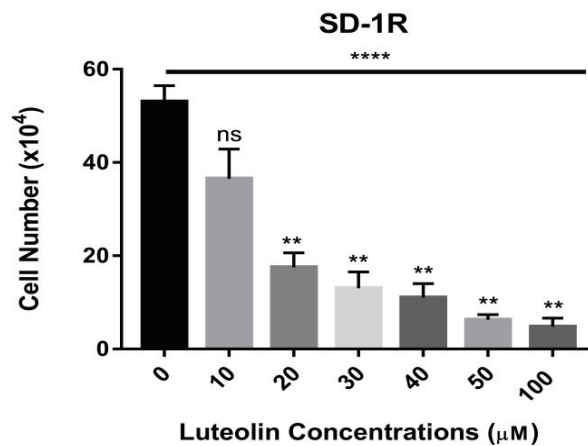
Figure 3.17. The dose dependent effect of luteolin on viability of SD-1 imatinib resistant (SD-1R) cells. Experiments were performed as two different experiments (n=2). Statistical analysis was done using paired t-test to compare the control and experiments while one-way Anova was used for comparison of all, $p < 0.05$: *, $p < 0.01$: **, $p < 0.001$: *** were accepted significant. The error bars represent the standard deviations. The error bars are not seen when they are smaller than the thickness of the lines on the graphs.

3.18. Cytotoxic Effects of Imatinib on SD-1 Cells

Before determining the therapeutic potential of combination of imatinib and luteolin for SD-1 cells, the cytotoxic effect of increasing concentration of imatinib (0-, 1-, 5-, 10-, 20-, and 50 μM) on SD-1 cell lines was determined by using MTT assay.
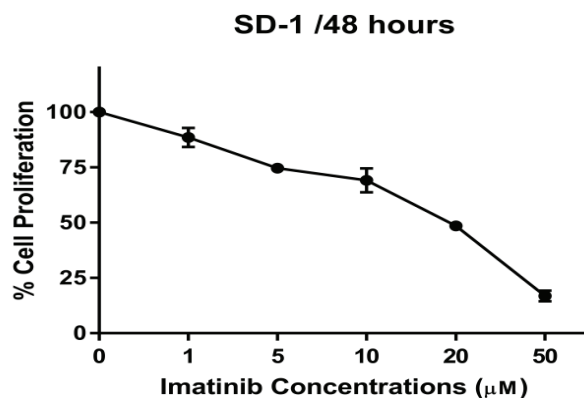
Figure 3.18A. The dose dependent anti-proliferative effect of imatinib on SD-1 cells. Experiments were performed as two different experiments (n=2). The error bars represent the standard deviations. The error bars are not seen when they are smaller than the thickness of the lines on the graphs.

As a consequence of the MTT results, imatinib had dose dependent cytotoxic effects on SD-1 cells for 48 hours (Figure 3.18A). IC50 value of imatinib on SD-1 cells was determined as 18 μM.

Previous studies demonstrated that tyrosine kinase inhibitor, imatinib, has cytotoxic effects on CML and ALL cell lines. According to a study, IC50 value of imatinib on SD-1 cell line was determined as more than 10 μM (Quentmeier, Eberth, Romani, Zaborski, & Drexler, 2011). Thus, the result of cytotoxic effect of imatinib on SD-1 cell line was supported.

Next, we confirmed that the cytotoxic effect of imatinib on SD-1 cell line (Figure 3.18A) through determining the effect of increasing concentration of imatinib on viability of SD-1 cell lines by using trypan-blue dye exclusion method. Following 48 hours increasing imatinib application (0-1-5-10-20-50 μM) to cells, cell numbers of each cell types were determined.

After 48 hours imatinib application, the cell viability of SD-1 cells were significantly decreased (Figure 3.18B). 5 μM imatinib decreased the cell viability of SD-1 cells as approximately 50%. The result of the cytotoxic effect of imatinib on SD-1 cell viability confirmed that the MTT result of Figure 3.18A.
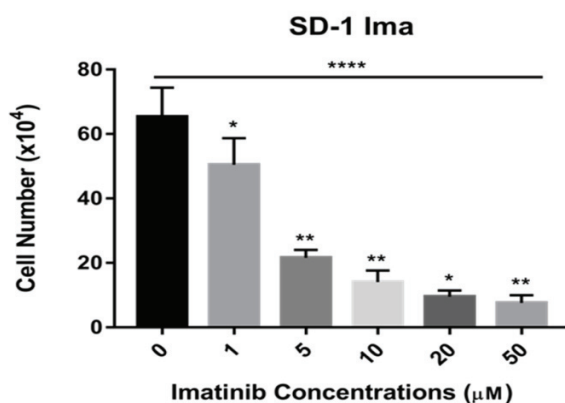
Figure 3.18B. The dose dependent effect of imatinib on viability of SD-1 cells. Experiments were performed as two different experiments (n=2). Statistical analysis was done using paired t-test to compare the control and experiments while one-way Anova was used for comparison of all, $p < 0.05$: *, $p < 0.01$: **, $p < 0.001$: *** were accepted significant. The error bars represent the standard deviations. The error bars are not seen when they are smaller than the thickness of the lines on the graphs.

Previous study demonstrated that the tyrosine kinase inhibitor, imatinib has cytotoxic effect on CML and ALL cell lines. According to a study, IC50 value of imatinib on SD-1 cell line was determined as more than 10 μM (Quentmeier et al., 2011). Thus, the result of cytotoxic effect of imatinib on SD-1 cell line was supported.

3.19. Cytotoxic Effect of Imatinib and Luteolin Combination on SD-1

The cytotoxic effect of increasing concentration of luteolin (0-, 10-, 20-, 30-, 40- and 50 μM) and imatinib combination (0-, 1-, 2-, 3-, 4-, and 5 μM or 0-, 0.5-, 1-, 1.5-, 2- and 2.5 μM) on SD-1 cell lines was determined by using MTT assay. Based on the graphs the IC value was determined.

Our preliminary data demonstrated that luteolin and imatinib combination as 1:10 and 1:20 ratio (Imatinib:Luteolin) had cytotoxic effect on SD-1 cells following 48 hours exposure (Figure 3.19). IC50 value of imatinib and luteolin combination on SD-1 cells was determined as combination of 10 μM luteolin + 1 μM imatinib.

Combination of Ima & Lut

Agents	Concentrations (μM)				
Lut	10	20	30	40	50
Ima (1:10)	1	2	3	4	5
Ima (1:20)	0,5	1	1,5	2	2,5
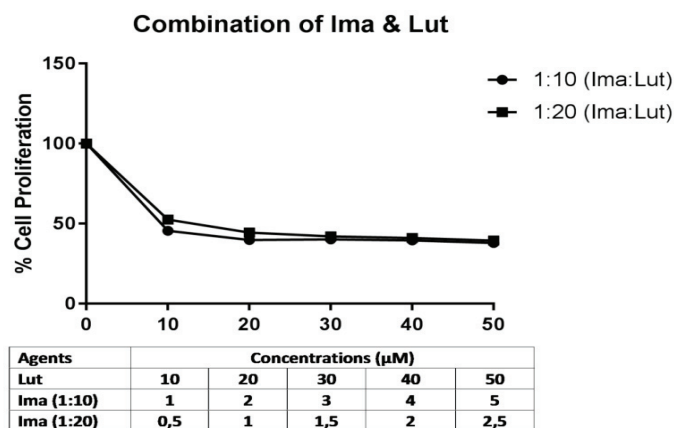
Figure 3.19. The effect of combination of imatinib-luteolin on SD-1 cells. The error bars represent the standard deviations. The error bars are not seen when they are smaller than the thickness of the lines on the graphs.

In a study, cells were treated with combination of luteolin and 5-FU as 10:1 dose ratio and cytotoxic, apoptotic and cytostatic effects of the combination were determined. According to their results, the luteolin has synergistic anti-tumor effect with5-FU through apoptosis induction in hepatocellular carcinoma (H. Xu et al., 2016).

In light of this study, we will further analysis the therapeutic potential of the imatinib and luteolin combination.

CHAPTER 4

CONCLUSION

ALL is a hematologic malignancy is characterized by increased level of immature lymphoblasts in bone marrow and peripheral blood. In the process of leukemogenesis; the development of lymphoblasts are genetically/epigenetically inhibited. One of the most common genetic abnormalities in ALL is BCR/ABL translocation which regulates the several pathways related to proliferation, anti-apoptotic and drug resistance through its aberrant tyrosine kinase activity. Although the current treatment strategies include targeting BCR/ABL; complete remission, overall survival and mortality of Ph+ ALL patients are still poor as compared to Ph- ALL patients. Therefore, new strategies combined with current treatments have vital importance for Ph+ ALL patients who are classified as high-risk group of ALL.

Bioactive sphingolipids which are a class of lipids in cancer have been investigated in wide range. Since bioactive sphingolipids regulates several very important biological processes in cells, they are considered as therapeutic target. In addition to chemotherapeutic drugs, inhibitors or analogs of bioactive sphingolipids have been investigated for new cancer treatment strategies. Besides, some studies showed that flavonoids contribute the bioactive sphingolipids-based cell death or inhibition of cell proliferation in cancer cells. Only one study showed that luteolin induces apoptosis through increasing endogenous ceramide levels in colon cancer cells. Moreover, luteolin has been shown to inhibit both expression and activity levels of SK-1 and -2 resulting in the reduction of S1P (Abdel Hadi et al., 2015).

Based on these studies in the literature, we hypothesized that luteolin could have anti-proliferative and apoptotic effects on Philadelphia chromosome positive acute lymphoblastic leukemia cells. Besides, luteolin might be regulating bioactive sphingolipids genes and induce apoptosis through affecting the expression levels of bioactive sphingolipid genes for its mechanism which strengthen therapeutic potential of luteolin.

We found that increasing concentration of luteolin has cytotoxic effect on SD-1 cells and HCC1937 BL cells by a time and dose dependent manner. However, luteolin was more effective on proliferation of SD-1 cells compared to HCC1937 BL cells. In contrast, there is no significant change determined in proliferation of healthy BEAS-2B cells. Moreover, the apoptotic effects of luteolin on SD-1 cells were also determined and the results were in agreement with each other and demonstrated that increasing concentrations of luteolin enhances the apoptosis in SD-1 cells.

Furthermore, cytostatic effect of luteolin on SD-1 cells were determined and we found that luteolin caused to cell cycle arrest at G2 phase while the cells were arrested at S phase in response to higher concentration of luteolin.

In order to determine the changes in bioactive sphingolipids genes in luteolin treated SD-1 cells, mRNA and protein levels of the genes were determined. According to qRT-PCR results following 48 hours application of luteolin in different dose, the expression levels of CERS genes increased except for CERS6 gene. On the other hand, luteolin did not change the expression level of sphingosine kinase 1 (SK-1) gene. On the other hand, the expression level of sphingosine kinase 2 (SK-2) gene fluctuated depending on the dose of luteolin. Furthermore, western blotting results showed that after 48 hours of luteolin exposure, the protein levels of *SK-1* significantly decreased while the changes in protein levels of *SK-2* and *GCS* were not statistically significant. Our results in line with the study by Abdel Hadi *et al*, which showed that luteolin induced apoptosis in colon cancer cells through increasing endogenous ceramide levels and decreasing SK-1 and SK-2 activity (Abdel Hadi et al., 2015).

In addition to determination of therapeutic potential of luteolin for SD-1 cells and the roles of bioactive sphingolipids genes in this therapeutic potential, we further investigated the therapeutic potential of luteolin for imatinib-resistant SD-1 cells (SD-1R) generated in our lab. We also tested therapeutic potential of luteolin and imatinib combination for SD-1 cells. Our preliminary data showed that luteolin might have anti-cancer effects on imatinib resistant SD-1R cell line. Likewise, luteolin and imatinib combination show a potential synergistic effect on SD-1 cells. Therapeutic potential of both luteolin for SD-1R and combination of luteolin-imatinib for SD-1 cells will be determined.

Here, for the first time, cytotoxic, apoptotic and cytostatic effects of luteolin on Philadelphia chromosome positive acute lymphoblastic leukemia cells were determined by this study. Moreover, the roles of bioactive sphingolipids genes in the therapeutic

potential of luteolin on Ph positive ALL cells were investigated for the first time as well. Luteolin enhanced the apoptosis rate in SD-1 cells by increasing ceramide synthase genes in mRNA level and decreased *SK-1*protein level as schemed in Figure 4.1.
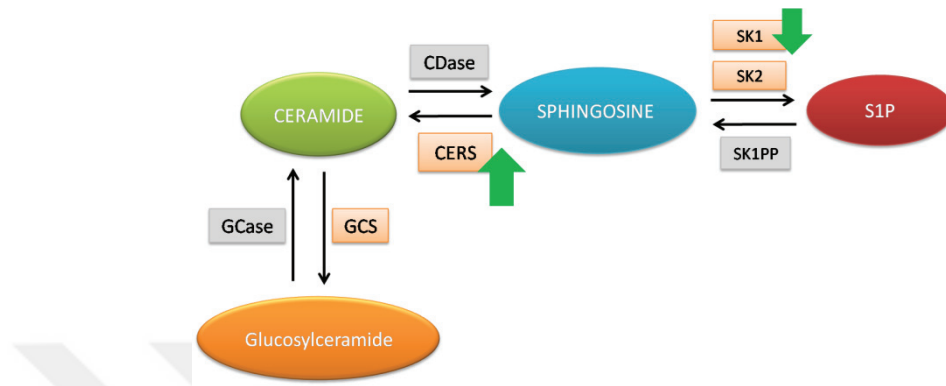
Figure 4.1. Luteolin has therapeutic potential for Ph positive ALL cells. Increasing level of *CERS* genes expression and decreasing *SKI* protein level contribute to luteolin-induced apoptosis in SD-1 cells.

For future studies, luteolin will be investigated step by step for Ph positive ALL patients from bench to clinic. The underlying mechanisms related to therapeutic potential should be investigated before determining pharmacokinetic, pharmacodynamic, genotoxicity analyses of luteolin. Studying on patient samples and/or *in vivo* studies might be helpful to understand the therapeutic potential of luteolin as a chemotherapeutic drug for Ph positive ALL patients in clinic.
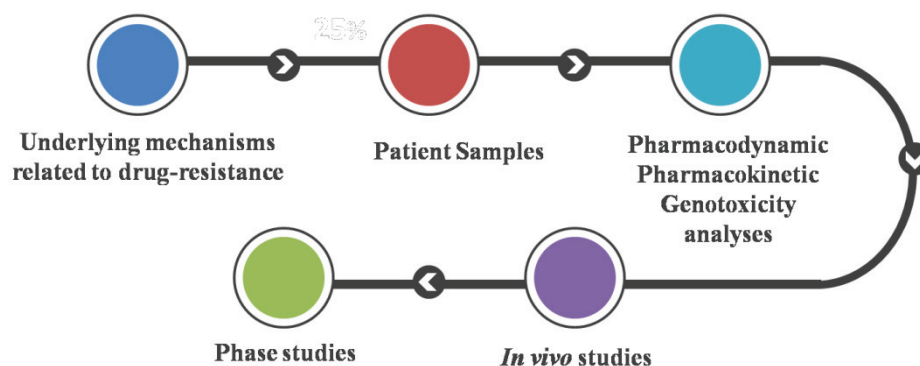
Figure 4.2.The steps luteolin might have investigated from bench to clinic.

REFERENCE

Abdel Hadi, L., Di Vito, C., Marfia, G., Ferraretto, A., Tringali, C., Viani, P., & Riboni, L. (2015). Sphingosine Kinase 2 and Ceramide Transport as Key Targets of the Natural Flavonoid Luteolin to Induce Apoptosis in Colon Cancer Cells. *PLoS One, 10*(11), e0143384. doi:10.1371/journal.pone.0143384

Adan-Gokbulut, A., Kartal-Yandim, M., Iskender, G., & Baran, Y. (2013). Novel agents targeting bioactive sphingolipids for the treatment of cancer. *Curr Med Chem, 20*(1), 108-122.

Advani, A. S., McDonough, S., Coutre, S., Wood, B., Radich, J., Mims, M., . . . Appelbaum, F. R. (2014). SWOG S0910: a phase 2 trial of clofarabine/cytarabine/epratuzumab for relapsed/refractory acute lymphocytic leukaemia. *Br J Haematol, 165*(4), 504-509. doi:10.1111/bjh.12778

Aldoghachi, A. F., Baharudin, A., Ahmad, U., Chan, S. C., Ong, T. A., Yunus, R., . . . Veerakumarasivam, A. (2019). Evaluation of CERS2 Gene as a Potential Biomarker for Bladder Cancer. *Dis Markers, 2019*, 3875147. doi:10.1155/2019/3875147

Annino, L., Vegna, M. L., Camera, A., Specchia, G., Visani, G., Fioritoni, G., . . . Mandelli, F. (2002). Treatment of adult acute lymphoblastic leukemia (ALL): long-term follow-up of the GIMEMA ALL 0288 randomized study. *Blood, 99*(3), 863-871. doi:10.1182/blood.v99.3.863

Awasthi, A., Ayello, J., Van de Ven, C., Elmacken, M., Sabulski, A., Barth, M. J., . . . Cairo, M. S. (2015). Obinutuzumab (GA101) compared to rituximab significantly enhances cell death and antibody-dependent cytotoxicity and improves overall survival against CD20(+) rituximab-sensitive/-resistant Burkitt lymphoma (BL) and precursor B-acute lymphoblastic leukaemia (pre-B-ALL): potential targeted therapy in patients with poor risk CD20(+) BL and pre-B-ALL. *Br J Haematol, 171*(5), 763-775. doi:10.1111/bjh.13764

Azam, M., Latek, R. R., & Daley, G. Q. (2003). Mechanisms of autoinhibition and STI-571/imatinib resistance revealed by mutagenesis of BCR-ABL. *Cell, 112*(6), 831-843. doi:10.1016/s0092-8674(03)00190-9

Baran, Y., Salas, A., Senkal, C. E., Gunduz, U., Bielawski, J., Obeid, L. M., & Ogretmen, B. (2007). Alterations of ceramide/sphingosine 1-phosphate rheostat involved in the regulation of resistance to imatinib-induced apoptosis in K562 human chronic myeloid leukemia cells. *J Biol Chem, 282*(15), 10922-10934. doi:10.1074/jbc.M610157200

Baranowski, M., & Gorski, J. (2011). Heart sphingolipids in health and disease. *Adv Exp Med Biol, 721*, 41-56. doi:10.1007/978-1-4614-0650-1_3

Barrett, D., Brown, V. I., Grupp, S. A., & Teachey, D. T. (2012). Targeting the PI3K/AKT/mTOR signaling axis in children with hematologic malignancies. *Paediatr Drugs, 14*(5), 299-316. doi:10.2165/11594740-000000000-00000

Bartke, N., & Hannun, Y. A. (2009). Bioactive sphingolipids: metabolism and function. *J Lipid Res, 50 Suppl*, S91-96. doi:10.1194/jlr.R800080-JLR200

Bartram, C. R., de Klein, A., Hagemeijer, A., van Agthoven, T., Geurts van Kessel, A., Bootsma, D., . . . et al. (1983). Translocation of c-ab1 oncogene correlates with the presence of a Philadelphia chromosome in chronic myelocytic leukaemia. *Nature, 306*(5940), 277-280. doi:10.1038/306277a0

Bassan, R., Bruggemann, M., Radcliffe, H. S., Hartfield, E., Kreuzbauer, G., & Wetten, S. (2019). A systematic literature review and meta-analysis of minimal residual disease as a prognostic indicator in adult B-cell acute lymphoblastic leukemia. *Haematologica*. doi:10.3324/haematol.2018.201053

Bassoy, E. Y., & Baran, Y. (2012). Bioactive sphingolipids in docetaxel-induced apoptosis in human prostate cancer cells. *Biomed Pharmacother, 66*(2), 103-110. doi:10.1016/j.biopha.2011.10.003

Baum, K. J., & Ren, R. (2008). Effect of Ras inhibition in hematopoiesis and BCR/ABL leukemogenesis. *J Hematol Oncol, 1*, 5. doi:10.1186/1756-8722-1-5

Bazarbachi, A. H., Yilmaz, M., Ravandi, F., Thomas, D. A., Khouri, M., Garcia-Manero, G., . . . Kantarjian, H. M. (2018). A phase 2 study of hyper-CVAD plus ofatumumab as frontline therapy in CD20+ acute lymphoblastic leukemia (ALL): Updated results. *Journal of Clinical Oncology, 36*(15_suppl), 7041-7041. doi:10.1200/JCO.2018.36.15_suppl.7041

Beissert, T., Hundertmark, A., Kaburova, V., Travaglini, L., Mian, A. A., Nervi, C., & Ruthardt, M. (2008). Targeting of the N-terminal coiled coil oligomerization interface by a helix-2 peptide inhibits unmutated and imatinib-resistant BCR/ABL. *Int J Cancer, 122*(12), 2744-2752. doi:10.1002/ijc.23467

Benjamini, O., Dumlao, T. L., Kantarjian, H., O'Brien, S., Garcia-Manero, G., Faderl, S., . . . Ravandi, F. (2014). Phase II trial of hyper CVAD and dasatinib in patients with relapsed Philadelphia chromosome positive acute lymphoblastic leukemia or blast phase chronic myeloid leukemia. *Am J Hematol, 89*(3), 282-287. doi:10.1002/ajh.23624

Bennett, J. M., Catovsky, D., Daniel, M. T., Flandrin, G., Galton, D. A., Gralnick, H. R., & Sultan, C. (1976). Proposals for the classification of the acute leukaemias. French-American-British (FAB) co-operative group. *Br J Haematol, 33*(4), 451-458. doi:10.1111/j.1365-2141.1976.tb03563.x

Bennett, J. M., Catovsky, D., Daniel, M. T., Flandrin, G., Galton, D. A., Gralnick, H. R., & Sultan, C. (1985). Proposed revised criteria for the classification of acute myeloid leukemia. A report of the French-American-British Cooperative Group. *Ann Intern Med, 103*(4), 620-625. doi:10.7326/0003-4819-103-4-620

Brachtendorf, S., El-Hindi, K., & Grosch, S. (2019). Ceramide synthases in cancer therapy and chemoresistance. *Prog Lipid Res, 74*, 160-185. doi:10.1016/j.plipres.2019.04.002

Brachtendorf, S., Wanger, R. A., Birod, K., Thomas, D., Trautmann, S., Wegner, M.-S., . . . Grösch, S. (2018). Chemosensitivity of human colon cancer cells is influenced by a p53-dependent enhancement of ceramide synthase 5 and induction of autophagy. *Biochimica et Biophysica Acta (BBA) - Molecular and Cell Biology of Lipids, 1863*(10), 1214-1227. doi:https://doi.org/10.1016/j.bbalip.2018.07.011

Bradeen, H. A., Eide, C. A., O'Hare, T., Johnson, K. J., Willis, S. G., Lee, F. Y., . . . Deininger, M. W. (2006). Comparison of imatinib mesylate, dasatinib (BMS-354825), and nilotinib (AMN107) in an N-ethyl-N-nitrosourea (ENU)-based mutagenesis screen: high efficacy of drug combinations. *Blood, 108*(7), 2332-2338. doi:10.1182/blood-2006-02-004580

Bray, F., Ferlay, J., Soerjomataram, I., Siegel, R. L., Torre, L. A., & Jemal, A. (2018). Global cancer statistics 2018: GLOBOCAN estimates of incidence and mortality worldwide for 36 cancers in 185 countries. *CA Cancer J Clin, 68*(6), 394-424. doi:10.3322/caac.21492

Burmeister, T., Schwartz, S., Bartram, C. R., Gokbuget, N., Hoelzer, D., Thiel, E., & group, G. s. (2008). Patients' age and BCR-ABL frequency in adult B-precursor ALL: a retrospective analysis from the GMALL study group. *Blood, 112*(3), 918-919. doi:10.1182/blood-2008-04-149286

Caino, M. C., Ghosh, J. C., Chae, Y. C., Vaira, V., Rivadeneira, D. B., Faversani, A., . . . Altieri, D. C. (2015). PI3K therapy reprograms mitochondrial trafficking to fuel tumor cell invasion. *Proc Natl Acad Sci U S A, 112*(28), 8638-8643. doi:10.1073/pnas.1500722112

Cakir, Z., Saydam, G., Sahin, F., & Baran, Y. (2011). The roles of bioactive sphingolipids in resveratrol-induced apoptosis in HL60: acute myeloid leukemia cells. *J Cancer Res Clin Oncol, 137*(2), 279-286. doi:10.1007/s00432-010-0884-x

Camgoz, A., Gencer, E. B., Ural, A. U., Avcu, F., & Baran, Y. (2011). Roles of ceramide synthase and ceramide clearence genes in nilotinib-induced cell death in chronic myeloid leukemia cells. *Leuk Lymphoma, 52*(8), 1574-1584. doi:10.3109/10428194.2011.568653

Campo, E., Swerdlow, S. H., Harris, N. L., Pileri, S., Stein, H., & Jaffe, E. S. (2011). The 2008 WHO classification of lymphoid neoplasms and beyond: evolving concepts and practical applications. *Blood, 117*(19), 5019-5032. doi:10.1182/blood-2011-01-293050

Castillo, J., Milani, C., & Mendez-Allwood, D. (2009). Ofatumumab, a second-generation anti-CD20 monoclonal antibody, for the treatment of lymphoproliferative and autoimmune disorders. *Expert Opin Investig Drugs, 18*(4), 491-500. doi:10.1517/13543780902832679

Chan, L. C., Karhi, K. K., Rayter, S. I., Heisterkamp, N., Eridani, S., Powles, R., . . . Wiedemann, L. M. (1987). A novel abl protein expressed in Philadelphia chromosome positive acute lymphoblastic leukaemia. *Nature, 325*(6105), 635-637. doi:10.1038/325635a0

Che, J., Huang, Y., Xu, C., & Zhang, P. (2017). Increased ceramide production sensitizes breast cancer cell response to chemotherapy. *Cancer Chemother Pharmacol, 79*(5), 933-941. doi:10.1007/s00280-017-3292-y

Chen, J., Li, X., Ma, D., Liu, T., Tian, P., & Wu, C. (2017). Ceramide synthase-4 orchestrates the cell proliferation and tumor growth of liver cancer in vitro and in vivo through the nuclear factor-kappaB signaling pathway. *Oncol Lett, 14*(2), 1477-1483. doi:10.3892/ol.2017.6365

Chen, P., Zhang, J. Y., Sha, B. B., Ma, Y. E., Hu, T., Ma, Y. C., . . . Li, P. (2017). Luteolin inhibits cell proliferation and induces cell apoptosis via down-regulation of mitochondrial membrane potential in esophageal carcinoma cells EC1 and KYSE450. *Oncotarget, 8*(16), 27471-27480. doi:10.18632/oncotarget.15832

Cheng, A. C., Huang, T. C., Lai, C. S., & Pan, M. H. (2005). Induction of apoptosis by luteolin through cleavage of Bcl-2 family in human leukemia HL-60 cells. *Eur J Pharmacol, 509*(1), 1-10. doi:10.1016/j.ejphar.2004.12.026

Chiaretti, S., Messina, M., & Foa, R. (2019). BCR/ABL1-like acute lymphoblastic leukemia: How to diagnose and treat? *Cancer, 125*(2), 194-204. doi:10.1002/cncr.31848

Chiaretti, S., Zini, G., & Bassan, R. (2014). Diagnosis and subclassification of acute lymphoblastic leukemia. *Mediterr J Hematol Infect Dis, 6*(1), e2014073. doi:10.4084/MJHID.2014.073

Chu, S., Li, L., Singh, H., & Bhatia, R. (2007). BCR-tyrosine 177 plays an essential role in Ras and Akt activation and in human hematopoietic progenitor transformation in chronic myelogenous leukemia. *Cancer Res, 67*(14), 7045-7053. doi:10.1158/0008-5472.Can-06-4312

Chung, E. Y., Psathas, J. N., Yu, D., Li, Y., Weiss, M. J., & Thomas-Tikhonenko, A. (2012). CD19 is a major B cell receptor-independent activator of MYC-driven B-lymphomagenesis. *J Clin Invest, 122*(6), 2257-2266. doi:10.1172/jci45851

Cook, M. T., Liang, Y., Besch-Williford, C., & Hyder, S. M. (2017). Luteolin inhibits lung metastasis, cell migration, and viability of triple-negative breast cancer cells. *Breast Cancer (Dove Med Press), 9*, 9-19. doi:10.2147/BCTT.S124860

Cruickshanks, N., Roberts, J. L., Bareford, M. D., Tavallai, M., Poklepovic, A., Booth, L., . . . Dent, P. (2015). Differential regulation of autophagy and cell viability by ceramide species. *Cancer Biol Ther, 16*(5), 733-742. doi:10.1080/15384047.2015.1026509

Dany, M., Gencer, S., Nganga, R., Thomas, R. J., Oleinik, N., Baron, K. D., . . . Ogretmen, B. (2016). Targeting FLT3-ITD signaling mediates ceramide-

dependent mitophagy and attenuates drug resistance in AML. *Blood, 128*(15), 1944-1958. doi:10.1182/blood-2016-04-708750

Daver, N., Thomas, D., Ravandi, F., Cortes, J., Garris, R., Jabbour, E., . . . O'Brien, S. (2015). Final report of a phase II study of imatinib mesylate with hyper-CVAD for the front-line treatment of adult patients with Philadelphia chromosome-positive acute lymphoblastic leukemia. *Haematologica, 100*(5), 653-661. doi:10.3324/haematol.2014.118588

Den Boer, M. L., van Slegtenhorst, M., De Menezes, R. X., Cheok, M. H., Buijs-Gladdines, J. G., Peters, S. T., . . . Pieters, R. (2009). A subtype of childhood acute lymphoblastic leukaemia with poor treatment outcome: a genome-wide classification study. *Lancet Oncol, 10*(2), 125-134. doi:10.1016/s1470-2045(08)70339-5

Dia, V. P., & Pangloli, P. (2017). Epithelial-to-Mesenchymal Transition in Paclitaxel-Resistant Ovarian Cancer Cells Is Downregulated by Luteolin. *J Cell Physiol, 232*(2), 391-401. doi:10.1002/jcp.25436

Dombret, H., Gabert, J., Boiron, J. M., Rigal-Huguet, F., Blaise, D., Thomas, X., . . . Fiere, D. (2002). Outcome of treatment in adults with Philadelphia chromosome-positive acute lymphoblastic leukemia--results of the prospective multicenter LALA-94 trial. *Blood, 100*(7), 2357-2366. doi:10.1182/blood-2002-03-0704

Dorey, K., Engen, J. R., Kretzschmar, J., Wilm, M., Neubauer, G., Schindler, T., & Superti-Furga, G. (2001). Phosphorylation and structure-based functional studies reveal a positive and a negative role for the activation loop of the c-Abl tyrosine kinase. *Oncogene, 20*(56), 8075-8084. doi:10.1038/sj.onc.1205017

Dressler, K., Mathias, S., & Kolesnick, R. (1992). Tumor necrosis factor-alpha activates the sphingomyelin signal transduction pathway in a cell-free system. *Science, 255*(5052), 1715-1718. doi:10.1126/science.1313189

Druker, B. J., Sawyers, C. L., Kantarjian, H., Resta, D. J., Reese, S. F., Ford, J. M., . . . Talpaz, M. (2001). Activity of a specific inhibitor of the BCR-ABL tyrosine kinase in the blast crisis of chronic myeloid leukemia and acute lymphoblastic leukemia with the Philadelphia chromosome. *N Engl J Med, 344*(14), 1038-1042. doi:10.1056/nejm200104053441402

Edmond, V., Dufour, F., Poiroux, G., Shoji, K., Malleter, M., Fouque, A., . . . Legembre, P. (2015). Downregulation of ceramide synthase-6 during epithelial-to-mesenchymal transition reduces plasma membrane fluidity and cancer cell motility. *Oncogene, 34*(8), 996-1005. doi:10.1038/onc.2014.55

Erez-Roman, R., Pienik, R., & Futerman, A. H. (2010). Increased ceramide synthase 2 and 6 mRNA levels in breast cancer tissues and correlation with sphingosine kinase expression. *Biochem Biophys Res Commun, 391*(1), 219-223. doi:10.1016/j.bbrc.2009.11.035

Fainstein, E., Marcelle, C., Rosner, A., Canaani, E., Gale, R. P., Dreazen, O., . . . Croce, C. M. (1987). A new fused transcript in Philadelphia chromosome positive acute lymphocytic leukaemia. *Nature, 330*(6146), 386-388. doi:10.1038/330386a0

Fan, S. H., Wang, Y. Y., Lu, J., Zheng, Y. L., Wu, D. M., Zhang, Z. F., . . . Cheng, W. (2015). CERS2 suppresses tumor cell invasion and is associated with decreased V-ATPase and MMP-2/MMP-9 activities in breast cancer. *J Cell Biochem, 116*(4), 502-513. doi:10.1002/jcb.24978

Fang, Z. H., Dong, C. L., Chen, Z., Zhou, B., Liu, N., Lan, H. F., . . . Han, Z. C. (2009). Transcriptional regulation of survivin by c-Myc in BCR/ABL-transformed cells: implications in anti-leukaemic strategy. *J Cell Mol Med, 13*(8b), 2039-2052. doi:10.1111/j.1582-4934.2008.00549.x

Fekry, B., Esmaeilniakooshkghazi, A., Krupenko, S. A., & Krupenko, N. I. (2016). Ceramide Synthase 6 Is a Novel Target of Methotrexate Mediating Its Antiproliferative Effect in a p53-Dependent Manner. *PLoS One, 11*(1), e0146618. doi:10.1371/journal.pone.0146618

Ferlay, J., Colombet, M., Soerjomataram, I., Mathers, C., Parkin, D. M., Piñeros, M., . . . Bray, F. (2018). Estimating the global cancer incidence and mortality in 2018: GLOBOCAN sources and methods. *Int J Cancer*. doi:10.1002/ijc.31937

Fielding, A. K., Rowe, J. M., Richards, S. M., Buck, G., Moorman, A. V., Durrant, I. J., . . . Goldstone, A. H. (2009). Prospective outcome data on 267 unselected adult patients with Philadelphia chromosome-positive acute lymphoblastic leukemia confirms superiority of allogeneic transplantation over chemotherapy in the pre-imatinib era: results from the International ALL Trial MRC UKALLXII/ECOG2993. *Blood, 113*(19), 4489-4496. doi:10.1182/blood-2009-01-199380

Fitzgerald, S., Sheehan, K. M., Espina, V., O'Grady, A., Cummins, R., Kenny, D., . . . Kijanka, G. S. (2014). High CerS5 expression levels associate with reduced patient survival and transition from apoptotic to autophagy signalling pathways in colorectal cancer. *The journal of pathology. Clinical research, 1*(1), 54-65. doi:10.1002/cjp2.5

Frank, D., & Varticovski, L. (1996). BCR/abl leads to the constitutive activation of Stat proteins, and shares an epitope with tyrosine phosphorylated Stats. *Leukemia : official journal of the Leukemia Society of America, Leukemia Research Fund, U.K, 10*, 1724-1730.

Fujimoto, M., Poe, J. C., Jansen, P. J., Sato, S., & Tedder, T. F. (1999). CD19 amplifies B lymphocyte signal transduction by regulating Src-family protein tyrosine kinase activation. *J Immunol, 162*(12), 7088-7094.

Futerman, A. H., & Hannun, Y. A. (2004). The complex life of simple sphingolipids. *EMBO Rep, 5*(8), 777-782. doi:10.1038/sj.embor.7400208

Gault, C. R., Obeid, L. M., & Hannun, Y. A. (2010). An overview of sphingolipid metabolism: from synthesis to breakdown. *Adv Exp Med Biol, 688*, 1-23. doi:10.1007/978-1-4419-6741-1_1

Gencer Akcok, E., Ural, A., Avcu, F., & Baran, Y. (2011). A novel mechanism of dasatinib-induced apoptosis in chronic myeloid leukemia; Ceramide synthase

and ceramide clearance genes. *Annals of hematology, 90*, 1265-1275. doi:10.1007/s00277-011-1212-5

Gencer, S., Oleinik, N., Kim, J., Panneer Selvam, S., De Palma, R., Dany, M., . . . Ogretmen, B. (2017). TGF-β receptor I/II trafficking and signaling at primary cilia are inhibited by ceramide to attenuate cell migration and tumor metastasis. *Science Signaling, 10*(502), eaam7464. doi:10.1126/scisignal.aam7464

Giebel, S., Stella-Holowiecka, B., Krawczyk-Kulis, M., Gokbuget, N., Hoelzer, D., Doubek, M., . . . Holowiecki, J. (2010). Status of minimal residual disease determines outcome of autologous hematopoietic SCT in adult ALL. *Bone Marrow Transplant, 45*(6), 1095-1101. doi:10.1038/bmt.2009.308

Gleissner, B., Gokbuget, N., Bartram, C. R., Janssen, B., Rieder, H., Janssen, J. W., . . . Thiel, E. (2002). Leading prognostic relevance of the BCR-ABL translocation in adult acute B-lineage lymphoblastic leukemia: a prospective study of the German Multicenter Trial Group and confirmed polymerase chain reaction analysis. *Blood, 99*(5), 1536-1543. doi:10.1182/blood.v99.5.1536

Goni, F. M., & Alonso, A. (2006). Biophysics of sphingolipids I. Membrane properties of sphingosine, ceramides and other simple sphingolipids. *Biochim Biophys Acta, 1758*(12), 1902-1921. doi:10.1016/j.bbamem.2006.09.011

Groffen, J., Stephenson, J. R., Heisterkamp, N., de Klein, A., Bartram, C. R., & Grosveld, G. (1984). Philadelphia chromosomal breakpoints are clustered within a limited region, bcr, on chromosome 22. *Cell, 36*(1), 93-99. doi:10.1016/0092-8674(84)90077-1

Grosch, S., Schiffmann, S., & Geisslinger, G. (2012). Chain length-specific properties of ceramides. *Prog Lipid Res, 51*(1), 50-62. doi:10.1016/j.plipres.2011.11.001

Guillermet-Guibert, J., Davenne, L., Pchejetski, D., Saint-Laurent, N., Brizuela, L., Guilbeau-Frugier, C., . . . Bousquet, C. (2009). Targeting the sphingolipid metabolism to defeat pancreatic cancer cell resistance to the chemotherapeutic gemcitabine drug. *Mol Cancer Ther, 8*(4), 809-820. doi:10.1158/1535-7163.MCT-08-1096

Han, K., Meng, W., Zhang, J. J., Zhou, Y., Wang, Y. L., Su, Y., . . . Min, D. L. (2016). Luteolin inhibited proliferation and induced apoptosis of prostate cancer cells through miR-301. *Onco Targets Ther, 9*, 3085-3094. doi:10.2147/OTT.S102862

Hanada, K., Kumagai, K., Tomishige, N., & Yamaji, T. (2009). CERT-mediated trafficking of ceramide. *Biochim Biophys Acta, 1791*(7), 684-691. doi:10.1016/j.bbalip.2009.01.006

Hannun, Y., & Bell, R. (1987). Lysosphingolipids inhibit protein kinase C: implications for the sphingolipidoses. *Science, 235*(4789), 670-674. doi:10.1126/science.3101176

Hannun, Y. A., & Obeid, L. M. (2002). The Ceramide-centric universe of lipid-mediated cell regulation: stress encounters of the lipid kind. *J Biol Chem, 277*(29), 25847-25850. doi:10.1074/jbc.R200008200

Hannun, Y. A., & Obeid, L. M. (2008). Principles of bioactive lipid signalling: lessons from sphingolipids. *Nat Rev Mol Cell Biol, 9*(2), 139-150. doi:10.1038/nrm2329

Hannun, Y. A., & Obeid, L. M. (2011). Many ceramides. *J Biol Chem, 286*(32), 27855-27862. doi:10.1074/jbc.R111.254359

Hannun, Y. A., & Obeid, L. M. (2017). Sphingolipids and their metabolism in physiology and disease. *Nature Reviews Molecular Cell Biology, 19*, 175. doi:10.1038/nrm.2017.107

https://www.nature.com/articles/nrm.2017.107#supplementary-information

Harris, N. L., Jaffe, E. S., Diebold, J., Flandrin, G., Muller-Hermelink, H. K., Vardiman, J., . . . Bloomfield, C. D. (1999). World Health Organization Classification of Neoplastic Diseases of the Hematopoietic and Lymphoid Tissues: Report of the Clinical Advisory Committee Meeting—Airlie House, Virginia, November 1997. *Journal of Clinical Oncology, 17*(12), 3835-3849. doi:10.1200/jco.1999.17.12.3835

Hartmann, D., Lucks, J., Fuchs, S., Schiffmann, S., Schreiber, Y., Ferreirós, N., . . . Grösch, S. (2012). Long chain ceramides and very long chain ceramides have opposite effects on human breast and colon cancer cell growth. *The International Journal of Biochemistry & Cell Biology, 44*(4), 620-628. doi:https://doi.org/10.1016/j.biocel.2011.12.019

He, Y., Wertheim, J. A., Xu, L., Miller, J. P., Karnell, F. G., Choi, J. K., . . . Pear, W. S. (2002). The coiled-coil domain and Tyr177 of bcr are required to induce a murine chronic myelogenous leukemia-like disease by bcr/abl. *Blood, 99*(8), 2957-2968. doi:10.1182/blood.v99.8.2957

Hinman, L. M., Hamann, P. R., Wallace, R., Menendez, A. T., Durr, F. E., & Upeslacis, J. (1993). Preparation and characterization of monoclonal antibody conjugates of the calicheamicins: a novel and potent family of antitumor antibiotics. *Cancer Res, 53*(14), 3336-3342.

Hoelbl, A., Schuster, C., Kovacic, B., Zhu, B., Wickre, M., Hoelzl, M. A., . . . Sexl, V. (2010). Stat5 is indispensable for the maintenance of bcr/abl-positive leukaemia. *EMBO Mol Med, 2*(3), 98-110. doi:10.1002/emmm.201000062

Hoelzer, D., & Gokbuget, N. (2012). Chemoimmunotherapy in acute lymphoblastic leukemia. *Blood Rev, 26*(1), 25-32. doi:10.1016/j.blre.2011.08.001

Hoelzer, D., Huettmann, A., & Kaul, F. (2010). Immunochemotherapy with rituximab improves molecular CR rate and outcome in CD20+ B-lineage standard and high risk patients; Results of 263 CD20+ patients studied prospectively in GMALL study 07/2003. *Blood, 116*.

Horowitz, N. A., Akasha, D., & Rowe, J. M. (2018). Advances in the genetics of acute lymphoblastic leukemia in adults and the potential clinical implications. *Expert Rev Hematol, 11*(10), 781-791. doi:10.1080/17474086.2018.1509702

Huang, L., Jin, K., & Lan, H. (2019). Luteolin inhibits cell cycle progression and induces apoptosis of breast cancer cells through downregulation of human telomerase reverse transcriptase. *Oncol Lett, 17*(4), 3842-3850. doi:10.3892/ol.2019.10052

Huang, X., Dai, S., Dai, J., Xiao, Y., Bai, Y., Chen, B., & Zhou, M. (2015). Luteolin decreases invasiveness, deactivates STAT3 signaling, and reverses interleukin-6 induced epithelial-mesenchymal transition and matrix metalloproteinase secretion of pancreatic cancer cells. *Onco Targets Ther, 8*, 2989-3001. doi:10.2147/OTT.S91511

Ilaria, R. L., Jr., & Van Etten, R. A. (1996). P210 and P190(BCR/ABL) induce the tyrosine phosphorylation and DNA binding activity of multiple specific STAT family members. *J Biol Chem, 271*(49), 31704-31710. doi:10.1074/jbc.271.49.31704

Im, E., Yeo, C., & Lee, E. O. (2018). Luteolin induces caspase-dependent apoptosis via inhibiting the AKT/osteopontin pathway in human hepatocellular carcinoma SK-Hep-1 cells. *Life Sci, 209*, 259-266. doi:10.1016/j.lfs.2018.08.025

Jabbour, E., Kantarjian, H., Ravandi, F., Thomas, D., Huang, X., Faderl, S., . . . O'Brien, S. (2015). Combination of hyper-CVAD with ponatinib as first-line therapy for patients with Philadelphia chromosome-positive acute lymphoblastic leukaemia: a single-centre, phase 2 study. *Lancet Oncol, 16*(15), 1547-1555. doi:10.1016/s1470-2045(15)00207-7

Jang, C. H., Moon, N., Oh, J., & Kim, J. S. (2019). Luteolin Shifts Oxaliplatin-Induced Cell Cycle Arrest at G(0)/G(1) to Apoptosis in HCT116 Human Colorectal Carcinoma Cells. *Nutrients, 11*(4). doi:10.3390/nu11040770

Ji, C., Yang, Y. L., He, L., Gu, B., Xia, J. P., Sun, W. L., . . . Bi, Z. G. (2012). Increasing ceramides sensitizes genistein-induced melanoma cell apoptosis and growth inhibition. *Biochem Biophys Res Commun, 421*(3), 462-467. doi:10.1016/j.bbrc.2012.04.012

Jin, A., Kurosu, T., Tsuji, K., Mizuchi, D., Arai, A., Fujita, H., . . . Miura, O. (2006). BCR/ABL and IL-3 activate Rap1 to stimulate the B-Raf/MEK/Erk and Akt signaling pathways and to regulate proliferation, apoptosis, and adhesion. *Oncogene, 25*, 4332. doi:10.1038/sj.onc.1209459

Jin, J., Mullen, T. D., Hou, Q., Bielawski, J., Bielawska, A., Zhang, X., . . . Hsu, Y. T. (2009). AMPK inhibitor Compound C stimulates ceramide production and promotes Bax redistribution and apoptosis in MCF7 breast carcinoma cells. *J Lipid Res, 50*(12), 2389-2397. doi:10.1194/jlr.M900119-JLR200

Kang, K. A., Piao, M. J., Hyun, Y. J., Zhen, A. X., Cho, S. J., Ahn, M. J., . . . Hyun, J. W. (2019). Luteolin promotes apoptotic cell death via upregulation of Nrf2 expression by DNA demethylase and the interaction of Nrf2 with p53 in human colon cancer cells. *Exp Mol Med, 51*(4), 40. doi:10.1038/s12276-019-0238-y

Kang, K. A., Piao, M. J., Ryu, Y. S., Hyun, Y. J., Park, J. E., Shilnikova, K., . . . Hyun, J. W. (2017). Luteolin induces apoptotic cell death via antioxidant activity in

human colon cancer cells. *Int J Oncol, 51*(4), 1169-1178. doi:10.3892/ijo.2017.4091

Kang, Z. J., Liu, Y. F., Xu, L. Z., Long, Z. J., Huang, D., Yang, Y., . . . Liu, Q. (2016). The Philadelphia chromosome in leukemogenesis. *Chin J Cancer, 35*, 48. doi:10.1186/s40880-016-0108-0

Keeshan, K., Cotter, T. G., & McKenna, S. L. (2003). Bcr-Abl upregulates cytosolic p21WAF-1/CIP-1 by a phosphoinositide-3-kinase (PI3K)-independent pathway. *Br J Haematol, 123*(1), 34-44. doi:10.1046/j.1365-2141.2003.04538.x

Kim, M. K., Lee, W., Yoon, G.-H., Chang, E.-J., Choi, S.-C., & Kim, S. W. (2019). Links between accelerated replicative cellular senescence and down-regulation of SPHK1 transcription. *BMB Reports, 52*(3), 220-225. doi:10.5483/BMBRep.2019.52.3.012

Kitatani, K., Idkowiak-Baldys, J., & Hannun, Y. A. (2008). The sphingolipid salvage pathway in ceramide metabolism and signaling. *Cell Signal, 20*(6), 1010-1018. doi:10.1016/j.cellsig.2007.12.006

Kittiratphatthana, N., Kukongviriyapan, V., Prawan, A., & Senggunprai, L. (2016). Luteolin induces cholangiocarcinoma cell apoptosis through the mitochondrial-dependent pathway mediated by reactive oxygen species. *J Pharm Pharmacol, 68*(9), 1184-1192. doi:10.1111/jphp.12586

Kolter, T. (2011). A view on sphingolipids and disease. *Chem Phys Lipids, 164*(6), 590-606. doi:10.1016/j.chemphyslip.2011.04.013

Koybasi, S., Senkal, C. E., Sundararaj, K., Spassieva, S., Bielawski, J., Osta, W., . . . Ogretmen, B. (2004). Defects in cell growth regulation by C18:0-ceramide and longevity assurance gene 1 in human head and neck squamous cell carcinomas. *J Biol Chem, 279*(43), 44311-44319. doi:10.1074/jbc.M406920200

Kuroda, I., Inukai, T., Zhang, X., Kikuchi, J., Furukawa, Y., Nemoto, A., . . . Sugita, K. (2013). BCR-ABL regulates death receptor expression for TNF-related apoptosis-inducing ligand (TRAIL) in Philadelphia chromosome-positive leukemia. *Oncogene, 32*(13), 1670-1681. doi:10.1038/onc.2012.186

Kurz, J., Parnham, M. J., Geisslinger, G., & Schiffmann, S. (2019). Ceramides as Novel Disease Biomarkers. *Trends Mol Med, 25*(1), 20-32. doi:10.1016/j.molmed.2018.10.009

Kurzrock, R., Gutterman, J. U., & Talpaz, M. (1988). The molecular genetics of Philadelphia chromosome-positive leukemias. *N Engl J Med, 319*(15), 990-998. doi:10.1056/nejm198810133191506

Lahiri, S., & Futerman, A. H. (2007). The metabolism and function of sphingolipids and glycosphingolipids. *Cell Mol Life Sci, 64*(17), 2270-2284. doi:10.1007/s00018-007-7076-0

Lai, R., Hirsch-Ginsberg, C. F., & Bueso-Ramos, C. (2000). Pathologic diagnosis of acute lymphocytic leukemia. *Hematol Oncol Clin North Am, 14*(6), 1209-1235.

Larson, R. A. (2006). Management of acute lymphoblastic leukemia in

older patients. *Semin Hematol, 43*, 126-133.

Laviad, E. L., Albee, L., Pankova-Kholmyansky, I., Epstein, S., Park, H., Merrill, A. H., Jr., & Futerman, A. H. (2008). Characterization of ceramide synthase 2: tissue distribution, substrate specificity, and inhibition by sphingosine 1-phosphate. *J Biol Chem, 283*(9), 5677-5684. doi:10.1074/jbc.M707386200

Lee, Y., & Kwon, Y. H. (2019). Regulation of apoptosis and autophagy by luteolin in human hepatocellular cancer Hep3B cells. *Biochem Biophys Res Commun*. doi:10.1016/j.bbrc.2019.07.073

Levy, M., & Futerman, A. H. (2010). Mammalian ceramide synthases. *IUBMB Life, 62*(5), 347-356. doi:10.1002/iub.319

Li, C., Wang, Q., Shen, S., Wei, X., & Li, G. (2019). HIF-1alpha/VEGF signaling-mediated epithelial-mesenchymal transition and angiogenesis is critically involved in anti-metastasis effect of luteolin in melanoma cells. *Phytother Res, 33*(3), 798-807. doi:10.1002/ptr.6273

Li, S., Ilaria, R. L., Jr., Million, R. P., Daley, G. Q., & Van Etten, R. A. (1999). The P190, P210, and P230 forms of the BCR/ABL oncogene induce a similar chronic myeloid leukemia-like syndrome in mice but have different lymphoid leukemogenic activity. *J Exp Med, 189*(9), 1399-1412. doi:10.1084/jem.189.9.1399

Li, S., Wu, Y., Ding, Y., Yu, M., & Ai, Z. (2018). CerS6 regulates cisplatin resistance in oral squamous cell carcinoma by altering mitochondrial fission and autophagy. *J Cell Physiol, 233*(12), 9416-9425. doi:10.1002/jcp.26815

Li, W., Yu, C. P., Xia, J. T., Zhang, L., Weng, G. X., Zheng, H. Q., . . . Song, L. B. (2009). Sphingosine kinase 1 is associated with gastric cancer progression and poor survival of patients. *Clin Cancer Res, 15*(4), 1393-1399. doi:10.1158/1078-0432.CCR-08-1158

Li, Z., Zhang, Y., Chen, L., & Li, H. (2018). The dietary compound luteolin inhibits pancreatic cancer growth by targeting BCL-2. *Food Funct, 9*(5), 3018-3027. doi:10.1039/c8fo00033f

Lim, W., Yang, C., Bazer, F. W., & Song, G. (2016). Luteolin Inhibits Proliferation and Induces Apoptosis of Human Placental Choriocarcinoma Cells by Blocking the PI3K/AKT Pathway and Regulating Sterol Regulatory Element Binding Protein Activity. *Biol Reprod, 95*(4), 82. doi:10.1095/biolreprod.116.141556

Lin, D., Kuang, G., Wan, J., Zhang, X., Li, H., Gong, X., & Li, H. (2017). Luteolin suppresses the metastasis of triple-negative breast cancer by reversing epithelial-to-mesenchymal transition via downregulation of beta-catenin expression. *Oncol Rep, 37*(2), 895-902. doi:10.3892/or.2016.5311

Lingwood, D., & Simons, K. (2010). Lipid rafts as a membrane-organizing principle. *Science, 327*(5961), 46-50. doi:10.1126/science.1174621

Linn, S. C., Kim, H. S., Keane, E. M., Andras, L. M., Wang, E., & Merrill, A. H., Jr. (2001). Regulation of de novo sphingolipid biosynthesis and the toxic consequences of its disruption. *Biochem Soc Trans, 29*(Pt 6), 831-835. doi:10.1042/0300-5127:0290831

Liu, Y., Lang, T., Jin, B., Chen, F., Zhang, Y., Beuerman, R. W., . . . Zhang, Z. (2017). Luteolin inhibits colorectal cancer cell epithelial-to-mesenchymal transition by suppressing CREB1 expression revealed by comparative proteomics study. *J Proteomics, 161*, 1-10. doi:10.1016/j.jprot.2017.04.005

Liu, Y. Y., Patwardhan, G. A., Bhinge, K., Gupta, V., Gu, X., & Jazwinski, S. M. (2011). Suppression of glucosylceramide synthase restores p53-dependent apoptosis in mutant p53 cancer cells. *Cancer Res, 71*(6), 2276-2285. doi:10.1158/0008-5472.CAN-10-3107

Lu, P.-H., Chen, M.-B., Liu, Y.-Y., Wu, M.-H., Li, W.-T., Wei, M.-X., . . . Qin, S.-K. (2017). Identification of sphingosine kinase 1 (SphK1) as a primary target of icaritin in hepatocellular carcinoma cells. *Oncotarget, 8*(14), 22800-22810. doi:10.18632/oncotarget.15205

Luo, F. R., Yang, Z., Camuso, A., Smykla, R., McGlinchey, K., Fager, K., . . . Lee, F. Y. (2006). Dasatinib (BMS-354825) pharmacokinetics and pharmacodynamic biomarkers in animal models predict optimal clinical exposure. *Clin Cancer Res, 12*(23), 7180-7186. doi:10.1158/1078-0432.Ccr-06-1112

Luttgeharm, K. D., Cahoon, E. B., & Markham, J. E. (2015). A mass spectrometry-based method for the assay of ceramide synthase substrate specificity. *Anal Biochem, 478*, 96-101. doi:10.1016/j.ab.2015.02.016

Malagola, M., Papayannidis, C., & Baccarani, M. (2016). Tyrosine kinase inhibitors in Ph+ acute lymphoblastic leukaemia: facts and perspectives. *Ann Hematol, 95*(5), 681-693. doi:10.1007/s00277-016-2617-y

Malouf, C., & Ottersbach, K. (2018). Molecular processes involved in B cell acute lymphoblastic leukaemia. *Cell Mol Life Sci, 75*(3), 417-446. doi:10.1007/s00018-017-2620-z

Mancini, M., Scappaticci, D., Cimino, G., Nanni, M., Derme, V., Elia, L., . . . Foa, R. (2005). A comprehensive genetic classification of adult acute lymphoblastic leukemia (ALL): analysis of the GIMEMA 0496 protocol. *Blood, 105*(9), 3434-3441. doi:10.1182/blood-2004-07-2922

Mandanas, R. A., Leibowitz, D. S., Gharehbaghi, K., Tauchi, T., Burgess, G. S., Miyazawa, K., . . . Boswell, H. S. (1993). Role of p21 RAS in p210 bcr-abl transformation of murine myeloid cells. *Blood, 82*(6), 1838-1847.

Martinelli, G., Boissel, N., Chevallier, P., Ottmann, O., Gokbuget, N., Topp, M. S., . . . Stein, A. (2017). Complete Hematologic and Molecular Response in Adult Patients With Relapsed/Refractory Philadelphia Chromosome-Positive B-Precursor Acute Lymphoblastic Leukemia Following Treatment With Blinatumomab: Results From a Phase II, Single-Arm, Multicenter Study. *J Clin Oncol, 35*(16), 1795-1802. doi:10.1200/jco.2016.69.3531

Maru, Y., & Witte, O. N. (1991). The BCR gene encodes a novel serine/threonine kinase activity within a single exon. *Cell, 67*(3), 459-468. doi:10.1016/0092-8674(91)90521-y

Maury, S., Chevret, S., Thomas, X., Heim, D., Leguay, T., Huguet, F., . . . Dombret, H. (2016). Rituximab in B-Lineage Adult Acute Lymphoblastic Leukemia. *N Engl J Med, 375*(11), 1044-1053. doi:10.1056/NEJMoa1605085

Melo, J. V. (1996). The diversity of BCR-ABL fusion proteins and their relationship to leukemia phenotype. *Blood, 88*(7), 2375-2384.

Menaldino, D. S., Bushnev, A., Sun, A., Liotta, D. C., Symolon, H., Desai, K., . . . Merrill, A. H., Jr. (2003). Sphingoid bases and de novo ceramide synthesis: enzymes involved, pharmacology and mechanisms of action. *Pharmacol Res, 47*(5), 373-381. doi:10.1016/s1043-6618(03)00054-9

Mesicek, J., Lee, H., Feldman, T., Jiang, X., Skobeleva, A., Berdyshev, E. V., . . . Kolesnick, R. (2010). Ceramide synthases 2, 5, and 6 confer distinct roles in radiation-induced apoptosis in HeLa cells. *Cellular Signalling, 22*(9), 1300-1307. doi:https://doi.org/10.1016/j.cellsig.2010.04.006

Mizuchi, D., Kurosu, T., Kida, A., Jin, Z. H., Jin, A., Arai, A., & Miura, O. (2005). BCR/ABL activates Rap1 and B-Raf to stimulate the MEK/Erk signaling pathway in hematopoietic cells. *Biochem Biophys Res Commun, 326*(3), 645-651. doi:10.1016/j.bbrc.2004.11.086

Mizutani, Y., Kihara, A., & Igarashi, Y. (2005). Mammalian Lass6 and its related family members regulate synthesis of specific ceramides. *Biochem J, 390*(Pt 1), 263-271. doi:10.1042/BJ20050291

Mizutani, Y., Kihara, A., & Igarashi, Y. (2006). LASS3 (longevity assurance homologue 3) is a mainly testis-specific (dihydro)ceramide synthase with relatively broad substrate specificity. *Biochem J, 398*(3), 531-538. doi:10.1042/bj20060379

Moorman, A. V., Harrison, C. J., Buck, G. A., Richards, S. M., Secker-Walker, L. M., Martineau, M., . . . Dewald, G. W. (2007). Karyotype is an independent prognostic factor in adult acute lymphoblastic leukemia (ALL): analysis of cytogenetic data from patients treated on the Medical Research Council (MRC) UKALLXII/Eastern Cooperative Oncology Group (ECOG) 2993 trial. *Blood, 109*(8), 3189-3197. doi:10.1182/blood-2006-10-051912

Mullen, T. D., Hannun, Y. A., & Obeid, L. M. (2012). Ceramide synthases at the centre of sphingolipid metabolism and biology. *Biochem J, 441*(3), 789-802. doi:10.1042/BJ20111626

Mullighan, C. G., Su, X., Zhang, J., Radtke, I., Phillips, L. A., Miller, C. B., . . . Downing, J. R. (2009). Deletion of IKZF1 and prognosis in acute lymphoblastic leukemia. *N Engl J Med, 360*(5), 470-480. doi:10.1056/NEJMoa0808253

Nganga, R., Oleinik, N., & Ogretmen, B. (2018). Mechanisms of Ceramide-Dependent Cancer Cell Death. *Adv Cancer Res, 140*, 1-25. doi:10.1016/bs.acr.2018.04.007

Nimmanapalli, R., Porosnicu, M., Nguyen, D., Worthington, E., O'Bryan, E., Perkins, C., & Bhalla, K. (2019). Editor's Note: Cotreatment with STI-571 Enhances Tumor Necrosis Factor alpha-related Apoptosis-inducing Ligand (TRAIL or Apo-2L)-induced Apoptosis of Bcr-Abl-positive Human Acute Leukemia Cells. *Clin Cancer Res, 25*(13), 4195. doi:10.1158/1078-0432.Ccr-19-1602

Nowell, P. (1960). A minute chromosome in human chronic granulocytic

leukemia. . *Science, 132*(1497), 497–501.

Nowell, P. C. (2007). Discovery of the Philadelphia chromosome: a personal perspective. *J Clin Invest, 117*(8), 2033-2035. doi:10.1172/JCI31771

O'Dwyer, K. M., & Liesveld, J. L. (2017). Philadelphia chromosome negative B-cell acute lymphoblastic leukemia in older adults: Current treatment and novel therapies. *Best Pract Res Clin Haematol, 30*(3), 184-192. doi:10.1016/j.beha.2017.08.001

O'Hare, T., Walters, D. K., Stoffregen, E. P., Jia, T., Manley, P. W., Mestan, J., . . . Druker, B. J. (2005). In vitro activity of Bcr-Abl inhibitors AMN107 and BMS-354825 against clinically relevant imatinib-resistant Abl kinase domain mutants. *Cancer Res, 65*(11), 4500-4505. doi:10.1158/0008-5472.Can-05-0259

Obeid, L. M., Linardic, C. M., Karolak, L. A., & Hannun, Y. A. (1993). Programmed cell death induced by ceramide. *Science, 259*(5102), 1769-1771. doi:10.1126/science.8456305

Ogretmen, B., & Hannun, Y. A. (2004). Biologically active sphingolipids in cancer pathogenesis and treatment. *Nat Rev Cancer, 4*(8), 604-616. doi:10.1038/nrc1411

Okabe, S., Tauchi, T., Tanaka, Y., Kitahara, T., Kimura, S., Maekawa, T., & Ohyashiki, K. (2014). Efficacy of the dual PI3K and mTOR inhibitor NVP-BEZ235 in combination with nilotinib against BCR-ABL-positive leukemia cells involves the ABL kinase domain mutation. *Cancer Biol Ther, 15*(2), 207-215. doi:10.4161/cbt.26725

Okamoto, K., Karasawa, M., Sakai, H., Ogura, H., Morita, K., & Naruse, T. (1997). A novel acute lymphoid leukaemia type BCR/ABL transcript in chronic myelogenous leukaemia. *Br J Haematol, 96*(3), 611-613. doi:10.1046/j.1365-2141.1997.d01-2066.x

Organization, W. H. (2019). Cancer Today. Retrieved from http://gco.iarc.fr/today/explore

Otero, D. C., Omori, S. A., & Rickert, R. C. (2001). Cd19-dependent activation of Akt kinase in B-lymphocytes. *J Biol Chem, 276*(2), 1474-1478. doi:10.1074/jbc.M003918200

Ottmann, O., Dombret, H., Martinelli, G., Simonsson, B., Guilhot, F., Larson, R. A., . . . Coutre, S. (2007). Dasatinib induces rapid hematologic and cytogenetic responses in adult patients with Philadelphia chromosome positive acute

lymphoblastic leukemia with resistance or intolerance to imatinib: interim results of a phase 2 study. *Blood, 110*(7), 2309-2315. doi:10.1182/blood-2007-02-073528

Ottmann, O. G., & Pfeifer, H. (2009). Management of Philadelphia chromosome-positive acute lymphoblastic leukemia (Ph+ ALL). *Hematology Am Soc Hematol Educ Program*, 371-381. doi:10.1182/asheducation-2009.1.371

Pane, F., Intrieri, M., Quintarelli, C., Izzo, B., Muccioli, G. C., & Salvatore, F. (2002). BCR/ABL genes and leukemic phenotype: from molecular mechanisms to clinical correlations. *Oncogene, 21*(56), 8652-8667. doi:10.1038/sj.onc.1206194

Panjarian, S., Kozhaya, L., Arayssi, S., Yehia, M., Bielawski, J., Bielawska, A., . . . Dbaibo, G. S. (2008). De novo N-palmitoylsphingosine synthesis is the major biochemical mechanism of ceramide accumulation following p53 up-regulation. *Prostaglandins & Other Lipid Mediators, 86*(1), 41-48. doi:https://doi.org/10.1016/j.prostaglandins.2008.02.004

Park, J. W., Park, W. J., & Futerman, A. H. (2014). Ceramide synthases as potential targets for therapeutic intervention in human diseases. *Biochim Biophys Acta, 1841*(5), 671-681. doi:10.1016/j.bbalip.2013.08.019

Park, S. J., Kim, M. J., Kim, H. B., Kang, C. D., & Kim, S. H. (2009). Sensitization of imatinib-resistant CML cells to TRAIL-induced apoptosis is mediated through down-regulation of Bcr-Abl as well as c-FLIP. *Biochem J, 420*(1), 73-81. doi:10.1042/bj20082131

Patwardhan, G. A., Beverly, L. J., & Siskind, L. J. (2016). Sphingolipids and mitochondrial apoptosis. *J Bioenerg Biomembr, 48*(2), 153-168. doi:10.1007/s10863-015-9602-3

Pchejetski, D., Golzio, M., Bonhoure, E., Calvet, C., Doumerc, N., Garcia, V., . . . Cuvillier, O. (2005). Sphingosine kinase-1 as a chemotherapy sensor in prostate adenocarcinoma cell and mouse models. *Cancer Res, 65*(24), 11667-11675. doi:10.1158/0008-5472.CAN-05-2702

Pendergast, A. M., Gishizky, M. L., Havlik, M. H., & Witte, O. N. (1993). SH1 domain autophosphorylation of P210 BCR/ABL is required for transformation but not growth factor independence. *Molecular and cellular biology, 13*(3), 1728-1736. doi:10.1128/mcb.13.3.1728

Pewzner-Jung, Y., Ben-Dor, S., & Futerman, A. H. (2006). When do Lasses (longevity assurance genes) become CerS (ceramide synthases)?: Insights into the regulation of ceramide synthesis. *J Biol Chem, 281*(35), 25001-25005. doi:10.1074/jbc.R600010200

Phelan, K. W., & Advani, A. S. (2018). Novel Therapies in Acute Lymphoblastic Leukemia. *Curr Hematol Malig Rep, 13*(4), 289-299. doi:10.1007/s11899-018-0457-7

Ponnusamy, S., Meyers-Needham, M., Senkal, C. E., Saddoughi, S. A., Sentelle, D., Selvam, S. P., . . . Ogretmen, B. (2010). Sphingolipids and cancer: ceramide and

sphingosine-1-phosphate in the regulation of cell death and drug resistance. *Future Oncol, 6*(10), 1603-1624. doi:10.2217/fon.10.116

Portell, C. A., & Advani, A. S. (2014). Novel targeted therapies in acute lymphoblastic leukemia. *Leuk Lymphoma, 55*(4), 737-748. doi:10.3109/10428194.2013.823493

Preyer, M., Vigneri, P., & Wang, J. Y. (2011). Interplay between kinase domain autophosphorylation and F-actin binding domain in regulating imatinib sensitivity and nuclear import of BCR-ABL. *PLoS One, 6*(2), e17020. doi:10.1371/journal.pone.0017020

Prochazkova, D., Bousova, I., & Wilhelmova, N. (2011). Antioxidant and prooxidant properties of flavonoids. *Fitoterapia, 82*(4), 513-523. doi:10.1016/j.fitote.2011.01.018

PubChem.

Pui, C. H., Relling, M. V., & Downing, J. R. (2004). Acute lymphoblastic leukemia. *N Engl J Med, 350*(15), 1535-1548. doi:10.1056/NEJMra023001

Pullarkat, V., Slovak, M. L., Kopecky, K. J., Forman, S. J., & Appelbaum, F. R. (2008). Impact of cytogenetics on the outcome of adult acute lymphoblastic leukemia: results of Southwest Oncology Group 9400 study. *Blood, 111*(5), 2563-2572. doi:10.1182/blood-2007-10-116186

Quentmeier, H., Eberth, S., Romani, J., Zaborski, M., & Drexler, H. G. (2011). BCR-ABL1-independent PI3Kinase activation causing imatinib-resistance. *J Hematol Oncol, 4*, 6. doi:10.1186/1756-8722-4-6

Raetz, E. A., Cairo, M. S., Borowitz, M. J., Lu, X., Devidas, M., Reid, J. M., . . . Carroll, W. L. (2015). Re-induction chemoimmunotherapy with epratuzumab in relapsed acute lymphoblastic leukemia (ALL): Phase II results from Children's Oncology Group (COG) study ADVL04P2. *Pediatr Blood Cancer, 62*(7), 1171-1175. doi:10.1002/pbc.25454

Rafei, H., Kantarjian, H. M., & Jabbour, E. J. (2019). Recent advances in the treatment of acute lymphoblastic leukemia. *Leuk Lymphoma, 60*(11), 2606-2621. doi:10.1080/10428194.2019.1605071

Raimondo, S., Naselli, F., Fontana, S., Monteleone, F., Lo Dico, A., Saieva, L., . . . Alessandro, R. (2015). Citrus limon-derived nanovesicles inhibit cancer cell proliferation and suppress CML xenograft growth by inducing TRAIL-mediated cell death. *Oncotarget, 6*(23), 19514-19527. doi:10.18632/oncotarget.4004

Ravandi, F., O'Brien, S., Thomas, D., Faderl, S., Jones, D., Garris, R., . . . Kantarjian, H. (2010). First report of phase 2 study of dasatinib with hyper-CVAD for the frontline treatment of patients with Philadelphia chromosome-positive (Ph+) acute lymphoblastic leukemia. *Blood, 116*(12), 2070-2077. doi:10.1182/blood-2009-12-261586

Ribera, J.-M. (2018). A step ahead in Philadelphia chromosome-positive acute lymphoblastic leukaemia. *The Lancet Haematology, 5*(12), e602-e603. doi:10.1016/s2352-3026(18)30195-9

Riebeling, C., Allegood, J. C., Wang, E., Merrill, A. H., Jr., & Futerman, A. H. (2003). Two mammalian longevity assurance gene (LAG1) family members, trh1 and trh4, regulate dihydroceramide synthesis using different fatty acyl-CoA donors. *J Biol Chem, 278*(44), 43452-43459. doi:10.1074/jbc.M307104200

Rieder, H., Ludwig, W. D., Gassmann, W., Maurer, J., Janssen, J. W., Gokbuget, N., . . . Fonatsch, C. (1996). Prognostic significance of additional chromosome abnormalities in adult patients with Philadelphia chromosome positive acute lymphoblastic leukaemia. *Br J Haematol, 95*(4), 678-691. doi:10.1046/j.1365-2141.1996.d01-1968.x

Roser, H. R. a. M. (2019). Causes of Death. Retrieved from https://ourworldindata.org/causes-of-death

Rowe, J. M., Buck, G., Burnett, A. K., Chopra, R., Wiernik, P. H., Richards, S. M., . . . Goldstone, A. H. (2005). Induction therapy for adults with acute lymphoblastic leukemia: results of more than 1500 patients from the international ALL trial: MRC UKALL XII/ECOG E2993. *Blood, 106*(12), 3760-3767. doi:10.1182/blood-2005-04-1623

Rowley, J. D. (1973). Letter: A new consistent chromosomal abnormality in chronic myelogenous leukaemia identified by quinacrine fluorescence and Giemsa staining. *Nature, 243*(5405), 290-293. doi:10.1038/243290a0

Ruan, H., Wang, T., Yang, C., Jin, G., Gu, D., Deng, X., . . . Jin, H. (2016). Co-expression of LASS2 and TGF-beta1 predicts poor prognosis in hepatocellular carcinoma. *Sci Rep, 6*, 32421. doi:10.1038/srep32421

Ruckhaberle, E., Rody, A., Engels, K., Gaetje, R., von Minckwitz, G., Schiffmann, S., . . . Kaufmann, M. (2008). Microarray analysis of altered sphingolipid metabolism reveals prognostic significance of sphingosine kinase 1 in breast cancer. *Breast Cancer Res Treat, 112*(1), 41-52. doi:10.1007/s10549-007-9836-9

Russo, S. B., Ross, J. S., & Cowart, L. A. (2013). Sphingolipids in obesity, type 2 diabetes, and metabolic disease. *Handb Exp Pharmacol*(216), 373-401. doi:10.1007/978-3-7091-1511-4_19

Saddoughi, S. A., & Ogretmen, B. (2013). Diverse functions of ceramide in cancer cell death and proliferation. *Adv Cancer Res, 117*, 37-58. doi:10.1016/B978-0-12-394274-6.00002-9

Saddoughi, S. A., Song, P., & Ogretmen, B. (2008). Roles of bioactive sphingolipids in cancer biology and therapeutics. *Subcell Biochem, 49*, 413-440. doi:10.1007/978-1-4020-8831-5_16

Saglio, G., Guerrasio, A., Rosso, C., Zaccaria, A., Tassinari, A., Serra, A., . . . Gavosto, F. (1990). New type of Bcr/Abl junction in Philadelphia chromosome-positive chronic myelogenous leukemia. *Blood, 76*(9), 1819-1824.

Saglio, G., Kim, D. W., Issaragrisil, S., le Coutre, P., Etienne, G., Lobo, C., . . . Kantarjian, H. M. (2010). Nilotinib versus imatinib for newly diagnosed chronic myeloid leukemia. *N Engl J Med, 362*(24), 2251-2259. doi:10.1056/NEJMoa0912614

Samanta, A., Perazzona, B., Chakraborty, S., Sun, X., Modi, H., Bhatia, R., . . . Arlinghaus, R. (2011). Janus kinase 2 regulates Bcr-Abl signaling in chronic myeloid leukemia. *Leukemia, 25*(3), 463-472. doi:10.1038/leu.2010.287

Sassa, T., Suto, S., Okayasu, Y., & Kihara, A. (2012). A shift in sphingolipid composition from C24 to C16 increases susceptibility to apoptosis in HeLa cells. *Biochimica et Biophysica Acta (BBA) - Molecular and Cell Biology of Lipids, 1821*(7), 1031-1037. doi:https://doi.org/10.1016/j.bbalip.2012.04.008

Sattler, M., & Griffin, J. D. (2003). Molecular mechanisms of transformation by the BCR-ABL oncogene. *Semin Hematol, 40*(2 Suppl 2), 4-10. doi:10.1053/shem.2003.50034

Sawyers, C. L. (1993). The role of myc in transformation by BCR-ABL. *Leuk Lymphoma, 11 Suppl 1*, 45-46. doi:10.3109/10428199309047862

Sayed, D., Badrawy, H., Gaber, N., & Khalaf, M. R. (2014). p-Stat3 and bcr/abl gene expression in chronic myeloid leukemia and their relation to imatinib therapy. *Leuk Res, 38*(2), 243-250. doi:10.1016/j.leukres.2013.11.012

Scarlatti, F., Sala, G., Ricci, C., Maioli, C., Milani, F., Minella, M., . . . Ghidoni, R. (2007). Resveratrol sensitization of DU145 prostate cancer cells to ionizing radiation is associated to ceramide increase. *Cancer Lett, 253*(1), 124-130. doi:10.1016/j.canlet.2007.01.014

Schiffmann, S., Sandner, J., Birod, K., Wobst, I., Angioni, C., Ruckhaberle, E., . . . Grosch, S. (2009). Ceramide synthases and ceramide levels are increased in breast cancer tissue. *Carcinogenesis, 30*(5), 745-752. doi:10.1093/carcin/bgp061

Schindler, T., Bornmann, W., Pellicena, P., Miller, W. T., Clarkson, B., & Kuriyan, J. (2000). Structural mechanism for STI-571 inhibition of abelson tyrosine kinase. *Science, 289*(5486), 1938-1942. doi:10.1126/science.289.5486.1938

Schultz, K. R., Pullen, D. J., Sather, H. N., Shuster, J. J., Devidas, M., Borowitz, M. J., . . . Camitta, B. M. (2007). Risk- and response-based classification of childhood B-precursor acute lymphoblastic leukemia: a combined analysis of prognostic markers from the Pediatric Oncology Group (POG) and Children's Cancer Group (CCG). *Blood, 109*(3), 926-935. doi:10.1182/blood-2006-01-024729

Score, J., Calasanz, M. J., Ottman, O., Pane, F., Yeh, R. F., Sobrinho-Simoes, M. A., . . . Grand, F. H. (2010). Analysis of genomic breakpoints in p190 and p210 BCR-ABL indicate distinct mechanisms of formation. *Leukemia, 24*(10), 1742-1750. doi:10.1038/leu.2010.174

Secker-Walker, L. M., Prentice, H. G., Durrant, J., Richards, S., Hall, E., & Harrison, G. (1997). Cytogenetics adds independent prognostic information in adults with acute lymphoblastic leukaemia on MRC trial UKALL XA. MRC Adult Leukaemia Working Party. *Br J Haematol, 96*(3), 601-610. doi:10.1046/j.1365-2141.1997.d01-2053.x

Senkal, C. E., Ponnusamy, S., Rossi, M. J., Bialewski, J., Sinha, D., Jiang, J. C., . . . Ogretmen, B. (2007). Role of human longevity assurance gene 1 and C18-ceramide in chemotherapy-induced cell death in human head and neck squamous cell carcinomas. *Mol Cancer Ther, 6*(2), 712-722. doi:10.1158/1535-7163.Mct-06-0558

Sentelle, R. D., Senkal, C. E., Jiang, W., Ponnusamy, S., Gencer, S., Selvam, S. P., . . . Ogretmen, B. (2012). Ceramide targets autophagosomes to mitochondria and induces lethal mitophagy. *Nat Chem Biol, 8*(10), 831-838. doi:10.1038/nchembio.1059

Shah, N. N., Stevenson, M. S., Yuan, C. M., Richards, K., Delbrook, C., Kreitman, R. J., . . . Wayne, A. S. (2015). Characterization of CD22 expression in acute lymphoblastic leukemia. *Pediatr Blood Cancer, 62*(6), 964-969. doi:10.1002/pbc.25410

Shah, N. P., Nicoll, J. M., Nagar, B., Gorre, M. E., Paquette, R. L., Kuriyan, J., & Sawyers, C. L. (2002). Multiple BCR-ABL kinase domain mutations confer polyclonal resistance to the tyrosine kinase inhibitor imatinib (STI571) in chronic phase and blast crisis chronic myeloid leukemia. *Cancer Cell, 2*(2), 117-125.

Shaw, J., Costa-Pinheiro, P., Patterson, L., Drews, K., Spiegel, S., & Kester, M. (2018). Novel Sphingolipid-Based Cancer Therapeutics in the Personalized Medicine Era. *Adv Cancer Res, 140*, 327-366. doi:10.1016/bs.acr.2018.04.016

Siegel, R. L., Miller, K. D., & Jemal, A. (2019). Cancer statistics, 2019. *CA Cancer J Clin, 69*(1), 7-34. doi:10.3322/caac.21551

Simons, K., & Ikonen, E. (1997). Functional rafts in cell membranes. *Nature, 387*(6633), 569-572. doi:10.1038/42408

Sobue, S., Nemoto, S., Murakami, M., Ito, H., Kimura, A., Gao, S., . . . Murate, T. (2008). Implications of sphingosine kinase 1 expression level for the cellular sphingolipid rheostat: relevance as a marker for daunorubicin sensitivity of leukemia cells. *Int J Hematol, 87*(3), 266-275. doi:10.1007/s12185-008-0052-0

Society, A. C. (2019). Cancer Facts and Figures.

Soekarman, D., van Denderen, J., Hoefsloot, L., Moret, M., Meeuwsen, T., van Baal, J., . . . Grosveld, G. (1990). A novel variant of the bcr-abl fusion product in Philadelphia chromosome-positive acute lymphoblastic leukemia. *Leukemia, 4*(6), 397-403.

Stock, W. (2008). Advances in the treatment of Philadelphia chromosome-positive acute lymphoblastic leukemia. *Clin Adv Hematol Oncol, 6*(7), 487-488.

Talpaz, M., Shah, N. P., Kantarjian, H., Donato, N., Nicoll, J., Paquette, R., . . . Sawyers, C. L. (2006). Dasatinib in imatinib-resistant Philadelphia chromosome-positive leukemias. *N Engl J Med, 354*(24), 2531-2541. doi:10.1056/NEJMoa055229

Tao, W. J., Lin, H., Sun, T., Samanta, A. K., & Arlinghaus, R. (2008). BCR-ABL oncogenic transformation of NIH 3T3 fibroblasts requires the IL-3 receptor. *Oncogene, 27*(22), 3194-3200. doi:10.1038/sj.onc.1210979

Tasian, S. K., Loh, M. L., & Hunger, S. P. (2017). Philadelphia chromosome-like acute lymphoblastic leukemia. *Blood, 130*(19), 2064-2072. doi:10.1182/blood-2017-06-743252

Terwilliger, T., & Abdul-Hay, M. (2017). Acute lymphoblastic leukemia: a comprehensive review and 2017 update. *Blood Cancer J, 7*(6), e577. doi:10.1038/bcj.2017.53

Thomas, D. A. (2007). Philadelphia chromosome positive acute lymphocytic leukemia: a new era of challenges. *Hematology Am Soc Hematol Educ Program*, 435-443. doi:10.1182/asheducation-2007.1.435

Thomas, D. A., O'Brien, S., Faderl, S., Garcia-Manero, G., Ferrajoli, A., Wierda, W., . . . Kantarjian, H. M. (2010). Chemoimmunotherapy with a modified hyper-CVAD and rituximab regimen improves outcome in de novo Philadelphia chromosome-negative precursor B-lineage acute lymphoblastic leukemia. *J Clin Oncol, 28*(24), 3880-3889. doi:10.1200/jco.2009.26.9456

Thomas, X., & Heiblig, M. (2016). Diagnostic and treatment of adult Philadelphia chromosome-positive acute lymphoblastic leukemia. *Int J Hematol Oncol, 5*(2), 77-90. doi:10.2217/ijh-2016-0009

Thomas, X., Thiebaut, A., Olteanu, N., Danaila, C., Charrin, C., Archimbaud, E., & Fiere, D. (1998). Philadelphia chromosome positive adult acute lymphoblastic leukemia: characteristics, prognostic factors and treatment outcome. *Hematol Cell Ther, 40*(3), 119-128.

Tian, H., & Yu, Z. (2015). Resveratrol induces apoptosis of leukemia cell line K562 by modulation of sphingosine kinase-1 pathway. *Int J Clin Exp Pathol, 8*(3), 2755-2762.

Tibes, R., Keating, M. J., Ferrajoli, A., Wierda, W., Ravandi, F., Garcia-Manero, G., . . . Faderl, S. (2006). Activity of alemtuzumab in patients with CD52-positive acute leukemia. *Cancer, 106*(12), 2645-2651. doi:10.1002/cncr.21901

Tidhar, R., Zelnik, I. D., Volpert, G., Ben-Dor, S., Kelly, S., Merrill, A. H., Jr., & Futerman, A. H. (2018). Eleven residues determine the acyl chain specificity of ceramide synthases. *J Biol Chem, 293*(25), 9912-9921. doi:10.1074/jbc.RA118.001936

Uen, Y. H., Fang, C. L., Lin, C. C., Hseu, Y. C., Hung, S. T., Sun, D. P., & Lin, K. Y. (2018). Ceramide synthase 6 predicts the prognosis of human gastric cancer: It

functions as an oncoprotein by dysregulating the SOCS2/JAK2/STAT3 pathway. *Mol Carcinog, 57*(12), 1675-1689. doi:10.1002/mc.22888

van Echten-Deckert, G., & Walter, J. (2012). Sphingolipids: critical players in Alzheimer's disease. *Prog Lipid Res, 51*(4), 378-393. doi:10.1016/j.plipres.2012.07.001

van Meer, G., Voelker, D. R., & Feigenson, G. W. (2008). Membrane lipids: where they are and how they behave. *Nat Rev Mol Cell Biol, 9*(2), 112-124. doi:10.1038/nrm2330

Vardiman, J. W., Thiele, J., Arber, D. A., Brunning, R. D., Borowitz, M. J., Porwit, A., . . . Bloomfield, C. D. (2009). The 2008 revision of the World Health Organization (WHO) classification of myeloid neoplasms and acute leukemia: rationale and important changes. *Blood, 114*(5), 937-951. doi:10.1182/blood-2009-03-209262

Venkataraman, K., Riebeling, C., Bodennec, J., Riezman, H., Allegood, J. C., Sullards, M. C., . . . Futerman, A. H. (2002). Upstream of growth and differentiation factor 1 (uog1), a mammalian homolog of the yeast longevity assurance gene 1 (LAG1), regulates N-stearoyl-sphinganine (C18-(dihydro)ceramide) synthesis in a fumonisin B1-independent manner in mammalian cells. *J Biol Chem, 277*(38), 35642-35649. doi:10.1074/jbc.M205211200

Verlekar, D., Wei, S. J., Cho, H., Yang, S., & Kang, M. H. (2018). Ceramide synthase-6 confers resistance to chemotherapy by binding to CD95/Fas in T-cell acute lymphoblastic leukemia. *Cell Death Dis, 9*(9), 925. doi:10.1038/s41419-018-0964-4

Vinhas, R., Lourenco, A., Santos, S., Lemos, M., Ribeiro, P., de Sousa, A. B., . . . Fernandes, A. R. (2018). A novel BCR-ABL1 mutation in a patient with Philadelphia chromosome-positive B-cell acute lymphoblastic leukemia. *Onco Targets Ther, 11*, 8589-8598. doi:10.2147/OTT.S177019

Wallington-Beddoe, C. T., Powell, J. A., Tong, D., Pitson, S. M., Bradstock, K. F., & Bendall, L. J. (2014). Sphingosine kinase 2 promotes acute lymphoblastic leukemia by enhancing MYC expression. *Cancer Res, 74*(10), 2803-2815. doi:10.1158/0008-5472.CAN-13-2732

Wang, H., Luo, Y., Qiao, T., Wu, Z., & Huang, Z. (2018). Luteolin sensitizes the antitumor effect of cisplatin in drug-resistant ovarian cancer via induction of apoptosis and inhibition of cell migration and invasion. *J Ovarian Res, 11*(1), 93. doi:10.1186/s13048-018-0468-y

Wang, H., Zuo, Y., Ding, M., Ke, C., Yan, R., Zhan, H., . . . Wang, J. (2017). LASS2 inhibits growth and invasion of bladder cancer by regulating ATPase activity. *Oncology letters, 13*(2), 661-668. doi:10.3892/ol.2016.5514

Wang, Q., Wang, H., Jia, Y., Ding, H., Zhang, L., & Pan, H. (2017). Luteolin reduces migration of human glioblastoma cell lines via inhibition of the p-IGF-1R/PI3K/AKT/mTOR signaling pathway. *Oncol Lett, 14*(3), 3545-3551. doi:10.3892/ol.2017.6643

Wang, Q., Wang, H., Jia, Y., Pan, H., & Ding, H. (2017). Luteolin induces apoptosis by ROS/ER stress and mitochondrial dysfunction in gliomablastoma. *Cancer Chemother Pharmacol, 79*(5), 1031-1041. doi:10.1007/s00280-017-3299-4

Wang, S. W., Chen, Y. R., Chow, J. M., Chien, M. H., Yang, S. F., Wen, Y. C., . . . Tseng, T. H. (2018). Stimulation of Fas/FasL-mediated apoptosis by luteolin through enhancement of histone H3 acetylation and c-Jun activation in HL-60 leukemia cells. *Mol Carcinog, 57*(7), 866-877. doi:10.1002/mc.22807

Wang, Z., Wen, L., Zhu, F., Wang, Y., Xie, Q., Chen, Z., & Li, Y. (2017). Overexpression of ceramide synthase 1 increases C18-ceramide and leads to lethal autophagy in human glioma. *Oncotarget, 8*(61), 104022-104036. doi:10.18632/oncotarget.21955

Warsch, W., Walz, C., & Sexl, V. (2013). JAK of all trades: JAK2-STAT5 as novel therapeutic targets in BCR-ABL1+ chronic myeloid leukemia. *Blood, 122*(13), 2167-2175. doi:10.1182/blood-2013-02-485573

Wegner, M.-S., Wanger, R. A., Oertel, S., Brachtendorf, S., Hartmann, D., Schiffmann, S., . . . Grösch, S. (2014). Ceramide synthases CerS4 and CerS5 are upregulated by 17β-estradiol and GPER1 via AP-1 in human breast cancer cells. *Biochemical Pharmacology, 92*(4), 577-589. doi:https://doi.org/10.1016/j.bcp.2014.10.007

Westbrook, C. A., Hooberman, A. L., Spino, C., Dodge, R. K., Larson, R. A., Davey, F., . . . Bloomfield, C. D. (1992). Clinical significance of the BCR-ABL fusion gene in adult acute lymphoblastic leukemia: a Cancer and Leukemia Group B Study (8762). *Blood, 80*(12), 2983-2990.

Wyatt, K. D., & Bram, R. J. (2019). Immunotherapy in pediatric B-cell acute lymphoblastic leukemia. *Hum Immunol, 80*(6), 400-408. doi:10.1016/j.humimm.2019.01.011

Xie, S., Lin, H., Sun, T., & Arlinghaus, R. B. (2002). Jak2 is involved in c-Myc induction by Bcr-Abl. *Oncogene, 21*(47), 7137-7146. doi:10.1038/sj.onc.1205942

Xu, H., Yang, T., Liu, X., Tian, Y., Chen, X., Yuan, R., . . . Du, G. (2016). Luteolin synergizes the antitumor effects of 5-fluorouracil against human hepatocellular carcinoma cells through apoptosis induction and metabolism. *Life Sci, 144*, 138-147. doi:10.1016/j.lfs.2015.12.002

Xu, W., Harrison, S. C., & Eck, M. J. (1997). Three-dimensional structure of the tyrosine kinase c-Src. *Nature, 385*(6617), 595-602. doi:10.1038/385595a0

Yanada, M., Ohno, R., & Naoe, T. (2009). Recent advances in the treatment of Philadelphia chromosome-positive acute lymphoblastic leukemia. *Int J Hematol, 89*(1), 3-13. doi:10.1007/s12185-008-0223-z

Yang, Y., & Uhlig, S. (2011). The role of sphingolipids in respiratory disease. *Ther Adv Respir Dis, 5*(5), 325-344. doi:10.1177/1753465811406772

Yao, X., Jiang, W., Yu, D., & Yan, Z. (2019). Luteolin inhibits proliferation and induces apoptosis of human melanoma cells in vivo and in vitro by suppressing MMP-2 and MMP-9 through the PI3K/AKT pathway. *Food Funct, 10*(2), 703-712. doi:10.1039/c8fo02013b

Yao, Y., Rao, C., Zheng, G., & Wang, S. (2019). Luteolin suppresses colorectal cancer cell metastasis via regulation of the miR384/pleiotrophin axis. *Oncol Rep, 42*(1), 131-141. doi:10.3892/or.2019.7136

Yu, Q., Zhang, M., Ying, Q., Xie, X., Yue, S., Tong, B., . . . Ma, L. (2019). Decrease of AIM2 mediated by luteolin contributes to non-small cell lung cancer treatment. *Cell Death Dis, 10*(3), 218. doi:10.1038/s41419-019-1447-y

Zang, M. D., Hu, L., Fan, Z. Y., Wang, H. X., Zhu, Z. L., Cao, S., . . . Liu, B. Y. (2017). Luteolin suppresses gastric cancer progression by reversing epithelial-mesenchymal transition via suppression of the Notch signaling pathway. *J Transl Med, 15*(1), 52. doi:10.1186/s12967-017-1151-6

Zhang, X., Subrahmanyam, R., Wong, R., Gross, A. W., & Ren, R. (2001). The NH(2)-terminal coiled-coil domain and tyrosine 177 play important roles in induction of a myeloproliferative disease in mice by Bcr-Abl. *Molecular and cellular biology, 21*(3), 840-853. doi:10.1128/mcb.21.3.840-853.2001

Zhao, S., Asgary, Z., Wang, Y., Goodwin, R., Andreeff, M., & Younes, A. (1999). Functional expression of TRAIL by lymphoid and myeloid tumour cells. *Br J Haematol, 106*(3), 827-832. doi:10.1046/j.1365-2141.1999.01630.x

Zheng, X., Li, W., Ren, L., Liu, J., Pang, X., Chen, X., . . . Du, G. (2019). The sphingosine kinase-1/sphingosine-1-phosphate axis in cancer: Potential target for anticancer therapy. *Pharmacol Ther, 195*, 85-99. doi:10.1016/j.pharmthera.2018.10.011

Zhou, T., Commodore, L., Huang, W. S., Wang, Y., Thomas, M., Keats, J., . . . Zhu, X. (2011). Structural mechanism of the Pan-BCR-ABL inhibitor ponatinib (AP24534): lessons for overcoming kinase inhibitor resistance. *Chem Biol Drug Des, 77*(1), 1-11. doi:10.1111/j.1747-0285.2010.01054.x

Zuo, Q., Wu, R., Xiao, X., Yang, C., Yang, Y., Wang, C., . . . Kong, A. N. (2018). The dietary flavone luteolin epigenetically activates the Nrf2 pathway and blocks cell transformation in human colorectal cancer HCT116 cells. *J Cell Biochem, 119*(11), 9573-9582. doi:10.1002/jcb.27275